The Radio Science Bulletin

ISSN 1024-4530

INTERNATIONAL
UNION OF
RADIO SCIENCE

UNION
RADIO-SCIENTIFIQUE
INTERNATIONALE

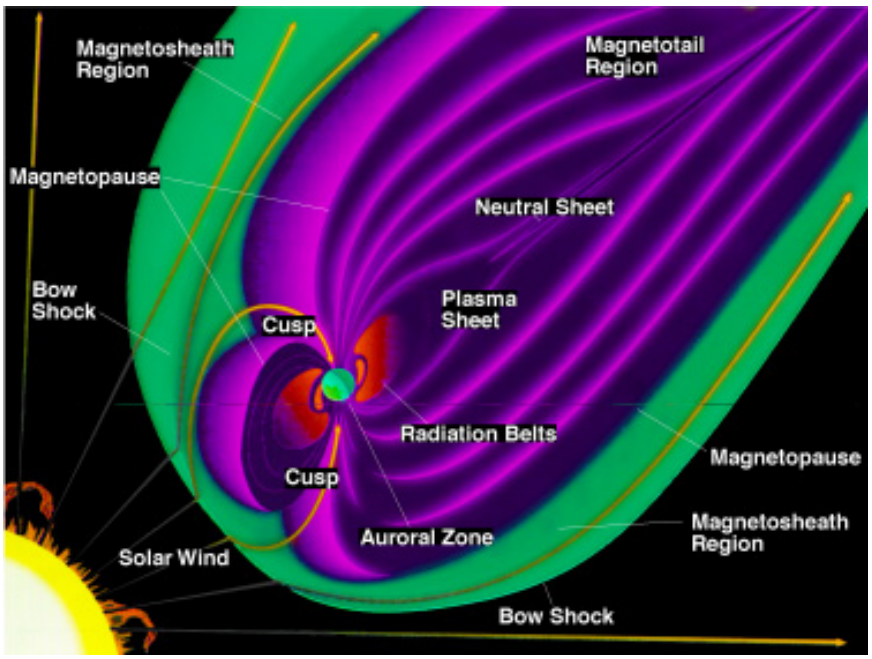

No 316
March 2006

Publié avec l'aide financière de l'ICSU
URSI, c/o Ghent University (INTEC)
St.-Pietersnieuwstraat 41, B-9000 Gent (Belgium)

Contents

Front cover: The internal structure of the Earth's magnetosphere (courtesy of Goddard Space Flight Center). See the paper by H.C. Koons and J.F. Fennell on pp. 27-41.

For information, please contact :
The URSI Secretariat
c/o Ghent University (INTEC)
Sint-Pietersnieuwstraat 41, B-9000 Gent, Belgium
Tel.: (32) 9-264 33 20, Fax: (32) 9-264 42 88
E-mail: info@ursi.org

Editorial

In this issue of the *Radio Science Bulletin*, we have three *Reviews of Radio Science*, Jim Lin's column, and a report on the status of ITU-R Study Group 7, along with other reports.

MIMO (multiple-input, multiple-output) communications technology has had a profound effect on wireless channel capacity and reliability. MIMO systems benefit from two aspects. Spatial multiplexing makes use of multiple spatially separated data channels (e.g., along multiple propagation paths) to improve the data rate. Spatial diversity makes use of an increased number of degrees of freedom in the fading channel to improve the reliability of communications. In their invited Commission C *Review*, Christoph Mecklenbräuker and Helmut Hofstetter explain the science and engineering of applying MIMO technology to wireless communications, and, in particular, look at the implications of applying it to mobile radio and cellular communications. The role and importance of scattering is first considered, and this is then used to develop a model of the MIMO radio channel. A model is then developed for the antenna arrays that are at both ends of a MIMO system, including the effects of polarization. These models are then used to describe recent developments in the various aspects of MIMO system design, including transmitter-side and receiver-side processing, coding, and channel estimation. The paper ends with a survey of open issues in the field. I think you will find this to be a very interesting and insightful look at one of today's most important communications technologies, in terms of the impact it is having on current and future communications systems.

Thanks go to Andy Molisch for his efforts in bringing us this *Review*.

Traditionally, a deterministic approach has been taken to the modeling of electromagnetic compatibility (EMC) problems and the interpretation of experimental EMC data. However, in his invited Commission E *Review*, Sergio Pignari presents a convincing argument for the value of statistical approaches to such problems. As he notes, complex systems are often not adequately well known to permit a fully deterministic approach. Even in simple systems, the parasitic nature of the coupling and the random nature of much of the electromagnetic interference make a statistical approach useful. Furthermore, a statistical approach often does not become more complex as the complexity of the system increases. Indeed, if an increase in complexity is due to repetition of some basic structure, a probabilistic approach can actually become more accurate with increasing complexity. The paper begins by looking at probabilistic models of electromagnetic interference in three classes, differentiated by the relationship of the bandwidth of the interference to the bandwidth of the system receiving the interference. Statistical aspects of EMC compliance testing are then considered, including measurement uncertainty, noise effects in time-domain electromagnetic interference measurements, and statistical aspects of radiated emissions and safety assessment. This is followed by a most interesting look at how a probabilistic approach can be used to predict interference effects on a variety of complex wiring structures. Finally, the application of statistics to system-level EMC assessment is considered. One of the nice aspects of this paper is that it is written so that it can be understood without a detailed knowledge of statistics.

The efforts of Flavio Canavero in bringing us this review are gratefully acknowledged.

The effects of space weather on communications satellites is the topic of the invited Commission H review by H. C. Koons and J. F. Fennell. In particular, this paper looks at the hazards space weather presents to communications satellites. It begins with a characterization of the space environment, including such sources of hazards as the sun, galactic sources, and the Earth's magnetosphere. It then considers the major types of environmental hazards, including single-event effects, surface charging, internal charging, total radiation dose, solar-cell degradation, atmospheric effects, and solar-cycle effects. The discussion is concluded with some examples of extreme events and anomalies. This paper provides an excellent and easy-to-understand introduction to the hazards to which communications satellites are subjected.

Regrettably, Harry Koons passed away after this paper was finished. It was his last completed scientific effort. Please remember him as you read this contribution.

Richard Horne is the Commission H Associate Editor, and his efforts in bring us this *Review* are much appreciated.

As always, Phil Wilkinson is the Senior Associate Editor in charge of the *Reviews of Radio Science*, and it is also because of his efforts that we have these *Reviews*.

The National Radiological Protection Board in the UK has issued an advisory to parents not to let children under the age of eight use mobile phones. In his column in this issue, Jim Lin examines this advisory in light of two

studies done on the reaction time and cognitive functions of children. One study showed a slight improvement in reaction time after exposure to mobile-phone radiation, and the other did not note any effects. In neither study did the effects observed achieve statistical significance. All of this makes for very interesting reading.

Alexandre Vassilliev and Kevin Hughes have brought us an update of the activities and status of the International Telecommunications Union (ITU-R) Radiocommunication Study Group 7. SG7 deals with "science services," including standard frequency and time signals, space research, space operation, remote sensing using Earth exploration satellites, meteorological satellites, meteorological aids, and radio astronomy. These are all primary areas of interest for URSI, and this report on SG7's activities is thus most welcome.

While this March issue of the *Radio Science Bulletin* will go to the printer perhaps a couple of weeks after March (still entirely my responsibility), it was close to being produced in March. Furthermore, I am back to my normal level of editing with this issue. Hopefully, we are thus back on schedule, and will remain so for future issues. I appreciate your patience in all of this.

We do have space available in future issues for your contributions. I hope you will consider sharing the results of your work with the URSI radio science community through the pages of this *Bulletin*.

W. Ross Stone

Letter to the Editor

Closure of the UK Ionosondes at Chilton and Port Stanley

This letter is intended to alert our users and the scientific community to the decision of the UK's Particle Physics and Astronomy Research Council (PPARC) to withdraw all funding from the UK ionosondes program. This will mean the closure of the ionospheric monitoring stations at Chilton in the UK and at Port Stanley in the Falkland Islands within the next six months.

The Chilton ionosonde continues the data series begun at Slough in 1931 and has just celebrated 75 years of regular soundings of the ionosphere, the longest sequence of ionospheric data anywhere in the world. The Port Stanley ionosonde has been taking data since 1945, making it one of the longest time series of ionospheric data anywhere in the southern hemisphere.

Closure of the Chilton and Port Stanley ionosondes will cut off long-term data series and leave crucial gaps in coverage at the north-western edge of Europe and in the South Atlantic. This would be a significant loss to ionospheric, solar-terrestrial, upper atmosphere, and radio science.

If you wish to express your concern about these closures, I suggest you write to the contact at PPARC given below. Please copy any letters to me. I would also welcome suggestions and support in finding alternative funding sources, to maintain these facilities.

Also included below is a brief summary of some of the key issues about the Chilton and Port Stanley ionosondes. You may wish to elaborate on those points most important to your own area of interest in your comments to PPARC.

Many thanks in advance for your support,

Sarah James
Head of Ionospheric Monitoring at RAL

Please send letters or e-mails to the following: Sue Horne (sue.horne@pparc.ac.uk), Particle Physics and Astronomy Research Council, Polaris House, North Star Avenue, Swindon SN2 1ET UK;

and copy to:

Sarah James (s.f.james@rl.ac.uk), Ionospheric Monitoring Group, Rutherford Appleton Laboratory, Chilton, Didcot OX11 0QX UK.

Continued on page 12

Wireless MIMO Communications - Waves, Scattering, and System Design

C.F. Mecklenbräuker
H. Hofstetter

Abstract

A wireless multiple-input multiple-output (MIMO) communications transceiver is a promising candidate for next generation wireless systems. It can enhance the capacity and reliability of the communication link. MIMO is enabled by the presence of multiple transmitting antennas and multiple receiving antennas in the communication link. The benefits of MIMO communication are obtained through a combination of antenna arrays, signal processing, and coding algorithms, which adapt the link to the changing channel. In this critical review paper, a propagation-oriented viewpoint is adopted to discuss wireless MIMO. We give an overview of current research areas and discuss some open problems.

1. Introduction

Recently, the use of multiple antennas at both ends of the communication link has been found to enable a dramatic boost in wireless channel capacity, even for fixed available signal bandwidth [1, 2, 3, 4]. Multiple antennas provide a vector-valued interface to the radio channel. The field of research that studies communications over general vector channels has come to be known as MIMO communications.

The MIMO communications field has become one of the most active research segments in wireless communications [5, 6, 7]. The first standards incorporating MIMO technology have already been defined. Despite the significant research efforts on MIMO communications, numerous problems related to performance limits, code design, and receiver design remain to be solved.

In MIMO communication systems, two signaling schemes are considered to be of fundamental importance: *spatial multiplexing* and *exploiting spatial diversity*. The former aims at increasing the data rate, whereas the latter targets an increase in link reliability. In short, the former multiplexes independent data streams to multiple transmit antennas, thereby increasing the data rate. On the other hand, the use of *spatial diversity* increases the number of spatial degrees of freedom of the fading channel to decrease the outage probability.

From a systems-engineering viewpoint, the *scalability* of data rates and link reliability are of primary interest. Therefore, the choice of the MIMO signaling scheme in a real-world system must be able to trade off data rate against link reliability in a flexible manner. It is therefore desirable to flexibly allocate the channel's degrees of freedom in space and time to multiplexing and diversity schemes.

Though not critical for single-input single-output (SISO) channels, channel estimation can be a major obstacle on MIMO channels for the following reason. The number of parameters to be estimated to characterize a general linear MIMO channel with T inputs (transmitting antennas), R outputs (receiving antennas), and L non-zero taps of the matrix-valued impulse response is RTL.

Having in mind boosting the capacity of cellular mobile radio systems by installing antenna arrays in both handsets and base stations, the considerations given above seem discouraging, or at least seem to limit the number of antennas that may contribute to a significant benefit. Fortunately, the radio-propagation channel, with antenna arrays at both ends of the link, is not a fully general MIMO fading channel. In contrast, the channel within one coherence interval does not necessarily need to be characterized by an RTL-dimensional vector state. This is due to dependencies among the matrix entries of the MIMO impulse response, created by the geometry of the arrays and the locations of the scattering objects. Moreover, there are actually different scales of channel coherence. One is the small-scale coherence time, which is determined by the time either the transmitter

---

Christoph F. Mecklenbräuker and Helmut Hofstetter are with ftw. Forschungszentrum Telekommunikation Wien, A-1220 Wien (Vienna), Austria;
E-mail: cfm@ftw.at, hofstetter@ftw.at.

This is one of the invited Commission C *Reviews of Radio Science*.

or the receiver needs to travel distances on the scale of wavelengths to account for independent Rayleigh fading. Further, a larger-scale coherence time is determined by the time required for changing the scattering environment, i.e., to travel distances comparable to the size of the scattering objects. Admittedly, both time scales can be similar for propagation in indoor environments. However, outdoors they may differ significantly.

This paper is devoted to discussing the structure that is inherent in the antenna-array channel. As such, the results are applicable to channels where the assumed structure holds, but are not applicable for arbitrary MIMO fading channels.

We briefly mention that Hanlen and Fu [8] proposed a volumetric approach to spatial diversity. They introduced an (unspecified) set of basis functions for defining *connection strengths* between the receiving (Rx) and transmitting (Tx) array volumes.

2. Scattering

The physical theory of wave scattering provides a starting point for understanding the structure of the MIMO mobile-radio fading channel. In the Introduction, it was described that the unstructured fading channel possesses *RTL* degrees of freedom.

In this paper, a physically motivated structure is imposed on the MIMO mobile radio channel that allows reducing the number of degrees of freedom to significantly below *RTL*. Hence, less pilot symbols will be required for estimating the state of such a constrained channel.

Physical insight into the propagation and scattering that account for the structure of the matrix-valued impulse response is obtained by the association of departure and arrival angles [9]. First, the linear time-invariant case is studied. A probabilistic model for the faded channel-transfer matrix, $\mathbf{H}(w)$, is given by the stochastic integral

$$\mathbf{H} = \int_{\vec{r}\in R^3} \int_{\vec{r}'\in R^3} \mathbf{a}(\vec{r})\, d(\vec{r},\vec{r}')\, \mathbf{b}(\vec{r}')\, dN(\vec{r})\, dN(\vec{r}') . \quad (1)$$

Here, the column vector $\mathbf{a} \in C^{R\times 1}$ describes the receiver array response to a wavefront scattered by an object at location $\vec{r}$. Similarly, the row vector $\mathbf{b} \in C^{1\times T}$ describes the weighting coefficients of the transmitting array elements such that the elemental wavefronts interfere at location $\vec{r}'$. In short, the vectors $\mathbf{a}$, $\mathbf{b}$ describe the complex-valued coupling of the receiving and transmitting array elements to a scattering object at location $\vec{r}$. It is further assumed that the scattering objects are located in the far field of both antenna arrays. The vectors $\mathbf{a}$, $\mathbf{b}$ become plane-wave steering vectors, which can be described by the direction of arrival and direction of departure, respectively. The quantity $d(\vec{r},\vec{r}')$ describes the complex propagator, which links the scattering objects at locations $\vec{r}$ and $\vec{r}'$. If we assume that the wave propagation is reciprocal, the complex propagator, $d(\vec{r},\vec{r}')$, in Equation (1) is a symmetric function of its arguments (not conjugate-symmetric). Due to multipath effects among the scatterers, the function $d(\vec{r},\vec{r}')$ fluctuates on a fast time scale [10]. For the purposes of this paper, $d(\vec{r},\vec{r}')$ is modeled as a random field. A graphical representation of the propagation and scattering model is shown in Figure 1.

Furthermore, the stochastic process, $N(\vec{r})$, is assumed to be a Poisson counting process, which describes the distribution of scatterers in space. For example, the stochastic integral $\int_{\vec{r}\in V} dN(\vec{r})$ gives the count of scatterers in the volume *V*. The counting process $N(\vec{r})$ is non-stationary, but its increments $dN(\vec{r})$ possess the properties of a stationary process.

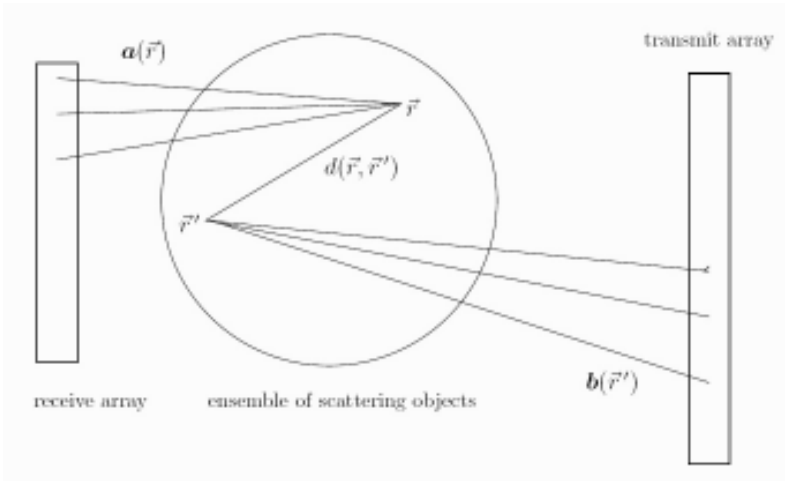

Figure 1. A schematic view of the MIMO channel with scattering objects.

Thus, $N(\vec{r})$ is conveniently characterized by the first- and second-order moments of its increments:

$$E\left[dN(\vec{r})\right] = c(\vec{r})d^3r,$$

$$E\left[dN(\vec{r})dN(\vec{r}')\right] = C(\vec{r})\delta(\vec{r}-\vec{r}')d^3r d^3r',$$

where d^3r denotes the volume element at location $\vec{r}$. Hence, $c(\vec{r})$ describes the expected volume scatterer count density. From the second moment, it is seen that the increments $dN(\vec{r})$ and $dN(\vec{r})$ are orthogonal for $\vec{r} \neq \vec{r}'$. The realizations of the increments are zero in all volumes without scattering objects: contributions to the stochastic integral of Equation (1) occur only at the locations of scattering objects. If the stochastic integral, Equation (1), is conditioned on the count of scattering objects *S*, cf. [11], it becomes a finite sum, so that

$$\mathbf{H} = \sum_{k=1}^{S}\sum_{l=1}^{S}\mathbf{a}(\vec{r}_k)d(\vec{r}_k,\vec{r}_l')\mathbf{b}(\vec{r}_l'), \qquad (2)$$

where the locations $\vec{r}_k, \vec{r}_l\ (k,l = 1,\ldots,S)$ are random variables.

2.1 The MIMO Mobile Radio Channel

Wave-propagation effects, like reflections, diffraction, scattering, refraction, and shadowing, result in multipath propagation scenarios. Each single path has a specific delay corresponding to its path length, is attenuated according to the propagation effects, and propagates into certain directions. Summed up, the channel becomes time dispersive and frequency selective.

Waves propagated from the transmitter are reflected by the cladding of buildings, scattered by trees, and diffracted around corners. Each interaction of the wave with its surrounding results in a new point source in space, spreading energy into certain directions. The scattering process is first investigated in more detail, and is then extended to all other propagation effects.

The finite size and typically rough surface of a scattering object yields a whole set of point sources per object. This set of point sources is called a cluster:

A cluster is a set of multipath components that is grouped together resulting in the same delay, direction of arrival (DoA), and direction of departure (DoD) statistics.

This definition is not limited to scattering processes themselves. The term *scattering* is often misused in the literature. Often, all propagation mechanisms are classified as scattering, since there is no clear separation. In [12], natural surface scattering is discussed, and a model for describing the scattering process is introduced. Measurements show that for natural surfaces, a combination of reflections and scattering occurs. Reflections are only visible at certain angles, while scattering propagates into all directions. Taking a rough surface yields specular reflections into variable directions. For channel modeling, this complex behavior is reduced to scattering objects that radiate into several directions with a certain power level [13].

In [14], the scattering process, including rough-surface scattering, is discussed in more detail. The results can be used to improve the model by adding backscattering diagrams to each scatterer. The backscattering diagram can be interpreted as an antenna pattern for each scatterer. This approach can be interpreted as replacing the dipole elements by arbitrary antenna elements. However, this idea increases the model complexity quite considerably, and is therefore not taken into account by most channel models.

The coexistence of scattering and specular reflections was discussed above. Similar arguments can be given to include diffraction and refraction. This results in clusters with a certain angular-delay power spectrum (ADPS) [15, 16]. A cluster can be characterized by its delay spread and by angular spreads in azimuth and elevation. Thus, spreads depend on the propagation mechanism. Reflections result in small and well-defined clusters in space, whereas scattering processes tend toward large clusters. Measurement results [17] show such sets of clusters in space. In [18], a new notation was introduced, talking more precisely about multipath components (MPCs), instead of scatterers. A multipath component describes a single propagation path from the transmitter to the receiver. The sum of all multipath components describes the propagation scenario. The total double-directional impulse responses (DDIR) can be written as the sum of the cluster double-directional impulse responses,

$$\mathbf{H} = \sum_{m=1}^{Cl}\sum_{n=1}^{Cl}\mathbf{H}_{m,n}$$

$$= \sum_{m=1}^{Cl}\sum_{n=1}^{Cl}\sum_{k=1}^{S_{Cl}}\sum_{l=1}^{S_{Cl}}\mathbf{a}_m(\vec{r}_k)d_{m,n}(\vec{r}_k,\vec{r}_l')\mathbf{b}_n(\vec{r}_l'), \qquad (3)$$

where *Cl* denotes the number of clusters, and S_{Cl} is the number of scatterers per cluster. If only one cluster at the base station (BS) couples exactly into one cluster at the mobile station (MS), $d_{m,n}(\vec{r}_k,\vec{r}_l')$ becomes block diagonal. If each scatterer at the base station couples into only one scatterer at the mobile station, *d* is a diagonal matrix. At first sight, this looks like a typical Kronecker model, but since there are no restrictions on the angles of the paths, paths with the same directions of departure may couple into different directions of arrivals.

A very popular description of the channel matrix is formulated in the delay-angular domain, describing not the scatterers themselves but each path by its directions of departure, directions of arrival, and delay, as

$$\mathbf{H} = \sum_{p=1}^{Cl} \sum_{s=1}^{S_{Cl}} \mathbf{H}_{p,s,\tau}(\tau)\mathbf{H}_{p,s,\theta}(\theta)$$

$$\mathbf{H}_{p,s,\varphi}(\varphi)\mathbf{H}_{p,s,\theta'}(\theta')\mathbf{H}_{p,s,\varphi'}(\varphi') \cdot \qquad (4)$$

θ and φ denote the angles in azimuth and elevation. The primed angles denote the directions at the mobile station, while the unprimed angles indicate the angles at the base station. Note that this model assumes independent delay and angular statistics within one cluster. A refinement of the model is given in [19], where the angular statistics at the mobile station depend on the cluster delay, so that

$$\mathbf{H} = \sum_{p=1}^{Cl} \sum_{s=1}^{S_{Cl}} \mathbf{H}_{p,s,\tau}(\tau)\mathbf{H}_{p,s,\theta}(\theta)$$

$$\mathbf{H}_{p,s,\varphi}(\varphi)\mathbf{H}_{p,s,\theta'}(\theta',\tau)\mathbf{H}_{p,s,\varphi'}(\varphi',\tau)$$

The two approaches described in Equations (3) and (4) are equivalent, and can be transformed into each other. Equation (4) directly reflects the measured statistics, whereas Equation (3) is commonly used for channel modeling, cf. [20, 21].

2.2 Antenna Arrays and Polarization

The discussion above makes no assumptions regarding the transmitting and receiving antennas. It can be seen as a case using isotropic antenna elements without any coupling and a single polarization. Polarization effects are gaining more and more interest for system design. Using dual-polarized antenna elements results in more or less uncorrelated received signals [22], while keeping the receiving unit small. This is very important for small mobile devices. To gain more information on the polarization behavior of the radio channel, antenna arrays using dual-polarized antenna elements were designed for channel-sounder measurements. In [23], an antenna array looking like a football was described that allowed dual-polarized measurements. Using such spherical antenna designs allows for the investigation of propagation effects in azimuth and elevation. In [24], other dual-polarized antenna arrays were discussed. All these arrays were designed for measurement purposes. Their major goal was to allow a detailed characterization of the air interface. Therefore, up to 64 antenna elements [25] were used for one array. For example, dual-polarized antennas for mobile devices were shown in [26, 27]. A cubic antenna array, exploiting space and a combination of polarization and pattern diversity, was discussed in [28].

To include polarization to the model, let us first assume that the transmitter emits only vertically polarized components. The multipath components interact at the scattering objects and become attenuated and depolarized. Depolarization can be described using the well-known cross-polarization discrimination (XPD) coefficient,

$$XPD = \frac{P_{VV} + P_{HH}}{P_{VH} + P_{HV}},$$

where P_{VV} denotes the power of the vertically co-polarized components and P_{VH} is the power in the cross-polarized components from vertical polarization to horizontal polarization. Investigations in [29] and [30] showed that the *XPD* coefficient depends on the distance between the transmitter and receiver, as well as on the delay and the angles of the multipath components. However, those results were insufficient to give a general parameterization relationship, and are therefore not taken into account. We assume that vertical and horizontal components of the received field have uncorrelated small-scale fading because of different propagation paths. One way of modeling uncorrelated small-scale fading is to use the same multipath components but to add random phases to each path for cross polarization. Equation (2) can thus be rewritten for the polarization case as

$$\mathbf{H}_V = \sum_{k=1}^{S} \sum_{l=1}^{S} \mathbf{a}_V(\vec{r}_k)\, d(\vec{r}_k, \vec{r}_l)\, \mathbf{b}_V(\vec{r}_l)$$

$$+\mathbf{a}_H(\vec{r}_k)\, XPD_{VH}\, e^{-j\phi_{VH}(\vec{r}_k,\vec{r}_l)}\, d(\vec{r}_k, \vec{r}_l)\, \mathbf{b}_V(\vec{r}_l),$$

where $\mathbf{H}_V$ denotes the vertically polarized part of the impulse response, XPD_{VH} is the power factor of the cross-polarized component, $\phi_{VH}(\vec{r}_k, \vec{r}_l)$ denotes a random phase coefficient for each multipath component, and $\mathbf{a}_{V/H}$ denotes the vertically/horizontally polarized transmitted signal, respectively. Note that the position vectors, $\vec{r}_k, \vec{r}_l$, are deterministic, but a random phase is added to the cross-polarized component to ensure that the small-scale statistics are independent. Adding horizontally polarized components to the transmitted signal is now straightforward. The impulse response is then given by the sum of the two polarized components.

Not only are scattering objects new point sources in space, but also are all antenna elements. This results in the well-known coupling between the elements of the array. The end-to-end impulse response, $\mathbf{H}_C$, which includes the antenna coupling, is given by

$$\mathbf{H}_C = \mathbf{C}_{Rx}\mathbf{H}\mathbf{C}_{Tx} ,$$

where $\mathbf{C}_{Rx}, \mathbf{C}_{Tx}$ denote the array coupling matrices [31] at the receiver and transmitter sides, respectively.

Using real-world antenna elements with non-isotropic antenna patterns yields a weighting of the propagation paths according to their steering vectors. Equation (3) can be redefined by introducing the antenna patterns, $p_{Tx}(\vec{r}_l)$ and $p_{Rx}(\vec{r}_k)$, for the transmitting and receiving elements, resulting in

$$\mathbf{H} = \sum_{k=1}^{S}\sum_{l=1}^{S} p_{Rx}(\vec{r}_k)\mathbf{a}(\vec{r}_k)d\left(\vec{r}_k, \vec{r}_l'\right)\mathbf{b}\left(\vec{r}_l'\right)p_{Tx}(\vec{r}_l).$$

3. System Design

3.1 Transmitter-Side Processing

3.1.1 Space-Time Codes

First, we consider the case when the transmitter lacks channel knowledge. Code-construction criteria that extract diversity gain and coding gain were given in [4]. Two families of codes can be distinguished: space-time block codes and space-time trellis codes. Thorough discussions of capacity issues and the performance of specific codes can be found in [5, 6, 32]. Historically, the excitement that space-time block codes raised in the research community started with orthogonal and unitary designs, upon the realization that such codes allow for linear receivers showing the performance of maximum-likelihood decoders. Subsequently, it was realized that strictly orthogonal/unitary codes sacrifice data rate beyond economic constraints when more than two transmitting antennas are used. This started the research interest in so-called quasi-orthogonal space-time codes. If the underlying modulation scheme is based on orthogonal frequency-division multiplexing (OFDM), space-frequency codes are more apt than space-time codes.

If, on the other hand, some channel knowledge is available at the transmitter, then the code designer may choose among a large number of transmitter processing schemes. The choice of scheme depends largely on the acceptable tradeoffs among data rate, link reliability, and fairness, if several users share a common MIMO channel.

3.1.2 Water-Filling

If channel-state information is available at the transmitter site, it can be utilized in order to improve the supported information rate. For perfect channel-state information, this is known as the *water-filling principle* [5]. According to this principle, the transmitter signals only through the channel's eigenmodes. The transmitter allocates more power to an eigenmode the higher is its gain. The naming of this strategy is derived from the optimum power-assignment strategy, which can be interpreted in analogy to pouring water into valleys.

If the channel-state information is only partially known to the transmitter, the optimum power-allocation scheme is generally unknown. However, this is the situation in communication via antenna arrays. Two time scales are acting on the fading in such a way that the small-scale fading is too fast to be made available to the transmitter via a feedback channel, but the directions of arrival and the directions of departure are varying slowly enough to justify the assumption that they are known to the transmitter.

3.1.3 Spatial Multiplexing

A simplistic form of space-time code is created when the symbol stream is multiplexed to the individual transmitting antenna elements. This is called spatial multiplexing. Several variants were investigated in the literature, and have become known as vertical, horizontal, or diagonal encoding schemes [5]. In vertical encoding, the (temporally encoded) symbol stream is de-multiplexed into several streams to be transmitted over the antennas. This form of encoding can reach channel capacity, because each information bit can be spread across all antennas. Vertical encoding requires sophisticated receiver types, and the associated signal processing and decoding can be demanding.

3.2 Receiver-Side Processing

In the frequency domain, we have the usual vector channel model for observations $\mathbf{X}(\omega)$, with additive noise, $\mathbf{N}(\omega)$, and transmitted signal, $\mathbf{S}(\omega)$:

$$\mathbf{X}(\omega) = \mathbf{H}(\omega)\mathbf{S}(\omega) + \mathbf{N}(\omega).$$

The random channel matrix from Equation (2) can be written concisely as

$$\mathbf{H}(\omega) = \mathbf{A}(\omega)\mathbf{D}(\omega)\mathbf{B}(\omega),$$

where the matrix $\mathbf{B}(\omega)$ describes the propagation of the transmitted signal to the scattering objects, the matrix $\mathbf{D}(\omega)$ models the coupling between scattering objects as well as any complex attenuation, and the matrix $\mathbf{A}(\omega)$ describes the propagation from the scattering objects to the receiver array.

3.2.1 Channel Estimation

Let us now look in greater detail at the structure of these matrices. For ease of notation, let us also drop the

dependency on frequency, as all the following consideration can be straightforwardly generalized to the frequency-selective case. Let S denote the number of scattering objects. Then, the matrix $\mathbf{B}(\omega)$ has size $S \times T$. However, it does not exhibit ST degrees of freedom, as it is completely determined by the optical distances, R_{st}/λ, between the locations of individual transmitting antenna elements and the locations of the scattering objects. It becomes

$$\left[\mathbf{B}(\omega)\right]_{st} = \frac{\exp\left[j\frac{2\pi}{\lambda} R_{st} \right]}{4\pi R_{st}}.$$

Actually, its number of degrees of freedom has an upper bound of $S+T$. An analogous argument yields the fact that an upper bound on the number of degrees of freedom of the matrix $\mathbf{A}(\omega)$ is $S+R$. Things are more complicated for the matrix $\mathbf{D}(\omega)$. Theoretically, the $S \times S$ matrix $\mathbf{D}(\omega)$ could be arbitrary. Physical constraints, however, ensure that it is a sparse matrix. Without multi-fold scattering, it is even diagonal. In any case, its number of degrees of freedom is also significantly less than S^2.

Let ξ_A, ξ_D, ξ_B be the unknown state vectors that characterize the channel matrices **A**, **D**, **B**, respectively. We have assumed

$$\dim \xi_A \le S+R,$$

$$\dim \xi_D \le S^2,$$

$$\dim \xi_B \le S+T \cdot$$

If we identified the $S+T+R$ parameters that uniquely determine the matrices **A** and **B**, the channel-estimation problem would reduce to the estimation of the sparse (or diagonal) matrix **D**.

Note that some of these parameters are geometrical in nature (e.g., angles of arrival), which do not depend strongly on frequency. For simplicity, it is assumed that ξ_A and ξ_B contain angular parameters that do not depend on frequency. The fluctuations in ξ_D, however, cannot be neglected among the frequencies of interest. This idealization of the channel takes into account the fact that the various channel parameters fluctuate on quite different time scales [21].

Assuming that there is no multi-fold scattering –i.e., the matrix **D** is diagonal – this would simplify the channel-estimation problem to estimating the S diagonal elements of **D**. If S is of the same order of magnitude as the number of antennas, the problem of channel estimation for MIMO antenna arrays is reduced to the order of channel estimation on SISO channels. The key tool to realize the latter promise is the availability of an algorithm that jointly estimates directions of arrival and directions of departure. Although such an algorithm has been reported in the literature [33], it relied on accurate estimation of the total channel matrix, **H**. Therefore, it does not simplify our original problem, which is to estimate **H**. Instead, we need an algorithm that does not require accurate estimation of the channel matrix, **H,** in order to jointly estimate directions of arrival and directions of departure.

3.1.4 Linear Equalization versus Joint Decoding

Currently, it seems that the number-crunching capabilities at the receiver side prohibit the implementation of maximum-likelihood receiver principles in the general case. The receiver-side baseband processing is more or less limited to linear reception (zero-forcing, linear minimum-mean-squared error equalizers) for reasons of numerical complexity. However, nonlinear approximations to maximum-likelihood receivers might be feasible. One example is the application of sphere decoding principles.

4. Open Issues

Currently, it is not well understood how the available diversity in the MIMO channel can be conveniently traded against available data rates with spatial multiplexing in practical realizations of transmitters and receivers.

We note that the diversity order and code gain of space-time codes translates into a space-time-code block-erasure ratio (BLER). However, the BLER translates into an average number of required retransmissions when some form of "Automatic Repeat reQuest" (ARQ) is employed. The average number of required retransmissions affects data output goodness at the medium access control (MAC) layer.

By sacrificing some diversity order of a space-time code, we can increase its data rate at the physical layer. However, we then increase outage and the average number of required retransmissions in ARQ. Thus, by *increasing* data rate in the physical layer, we might *decrease* the efficiency of the MAC layer.

Part of this lack of understanding stems from the fact that realistic models for MIMO channels are mathematically too complex when it comes to information-theoretic investigations. The major frontier in our understanding of MIMO techniques is the *joint optimization* of the physical, medium-access, and radio-link control sub-layers of a radio communications system. Design of multi-user MIMO techniques is of major importance to several standardization efforts (Third Generation cellular systems, IEEE 802.11n, WiMax, etc.), and a suitable cross-layer optimization is urgently required.

Little is known about the dynamics of channel quality and the "typical" rank of the channel matrix. This is important when the receiver side informs the transmitter side about observed channel qualities. Moreover, the behavior of realistic channels at high SNR differs substantially from (singular) worst-case models and from the simplistic/ optimistic stochastic models with independent identically distributed matrix elements.

If (partial) channel knowledge at the transmitter is to be exploited, the channel state vector needs to be quantized. We do not have analytical tools for evaluating the capacity if the channel state is known *approximately* at the transmitter.

In the case of a moving user, the MIMO channel becomes time-variant. In this case, such questions as how long some scatterer clusters are visible become very important. Furthermore, the changes of the channel eigenmodes over time are also not yet fully understood.

5. Acknowledgements

The authors would like to thank the Editor for inviting this contribution. This work was partly funded by Kplus through the projects C9 and I0 at Forschungszentrum Telekommunikation Wien (ftw.).

6. References

1. G. J. Foschini, "Layered Space-Time Architecture Wireless Communication in a Fading Environment When Using Multi-Element Antennas," *Bell Labs Technical Journal*, Autumn, 1996, pp. 41-59.
2. G. J. Foschini and M. J. Gans, "On Limits of Wireless Communications in a Fading Environment When Using Multiple Antennas," *Wireless Personal Communications*, **6**, 1998, pp. 311-335.
3. I.E. Telatar, "Capacity of Multi-Antenna Gaussian Channels," *European Transactions on Telecommunications*, **10**, 6, 1999, pp. 585-595, November.
4. V. Tarokh, N. Seshadri, and A. R. Calderbank, "Space-Time Codes for High Data Rate Wireless Communication: Performance Criterion and Code Construction," *IEEE Transactions on Information Theory*, **44**, 2, 1998, pp. 744-765.
5. A. J. Paulraj, D. A. Gore, R. U. Nabar, and H. Bölcskei, "An Overview of MIMO Communications – A Key to Gigabit Wireless," *Proceedings of the IEEE*, **92**, 2, 2004, pp. 198-218.
6. T. H. Liew, and L. Hanzo, "Space-Time Codes and Concatenated Channel Codes for Wireless Communications," *Proceedings of the IEEE*, **90**, 2, 2002, pp. 187-219.
7. S. N. Diggavi, N. Al-Dhahir, A. Stamoulis, and A. R. Calderbank, "Great Expectations: The Value of Spatial Diversity in Wireless Networks," *Proceedings of the IEEE*, **92**, 2, 2004, pp. 219-270.
8. L. W. Hanlen and M. Fu, "Wireless Communications Systems with Spatial Diversity: A Volumetric Approach," in *Proc. IEEE International Conference on Communications* (ICC), 2003, pp. 2673-2677.
9. M. Steinbauer, A. F. Molisch, and E. Bonek, "The Double-Directional Radio Channel," *IEEE Antennas and Propagation Magazine*, **43**, 4, 2001, pp. 51-63.
10. G. D. Durgin and T.S. Rappaport, "Theory of Multipath Shape Factors for Small-Scale Fading Wireless Channels," *IEEE Transactions on Antennas and Propagation*, **48**, 5, 2000, pp. 682-693.
11. R. Müller, "A Random Matrix Model of Communication via Antenna Arrays," *IEEE Transactions on Information Theory*, **48**, 9, 2002, pp. 2495-2506.
12. M. Pettersen, G. Stette, and J. Noll, "A Novel Approach to the Modelling of Natural Surface Scattering for 3D Channel Prediction," in Proc. *Vehicular Technology Conference 2001 Spring*, **1**, 2001, pp. 414-418.
13. J. Fuhl, A. F. Molisch, and E. Bonek, "Unified Channel Model for Mobile Radio Systems with Smart Antennas," *IEE Proceedings on Radar, Sonar and Navigation*, **145**, 1, 1998, pp. 32-41.
14. A. Ishimaru, "Wave Propagation and Scattering in Random Media and Rough Surfaces," *Proceedings of the IEEE*, **79**, 10, 1991, pp. 1359-1366.
15. J. Laurila, A.F. Molisch, and E. Bonek, "Influence of the Scatterer Distribution on Power Delay Profiles and Azimuthal Power Spectra of Mobile Radio," in Proc. ISSSTA'98, 1998, pp. 267-271, Sun City, South Africa, September.
16. H. Hofstetter, A. F. Molisch, and M. Steinbauer, "Implementation of a COST 259 Geometry Based Stochastic Channel Model for Macro- and Microcells," in *Proc. of the 4th European Personal Mobile Communications Conference (EPMCC 2001)*, Vienna, Austria, 20-22 February, 2001.
17. N. Czink, M. Herdin, H. Özcelik, and E. Bonek, "Number of Multipath Clusters in Indoor MIMO Propagation Environments," *Electronics Letters*, **40**, 23, 2004, pp. 1498-1499.
18. A. F. Molisch, H. Asplund, R. Heddergott, M. Steinbauer, and T. Zwick, "The COST 259 Directional Channel Model – I. Philosophy and General Aspects," *IEEE Transactions on Wireless Communications* (in press).
19. H. Asplund, A. F. Molisch, M. Steinbauer, and N. B. Mehta, "Clustering of Scatterers in Mobile Radio Channels – Evaluation and Modeling in the COST 259 Directional Channel Model," in Proc. *IEEE International Conference on Communications*, **2**, 28 April-2 May 2002.
20. Source: Ericsson, 3GPP Technical Specification Group, Radio Access Network, Working Group 4 (Radio), "Proposed Channel Models for Deployment Evaluation," TSG RAN WG4, Meeting #9, Bath, UK, **TSG R4#9 (99)818**, 1999, 7-10 December, available online at http://www.3gpp.org/ftp/tsg_ran/WG4_Radio/TSGR4_09/Docs/Zips/.
21. L. M. Correia (Ed.), *Wireless Flexible Personalised Communications*, Wiley, 2001.
22. J. J. A. Lempiainen and J. K. Laiho-Steffens, "The Performance of Polarization Diversity Schemes at a Base Station in Small/Micro Cells at 1800 MHz," *IEEE Transactions on Vehicular Technology*, **47**, 3, 1998, pp. 1087-1092.
23. K. Kalliola, H. Laitinen, L. Vaskelainen, and P. Vainikainen, "Directional 3D Real-Time Dual-Polarized Measurement of Wideband Mobile Radio Channel," in Proc. of the 16th *IEEE Instrumentation and Measurement Technology Conference* 1999 (IMTC/99), **1**, 1999, pp. 170-175, May.
24. S. Balling, M. Hein, M. Hennhöfer, G. Sommerkorn, R. Stephan, and R. Thomä, "Broadband Dual Polarized Antenna Arrays for Mobile Communication Applications," in Proc. of 33rd European Microwave Conference, Munich, Germany, 2003.
25. G. Sommerkorn, D. Hampicke, R. Klukas, A. Richter, A. Schneider, and R. Thomä, "Uniform Rectangular Antenna Array Design and Calibration Issues for 2-D ESPRIT Application," in Proc. of the 4th European Personal Mobile Communications Conference (EPMCC 2001), Vienna, Austria, 20-22 February, 2001.
26. J. Guterman, A. A. Moreira, and C. Peixeiro, "Two-Element Multi-Band Fractal PIFA for MIMO Applications in Small Size Terminals," in Proc. of the IEEE Antennas and Propagation Society International Symposium, Monterey, CA, USA, June 2004.

27.A. Pal, B. S. Lee, P. Rogers, G. Hilton, M. Beach, and A. Nix, "Effect of Antenna Element Properties and Array Orientation on Performance of MIMO Systems," in *Proc. 1st International Symposium on Wireless Communication Systems 2004*, pp. 120-124, September 2004.
28.B. N. Getu and J. Bach-Andersen, "The MIMO Cube – A Compact MIMO Antenna," *IEEE Transactions on Wireless Communications*, 4, 3, 2005, pp. 1136-1141, May.
29.K. Kalliola, K. Sulonen, H. Laitinen, O. Kivekas, J. Krogerus, and P. Vainikainen, "Angular Power Distribution and Mean Effective Gain of Mobile Antenna in Different Propagation Environments, *IEEE Transactions on Vehicular Technology*, **51**, 5, 2002, pp. 823-838.
30.M. Shafi, M. Zhang, A. L. Moustakas, P. J. Smith, A. F. Molisch, F. Tufvesson, and S. H. Simon, "Polarized MIMO Channels in 3D: Models, Measurements and Mutual Information," *IEEE Journal on Selected Areas in Communications*, Special issue on 4G, (submitted), 2005.
31.K. Pensel and J. A. Nossek, "*Uplink and Downlink Calibration of an Antenna Array in a Mobile Communication System*, 1997.
32.L. C. Godara, "Applications of Antenna Arrays to Mobile Communications, Part I: Performance Improvement, Feasibility, and System Considerations," *Proceedings of the IEEE*, **85**, 7, 1997, pp. 1031-1060
33.M. Steinbauer, D. Hampicke, G. Sommerkorn, A. Schneider, A. F. Molisch, and E. Bonek, "Array Measurement of the Double-Directional Mobile Radio Channel," in Proc. 50th IEEE Vehicular Technology Conference VTC'00, Tokyo, May 2000.

***Letter to the Editor**: Continued from page 4*

The Importance of the Chilton/ Slough and Port Stanley Ionospheric Data

The series of ionospheric measurements from Chilton/ Slough and Port Stanley are world leaders in length, quality, and consistency, making them uniquely valuable for studies of the long-term change of conditions in the upper atmosphere.

Their locations are important too, as Chilton data constrain, at the north-western edge, European efforts to predict and map ionospheric conditions. The ionosonde at Port Stanley is uniquely located in the South Atlantic, a region of particular interest due to the structure of the Earth's geomagnetic field, and the effect of global, atmospheric circulation patterns on the behavior of the ionosphere here.

The ionosondes' data are contributing to studies of long-term change in the upper atmosphere; to understanding the mechanisms by which solar variability could affect climate change on Earth; to the discovery of new mechanisms of energy transfer between the lower and upper atmosphere; to the understanding of planetary ionospheres in the rest of the Solar System; to the real-time monitoring and predictions of radio propagation conditions and space weather; and to the global, reciprocal exchange of geophysical data, without which a wide range of research in the UK would be damaged.

Statistics and EMC

S.A. Pignari

Abstract

In this paper, applications of statistics to electromagnetic-compatibility (EMC) investigations are reviewed. The description covers both prediction and experimental aspects, and includes well-established results as well as recently-developed models and techniques. The potential of using probabilistic and statistical modeling for EMC assessment is highlighted, especially where system complexity, partial unavailability of data, and randomness of electromagnetic interference play a role.

1. Introduction

Assessment of electromagnetic compatibility (EMC) requires identification of the dominant interference effects and understanding of the reasons that cause a system to be vulnerable. While in principle this can always be done by resorting to suitable experimental measurements, supplemented by deterministic modeling, system complexity often weakens or makes ineffective this classical approach to the interpretation and prediction of system EMC characteristics. As a matter of fact, even for a relatively simple system, incomplete knowledge and control of geometrical and electrical data, combined with the possibly parasitic nature of parameters involved in the coupling phenomena and with the inherent random nature of electromagnetic interference, make statistical approaches more attractive than deterministic modeling.

In general, probabilistic and statistical techniques have the potential of allowing for relating the precision and consistency of the system's predicted features to the amount and properties of available data. In contrast to deterministic modeling, probabilistic models (when applicable) do not become proportionally more complicated as the complexity of the system under analysis increases. Probabilistic models yield increasingly accurate results if this greater complexity arises from repetition of basic elements [1]. Additionally, statistical theory is intimately connected to instrumentation and measurements, which play a primary role in EMC assessment.

This article focuses on the main applications of statistics in EMC. The challenges related to using statistical theory in the framework of EMC assessment are highlighted. This is done by describing and discussing both well-established results and recent advances in the area of EMC probabilistic and statistical modeling. The topics addressed here include statistical characterization of electromagnetic interference (EMI), measurement uncertainty, additive-noise effects in time-domain EMI measurement systems, probabilistic and statistical modeling of crosstalk and radiated susceptibility of a wiring harness, and statistical approaches to system-level EMC assessment.

The important issue of the statistical characterization of the electromagnetic field in reverberation chambers is not considered here, since this topic has been already addressed in a recent paper published in the URSI *Radio Science Bulletin* [2].

2. Electromagnetic Interference

Different classifications of electromagnetic interference (EMI) can be given, depending on the selected criterion and objective. To the extent that the origin of the interference is the distinguishing element, natural and man-made interference are the two main categories into which EMI is typically subdivided. Alternatively, if the nature of the coupling phenomenon between the source and the victim of the interference is the crucial point, intentional or non-intentional EMI are the two possible alternatives [3].

From a mathematical viewpoint, and for the general aim of investigating degrading effects on electrical/electronic systems, an EMI environment can be modeled by resorting to the concept of a random process. For the investigation of the statistics of this process, the electromagnetic noise has been classified into three broad categories, based on the bandwidth of the interference with respect to the bandwidth of the receptor system [4]. Class A interference considers environments in which the spectrum of the offending electromagnetic disturbance is narrower than the receptor's bandwidth. Class B interference describes the case in which the bandwidth of the electromagnetic noise is larger than the bandwidth of the receptor. Class C interference consists of the superposition of the previous two classes.

Sergio A. Pignari is with the Politecnico di Milano, Dipartimento di Elettrotecnica, Piazza Leonardo da Vinci, 32, I-20133 Milano, Italy; Tel: +39-02-23993726; Fax: +39-02-23993703; E-mail: sergio.pignari@polimi.it.

This is one of the invited *Reviews of Radio Science* from Commission E.

According to this modeling approach, aimed at describing the global physical properties of EMI, statistical models were developed and closed-form expressions were derived in the 1970s for the envelope distribution of Class A and Class B interference [4-8]. In particular, for narrowband EMI (Class A), the result for the *a posteriori* probability distribution, P_A, is [4]

$$P_A\left(\varepsilon > \varepsilon_0\right) \equiv e^{-A_A} \sum_{m=0}^{\infty} \frac{A_A^m}{m!} e^{-\varepsilon_0^2/(2\hat{\sigma}_{mA}^2)}, \; 0 \le \varepsilon_0 < \infty, \tag{1}$$

where

$$\hat{\sigma}_{mA}^2 = \frac{m/A_A + \Gamma_A'}{2\left(1+\Gamma_A'\right)} \tag{2}$$

and

$$\varepsilon = \frac{E}{\sqrt{2\Omega_{2A}\left(1+\Gamma_A'\right)}}, \quad \varepsilon_0 = \frac{E_0}{\sqrt{2\Omega_{2A}\left(1+\Gamma_A'\right)}} \tag{3}$$

are normalized envelopes, E_0 being a pre-selected threshold value of the envelope, E. The probability P_A represents the exceedance probability, that is, the probability that at the receiver the instantaneous envelope exceeds some threshold, ε_0. The quantities A_A, Γ_A', and Ω_{2A} are the three global model parameters describing the emission events for Class A interference.

On the other hand, for wideband EMI (Class B), the *a posteriori* probability distribution, P_A, takes the form [4]

$$P_B\left(\varepsilon > \varepsilon_0\right) = \begin{cases} 1 - \hat{\varepsilon}_0^2 \displaystyle\sum_{n=0}^{\infty} \frac{(-1)^n \hat{A}^n}{n!} \Gamma\left(1+\frac{\alpha n}{2}\right) {}_1F_1\left(1+\frac{\alpha n}{2}; 2; -\hat{\varepsilon}_0^2\right), & 0 \le \varepsilon \le \varepsilon_B \\ \dfrac{e^{-A_B}}{4G_B^2} \displaystyle\sum_{m=0}^{\infty} \frac{A_B^m}{m!} e^{-\varepsilon_0^2/2\hat{\sigma}_{mB}^2}, & \varepsilon > \varepsilon_B \end{cases} \tag{4}$$

where

$$\hat{\sigma}_{mB}^2 = \frac{m/\hat{A}_B + \Gamma_B'}{2\left(1+\Gamma_B'\right)}, \; \hat{A}_B = \frac{2-\alpha}{4-\alpha} A_B \tag{5}$$

$$G_B^2 = \frac{1}{4\left(1+\Gamma_B'\right)}\left(\frac{4-\alpha}{2-\alpha} + \Gamma_B'\right) \tag{6}$$

and $\hat{A} = A_\alpha / \left(2G_B\right)^\alpha$, $\hat{\varepsilon}_0 = \left(\varepsilon_0 N_I\right)/\left(2G_B\right)$. The quantities A_α, α, A_B, Γ_B', Ω_{2B}, N_I, and Ω_{2A} are the six global model parameters describing the emission events for Class B interference.

The aforementioned statistical models provide a precise description of the general physical properties of a wide variety of electromagnetic disturbances. In particular, Class A interference describes the type of EMI often encountered in wireless applications, where the electromagnetic noise is often due to other communication systems. Conversely, Class B interference is typically associated with non-message-bearing noise, and it is highly impulsive [8]. These models have been successfully applied to the characterization of specific electromagnetic environments in the past decades. Selected examples are reported in the plots of Figures 1 and 2 (reproduced from Figures 2.2 and 2.4 of [4]), where the measured envelope distribution of electromagnetic noise due to different sources is compared with statistical predictions. Specifically,

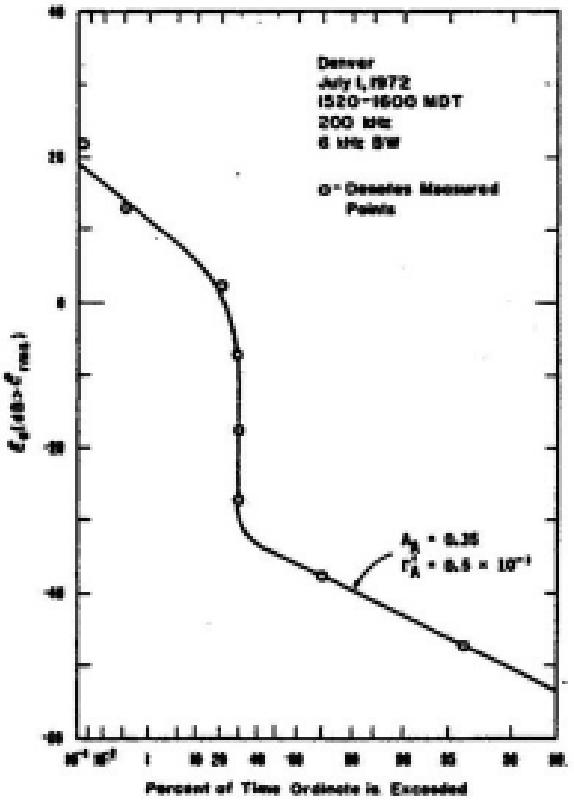

Figure 1. The a posteriori probability distribution of EMI due to a nearby power line (interference produced from equipment fed by the line): the Class A model versus measurement data. (Copyright ©1977 IEEE, reprinted with permission from D. Middleton, "Statistical-Physical Models of Electromagnetic Interference," *IEEE Transactions on Electromagnetic Compatibility*, **EMC-19**, 3, 1977, pp. 106-127.)

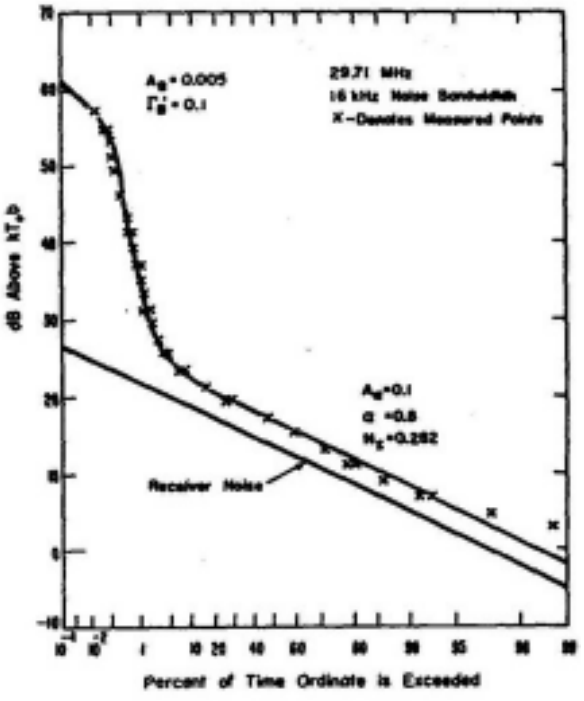

Figure 2. The a posteriori probability distribution of EMI due to automotive ignition noise from moving traffic: the Class B model versus measurement data. (Copyright ©1977 IEEE, reprinted with permission from D. Middleton, "Statistical-Physical Models of Electromagnetic Interference," IEEE Transactions on Electromagnetic Compatibility, ***EMC-19****, 3, 1977, pp. 106-127.)*

Figure 1 refers to Class A interference from a nearby power line, produced from equipment fed by the line; Figure 2 shows the case of Class B interference due to automotive ignition noise from moving traffic. It should be stressed that these statistical-physical models of EMI inherently account for the propagation and reception processes, and as a result are invariant with respect to the form and the occurrence of particular interference sources. That is, they are not specialized to individual noise mechanisms, source distributions, and emission waveforms. This modeling scheme has revealed that most man-made and natural electromagnetic noise is characterized by strongly non-Gaussian behavior [4-8] and, as such, it may have an impact on the performance of those systems in which electrical communications are designed for optimal performance in presence of Gaussian interference [4].

In recent years, the higher performance of today's measuring instrumentation and processing hardware has allowed the development of new procedures and setups for the experimental characterization of impulsive noise in wider frequency bands [9-12]. Results obtained for different electromagnetic environments (including EMI in hospitals [9], digital television channels [10], automotive ignition noise [11], and electromagnetic emissions due to microwave ovens [12]) have confirmed the general statistical properties of the analytical models derived in [4-8].

3. EMC Compliance Testing

3.1 Measurement Uncertainty

Another area of the application of statistics relates to testing for compliance. From the theoretical viewpoint, the use of statistics to characterize the overall uncertainty associated with an EMC measurement represents a necessary step for a statement of compliance. In general, statistical analysis is an important issue for the whole metrology area. However, as it relates to EMC testing, its relevance is even strengthened by aspects peculiar of this field. These include the numerous and sometimes large uncertainties in different parts of the measurement systems, and the EMC performance of the equipment under test (EUT) [13].

The targets of applying the basic principles of statistics to EMC testing are to estimate the measurement uncertainty, to give information on test repeatability and, therefore, to rank laboratories, measurement procedures, and setups from the viewpoint of measurement quality. In line with the aforementioned targets, normative documents were published in the 1990s by national and international committees working in the area of EMC [14-17]. These acknowledge the concept of measurement uncertainty as described in the *ISO Guide to the Expression of Uncertainty in Measurements* [18].

In general, measurement errors are composed of two contributions: random errors and systematic errors. Random errors are due to a number of sources, inherent in the measurement system, and reveal themselves as random fluctuations of subsequent observations. These measurement errors cannot be set to zero; however, statistics is a rigorous tool for characterizing them, and indicates how these errors are reduced by resorting to repeated measurements. Systematic errors are due to quantities that cause a systematic deviation (or bias) of the mean value of the measurement result. Even these errors, common in EMC measurement systems, cannot be eliminated. Nevertheless, a statistical description in terms of the mean value and standard deviation (i.e., systematic effects and superimposed fluctuations) permits finding suitable correction terms.

In short, the statistical description of an EMC measurement system requires identifying all the probable sources of error (the so-called "uncertainty budget"), the related probability distributions, and combining them in order to characterize the dispersion (i.e., the standard deviation) of the measurement values. As a result of this analysis, the system is attributed an overall uncertainty (the so-called "expanded uncertainty"), which represents an interval about the measured value that will encompass its true value with a specified confidence level [17].

There are statistical aspects worth noting in the estimation of the expanded uncertainty of an EMC measurement system. This is done in the following manner.

The overall uncertainty is specified in decibels, and this is obtained by combining uncertainties expressed in decibels. This originates from the fact that the quantity to be measured can often be written as a product of terms. From the statistical viewpoint, this brings up the normal and the lognormal probability density functions (pdfs) [19]. Another distinctive aspect is related to the characterization of the uncertainty associated with impedance mismatch. In EMC, this problem is typically encountered when a cable is connected to terminal devices with input impedances that do not exactly match the cable's characteristic impedance. In statistical terms, this phenomenon leads to the so-called "U-shaped" pdf [20, 21].

The first edition of the standards on EMC measurement uncertainty provided indications for the characterization of setups for the measurement of the principal EMI phenomena, and specified target measurement instrumentation uncertainty values. Within the last decade, those documents have been supplemented by new expanded versions, and by technical papers exploring details involved in the determination of uncertainty and providing characterization of specific setups. In particular, [22-27] contained investigations on the uncertainty in the measurement of radiated and conducted emissions, whereas [28] provided indications for the evaluation of the uncertainty budget of a setup for conducted susceptibility assessment via bulk current injection (BCI).

Although much has been done in the last decade to adapt the statistical approach – adopted in metrology measurements – to EMC compliance testing, the scientific community is still working to optimize the procedure for uncertainty estimation [29]. Essentially, the need for improvements arises from basic differences between EMC compliance testing and metrology measurements. One of the critical points in EMC is related to single or very limited executions of the measurement. As a matter of fact, carrying out repeated measurements is of primary importance to basic statistical considerations and, incidentally, this reduces the measurement uncertainty. However, the costs and economics of time often do not permit that. An extreme example in the area of transportation EMC concerns measurement of the emissions radiated to the outside world by rolling stock. In this case, the equipment under test is comprised of a train running along a railway line and the infrastructure. Repeated measurements are of paramount importance here in order to distinguish the contribution to emissions due to the train from EMI produced by the infrastructure and external noise sources. However, this clashes against very high costs due to train and railroad utilization. Another crucial aspect is that the statistics of some random parameters involved in the process of estimation of the overall uncertainty are often unknown [30]. Reproducibility – i.e., the ability to test the equipment under test at different labs – employing different operators and/or different instrumentation, and getting congruent results are also critical issues related to the partially non-deterministic EMC performance of the equipment under test when arranged in the setup foreseen by the standards [31].

3.2 Additive Noise Effects in Time-Domain EMI Measurement Systems

Over the above-discussed aspects, further challenging statistical issues in the field of EMC testing are those regarding novel procedures and setups. In this framework, an intriguing problem is the characterization of additive-noise effects in systems - recently introduced - for time-domain EMI measurements [32-33]. In these systems, the determination and reduction of noise effects is important for reliable estimation of interference levels and, consequently, to allow indisputable comparisons against threshold levels specified in the frequency domain by the regulatory agencies. In a time-domain EMI measurement system, additive noise is partly due to external environmental sources, and partly originates internally. The external noise is due to those electromagnetic emissions that are not intended to be measured, since they are not part of the interference phenomenon under investigation. This ambient noise may include white Gaussian noise (via the Central Limit Theorem [34]), as well as narrow-spectrum noise (e.g., message-bearing telecommunication signals). The spectral characteristics and the power, σ_{ext}^2, of the external noise can be determined by means of ad hoc measurements. On the other hand, internal noise is composed of electronic noise and quantization noise. The electronic noise (or thermal noise) is white and Gaussian. Its noise power, σ_e^2, is estimated by proper noise measurements, or deduced from the technical datasheets describing the units of the measurement system. Quantization noise is a further source of disturbance in high-speed data acquisition systems. It originates from the quantization process as a consequence of the fact that in practical analog-to-digital converters, high-frequency sampling and high resolution are contrasting requirements. Quantization is modeled as zero-mean white additive noise, uniformly distributed within the quantization step [35]. The quantization noise power, σ_q^2, is expressed in terms of the number of bits, b, and the full-scale value, FS, of an analog-to-digital converter with range equal to $2FS$:

$$\sigma_q^2 = \frac{FS^2}{3\left(2^{2b}\right)}. \qquad (7)$$

The total noise variance, σ_N^2, characterizing a time-domain EMI measurement system is therefore given by the sum of the variances of the external noise , σ_{ext}^2, the electronic noise, σ_e^2, and the quantization noise, σ_q^2, i.e.,

$$\sigma_N^2 = \sigma_{ext}^2 + \sigma_e^2 + \sigma_q^2. \qquad (8)$$

3.3 Radiated Emissions and Safety Assessment

In order to assess compliance with the limits, EMI measured in the time domain is translated into the frequency domain via the discrete Fourier transformation (DFT). Consequently, a statistical description of the measured emission levels in the frequency domain requires the analysis of noise propagation and transformation due to digital signal processing of the measured time series. This is especially important for systems designed for the measurement of non-stationary EMI, for which averaging techniques cannot be exploited.

An example of this kind of analysis can be found in [36], where a system for the measurement of radiated emissions was analyzed. Here, the system was designed to measure non-stationary magnetic-flux-density (MFD) radiated emissions, in order to assess safety conditions, i.e., to evaluate exposure levels via estimation of a safety parameter [37]. The statistical model was based on the representation of the spectral lines of the DFT of the measured field components in terms of random variables (RVs). In particular, by introducing the random variable

$$X_m = \frac{B_m^2}{\sigma_{DFT}^2} = \frac{B_{x,m}^2 + B_{y,m}^2 + B_{z,m}^2}{\sigma_{DFT}^2},\ m = 1,...,M \quad (9)$$

with $B_{x,m}$, $B_{y,m}$, $B_{z,m}$ being the amplitudes of the mth spectral lines of the three spatial components of the magnetic-flux-density vector, and σ_{DFT}^2 being the noise variance associated with the real (or imaginary) part of these three spectral components, it was shown that X_m is a non-central chi-squared random variable $\chi^2\left[\nu,\left(\delta_m/\sigma_{DFT}\right)^2\right]$ with $\nu = 6$ degrees of freedom and non-centrality parameter $\left(\delta_m/\sigma_{DFT}\right)^2$, i.e.,

$$f_{X_m}(X_m) = \frac{1}{8}\exp\left\{-\left[X_m + \left(\delta_m/\sigma_{DFT}\right)^2\right]/2\right\}\sum_{n=0}^{\infty}\frac{X_m^{n+2}\left(\delta_m/\sigma_{DFT}\right)^{2n}}{\Gamma(n+3)2^{2n}n!} \quad (10)$$

where δ_m represents the true amplitude of the magnetic-flux-density vector at the frequency under analysis, and σ_{DFT}^2 is a function of the total noise, σ_N^2, characterizing the measurement system. The measured amplitude of the magnetic-flux-density vector, normalized to σ_{DFT}, was obtained as $Y_m = \sqrt{X_m}$, and was characterized by the pdf

$$f_{Y_m}(Y_m) = 2Y_m f_{X_m}\left(Y_m^2\right),\ Y_m \geq 0. \quad (11)$$

The following analytical approximate expressions for the mean value, μ_{Y_m}, and the variance, $\sigma_{Y_m}^2$, of Y_m were obtained:

$$\mu_{Y_m} \cong \sqrt{6+\left(\delta_m/\sigma_{DFT}\right)^2} - \frac{3+\left(\delta_m/\sigma_{DFT}\right)^2}{2\left[6+\left(\delta_m/\sigma_{DFT}\right)^2\right]^{3/2}}, \quad (12)$$

$$\sigma_{Y_m}^2 \cong \frac{3+\left(\delta_m/\sigma_{DFT}\right)^2}{6+\left(\delta_m/\sigma_{DFT}\right)^2}. \quad (13)$$

Figure 3 reports plots of the pdf of Y_m for different values of the ratio δ_m/σ_{DFT}. The case $\delta_m/\sigma_{DFT} = 0$ refers to spectral lines due exclusively to noise.

Accordingly, the safety-parameter, I_B, defined as [37]

$$I_B = \frac{1}{\sqrt{2}}\sum_{m=1}^{M}\frac{B_m}{B_{L,m}}, \quad (14)$$

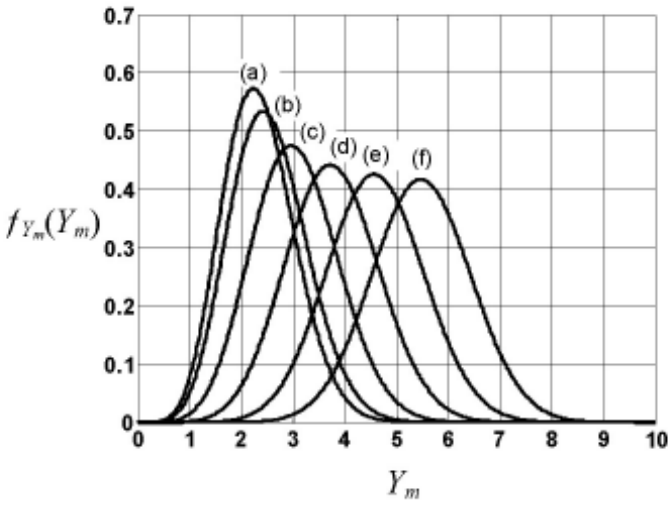

Figure 3. The pdf of the random variable Y_m for different values of the parameter δ_m/σ_{DFT}. The curves labeled (a), (b), ..., (f) correspond to $\delta_m/\sigma_{DFT} = 0,1,\ldots,5$, respectively.

where $B_{L,m}$ are frequency-dependent reference levels, is treated as a random variable, and the following approximate expressions for the mean value, $E\{I_B\}$, and the variance, $Var\{I_B\}$, were derived:

$$E\{I_B\} \cong \frac{\sigma_{DFT}}{\sqrt{2}} \sum_{m=1}^{M} \frac{1}{B_{L,m}} \left[\sqrt{6 + (\delta_m/\sigma_{DFT})^2} - \frac{3 + (\delta_m/\sigma_{DFT})^2}{2\left[6 + (\delta_m/\sigma_{DFT})^2\right]^{3/2}} \right], \quad (15)$$

$$Var\{I_B\} \cong \frac{1}{2}\sigma_{DFT}^2 \sum_{m=1}^{M} \frac{1}{B_{L,m}^2} \frac{3 + (\delta_m/\sigma_{DFT})^2}{6 + (\delta_m/\sigma_{DFT})^2}. \quad (16)$$

Knowledge of the statistics of I_B allowed locating a confidence interval around the measured value. This interval gave an estimated range of values that was likely to include (according to a specified probability) the true value of I_B. In practice, due to the non-stationary nature of the emissions, I_B is a function of time, i.e., $I_B = I_B(t)$, and safety requirements are fulfilled if $I_B(t)$ is less than or equal to one at any time instant in the observation period.

4. Wiring Structures

The development of prediction models for interference effects due to electromagnetic coupling in electrical and electronic subsystems is complicated by the presence of several unknown and uncontrolled parameters. As far as a wiring harness is considered, this modeling problem is especially pronounced. In the analysis of crosstalk, the matter originates from the fact that the relative positions of wires in wire bundles are typically unknown, and vary in an uncontrolled fashion along the bundle's length. From the standpoint of radiated susceptibility, the problem is even more complicated due to the inherent random nature of the interfering electromagnetic field.

4.1 Crosstalk

4.1.1 Circuit Models

Sensitivity of crosstalk to fluctuations of the bundle's cross section was firstly observed in [38-40] from the analysis of experimental data. In particular, in [38] it was pointed out that the sensitivity of unintentional coupling between wires in bundles is a function of the terminal impedances and, depending on the loads, the sensitivity may be sizable or slight. In [39-40], the statistics of crosstalk levels was investigated by fitting experimental data with known distribution functions, via hypothesis tests.

In order to derive information on crosstalk statistics, circuit models based on the chain connection of uniform multiconductor transmission lines (MTLs) were subsequently developed and experimentally validated [41-43]. This approach foresees modeling the non-uniformity of the bundle's cross section in terms of infinitesimal, random, abrupt changes, and representing the overall harness as a distributed multi-port device with random parameters. Information on the range and properties of crosstalk levels is then obtained by generating and analyzing a large set of wire-bundle realizations, via repeated runs. These numerical models prove to be suited for describing crosstalk statistics in densely packed wire bundles, provided some global information on the scale of non-uniformity is available, and provided the number of wires in the bundle is not too high.

From the standpoint of circuit modeling, in [44] the canonical deterministic model of crosstalk (based on a three-conductor uniform and lossless transmission line with resistive loads) was translated to probabilistic terms by assuming a rectangular uncertainty region for the wires in the line's cross section. Because of full uncertainty about wire position and separation, uniform pdfs were used, and an analytically implicit expression of the crosstalk pdf was derived. Numerical evaluations of this pdf evidenced a long tail for large crosstalk levels. This proved a crosstalk property observed in former times in the analysis of experimental data [40]. However, despite the idealized nature of the structure, the aforementioned probabilistic model is limited to electrically short transmission lines. An extension of this model was made available in [45], where a circuit model for crosstalk was developed in which the victim circuit embedded all the interference effects due to the presence of the generator circuit. Such effects were represented by a voltage and a current lumped noise sources and a distributed-parameter passive two-port. Under weak-

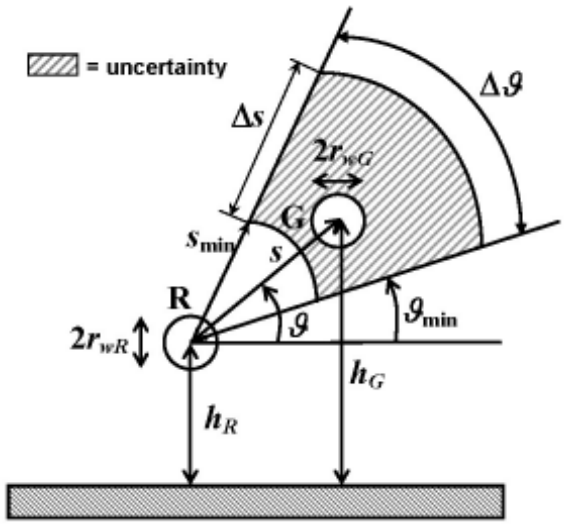

Figure 4. A three-conductor transmission-line cross section, adapted for the investigation of crosstalk statistics [45]. The parameters s and ϑ are used for tracking random fluctuations of the generator wire, G, around the receptor wire, R, in a fixed uncertainty region (dashed region).

coupling, a matched generator circuit, and by assuming random fluctuations of the generator wire in the transmission line's cross section (see Figure 4), the following closed-form expressions for the mean value and the variance of the near-end (NEXT) and the far-end (FEXT) crosstalk voltage transfer ratio were derived:

$$\mu_{XEXT} = F_{XE}\left(\beta L;\alpha_{RNE},\alpha_{RFE}\right)\mu_{\gamma}, \qquad (17)$$

$$\sigma^2_{XEXT} = F_{XE}\left(\beta L;\alpha_{RNE},\alpha_{RFE}\right)^2\sigma^2_{\gamma}, \qquad (18)$$

where $X = N, F$, and

$$F_{NE} \cong \frac{\left|\sin(\beta L)\right|}{\left|\left(1+\frac{\alpha_{RFE}}{\alpha_{RNE}}\right)\cos(\beta L)+ j\sin(\beta L)\left(\frac{1}{\alpha_{RNE}}+\alpha_{RFE}\right)\right|}$$

$$\times\frac{1+\alpha_{RFE}}{2}, \qquad (19)$$

$$F_{FE} \cong \frac{\left|\sin(\beta L)\right|}{\left|\left(1+\frac{\alpha_{RNE}}{\alpha_{RFE}}\right)\cos(\beta L)+ j\sin(\beta L)\left(\frac{1}{\alpha_{RFE}}+\alpha_{RNE}\right)\right|}$$

$$\times\frac{\left|\alpha_{RNE}-1\right|}{2}. \qquad (20)$$

In Equations (17)-(20), L is the line length, β is the phase constant (i.e., $\beta = \omega/v$, $\omega = 2\pi f$, where f is the frequency, and $v = 1/\sqrt{\mu\varepsilon}$ is the speed of light in the surrounding medium), $\alpha_{RNE} = R_{NE}/Z_{CR}$, $\alpha_{RFE} = R_{FE}/Z_{CR}$ are loading factors, $Z_{CR} = v\ell_R = 1/(vC_R)$ is the characteristic impedance of the receptor circuit, and γ is a random variable defined as

$$\gamma = \frac{l_m}{l_G} = \frac{1}{2}\frac{\log\left[1+4h_R\left(h_R + s\sin\vartheta\right)/s^2\right]}{\log\left[2(h_R + s\sin\vartheta)/r_{wG}\right]}. \qquad (21)$$

For limited-amplitude fluctuations of the generator wire, the mean value, μ_{γ}, and the variance, σ^2_{γ}, of the random variable γ can be expressed in terms of the statistical properties of s and ϑ by resorting to a Taylor-series approach [34, 45]. The expressions in Equations (17) and (18) are valid both at low frequencies and in the transmission-line standing-wave region. These expressions also allow for a sensitivity analysis of the frequency profile of the crosstalk transfer ratio to variations of the receptor loads. As a specific example, Figure 5 illustrates the NEXT transfer ratio for a line characterized by $L = 3$ m, $r_{wR} = r_{wG} = 0.1$ mm, $r_{wR} = r_{wG} = 0.1$ mm, $h_R = 10r_{wR}$, and receptor circuit loads such that $\alpha_{RNE} = 1.5$ and $\alpha_{RFE} = 0.5$. Fluctuations of the generator wire in the transmission-line cross section are modeled by considering s and ϑ to be independent random variables, uniformly distributed within the intervals defined by $s_{\min} = 10r_{wR}$, $s_{\max} = 30r_{wR}$, and $\vartheta_{\min} = 45°$, $\vartheta_{\max} = 135°$, respectively. In Figure 5, the solid curves represent the expected value and dispersion of the NEXT transfer ratio, as predicted by Equations (17) and (18), respectively. The dashed curves are numerical estimates of the same quantities, obtained as the output of a repeated-run analysis, and reported in the plot for validation purposes.

4.1.2 Telecommunication Systems

From the standpoint of transmission theory, the statistical characterization of crosstalk is relevant for performance analysis of communication systems employing multiple-pair cables for the transmission of digital or analog signals (e.g., the telephone cable plant). To this end, crosstalk properties have been investigated by modeling the interference phenomenon in the time domain. In particular, in [46] it was shown that the covariance of NEXT is the key quantity in determining the number of pulse-code modulation systems that can be allowed to operate in conjunction with a multi-pair cable. In general, in digital transmission systems, crosstalk manifests itself as a cyclostationary random process [47-48]. Basically, this is due to the fact that synchronous digital signals show periodic time-varying ensemble mean and variance, and decisions are made on periodic samples of the received signal. Consequently, the relationship between the sampling instant and the time-varying ensemble

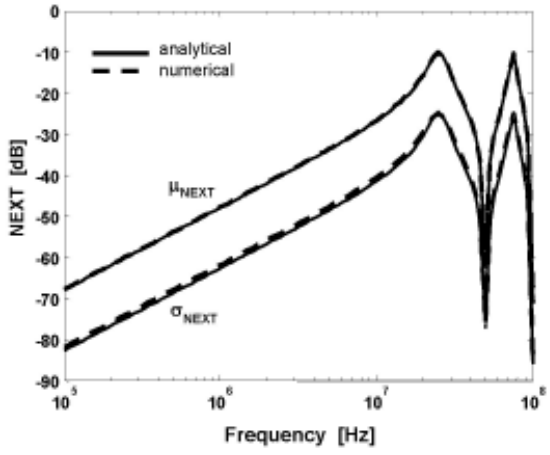

Figure 5. The mean value and standard deviation of the NEXT transfer ratio as a function of frequency for a uniform three-conductor transmission line (the line cross-section is shown in Figure 4). The receptor loads were such that $\alpha_{RNE} = 10$ and $\alpha_{RFE} = 0.1$.

statistics cannot be neglected. In [47], expressions were derived for the time-varying mean and variance of NEXT and FEXT, and it was shown that the time variation of NEXT is inherently smaller than the time variation of the FEXT interference. Additionally, conditions for signal shapes that minimize the expected value and dispersion of crosstalk were investigated. Unhappily, the relationship between the NEXT interference level and the shape of the transmitted signal involves the crosstalk transfer function, the frequency characteristics of which are not deterministic. Consequently, signal constraints for crosstalk minimization that take signal shape into account are too complex, and their application in real systems is unpractical. In general, it can be shown that even if the signal shapes that are worst for a given multi-pair cable cannot be deterministically known, a class of signal shapes exists that is more likely to cause excessive crosstalk interference [49]. To overcome this limitation, bounds on the maximum crosstalk at the near end have been identified by introducing constraints on transmitted signals that do not consider the shape of the transmitted signal, but only a measure of its level [50]. Accordingly, the energy transmitted in any time interval of a specified length should be constrained.

Crosstalk statistics also play an important role in the experimental characterization of digital transmission systems employing multi-pair cables (e.g., digital subscriber lines in telephone cables). Modem-based system-identification techniques have been proposed and used to measure crosstalk in such wiring structures; however, these methods suffer from the limitation of revealing only in-bandwidth interference effects. Conversely, from the standpoint of spectrum management, it is imperative to determine all the possible sources of interference. To overcome this problem, in [51] a set of canonical crosstalk power spectral densities was identified and used to estimate the correlation with the measured spectrum. This set may be viewed as a crosstalk "basis set." In this framework, the crucial point is that different types of crosstalk interferers may simultaneously contribute to the noise impairment of a victim wire pair, and these crosstalk sources have a joint probability distribution. Determination of this distribution is a complicated statistical problem, strictly related to the identification of a rigorous crosstalk summation method [52-53].

4.2 Radiated Susceptibility

Interference effects due to coupling of radiated disturbances with the wiring harness of a system strongly depend upon the characteristics of the impinging electromagnetic field, which are typically not known in practice except in a general way, or in very specific circumstances. As a consequence of this, the canonical deterministic approach to the characterization of radiated susceptibility is revealed to be inherently ineffective. Therefore, in recent years, efforts have been directed towards the extension of radiated susceptibility models by resorting to prediction schemes and techniques based on statistical approaches.

4.2.1 Analysis of Electromagnetic Pulse Effects

The first attempts date back to the 1970s, and refer to the characterization of electromagnetic-pulse (EMP) - induced effects [1], [54]. In particular, in [54], a probabilistic model was proposed for the representation of a densely-packed cable bundle. Here, the fluctuations of the bundle's geometrical configuration (i.e., bundle non-uniformity) were modeled by resorting to the concept of a random walk, and the reciprocity theorem was used to account for the external interfering field [34]. In [55], this approximate representation of a wiring harness was used for the estimation of crosstalk in large bundles of wires. It foresaw the segmentation of the whole bundle into a cascade of uniform sections, characterized by the same cross section, with random wire interchanges at section-to-section junctions. The merit of this model is that employs a unique cross section (this largely reduces the computational cost); the limitation resides in the discretization process that is responsible for frequency limitations.

A statistical approach is also required for the determination of the effects induced by an EMP onto a power line. In this case, the variety of parameters involved in the field-to-line coupling is too great and their number too large to allow definition of a typical conducted environment in a deterministic fashion. This problem was faced in [56], where a probabilistic approach was adopted to identify a typical current shape for the conducted environment. For a given polarization (horizontal or vertical), the probabilistic model also gives the cumulative density function of the peak current values induced by the pulse.

4.2.2 Two-Conductor Electrically Short Transmission Line

The potential of statistics for radiated susceptibility assessments is not limited to complex systems and environments. The probabilistic description of canonical wiring structures may also be useful in order to gain physical insight into the field-to-line coupling phenomenon. In line with this aim, investigations were recently accomplished and probabilistic models developed for the estimation of the response of a two-conductor transmission line exposed to an external random field. In particular, in [57] an electrically-short two-conductor transmission line was considered, the deterministic model assumptions were relaxed, and some of the parameters involved in the description of field-to-wire coupling were treated as random variables. Namely, that model assumed an external plane-wave field and investigated the impact of uncertainty in the knowledge of the wave polarization and direction of incidence (there, treated as random variables). Literal expressions are derived for the pdf of the magnitude of the current induced in the terminal loads for different selections of the pdfs of the external wave parameters. The probabilistic

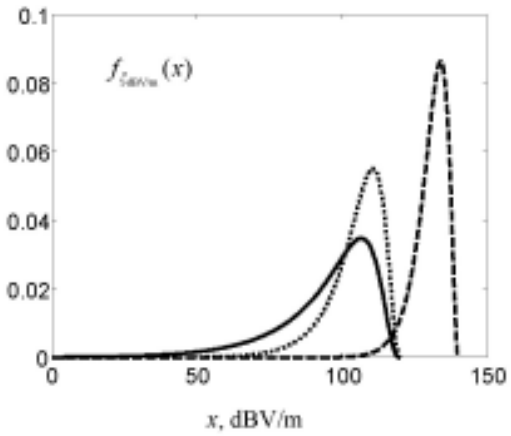

Figure 6. The pdf of the magnitude of the current induced in the right-end load (R_R) of a two-conductor line excited by an external plane wave with random amplitude, for different values of the ratio $a = Z_C / R_L$, where R_L is the left-end load. The solid curve refers to the case $a = 1$ (line matched at the left end), the dotted curve refers to $a = 1/10$, and the dashed curve to $a = 10$.

form of the results evidences the impact of partially unknown wave parameters and points out the role that different line characteristic impedances and load configurations play on susceptibility. A specific result is that matched loads are associated with the largest dispersion of the induced current (see Figure 6).

4.2.3 Two-Conductor Transmission Line of Arbitrary Length

The above-described probabilistic model is limited to electrically-short transmission lines. If all the wave parameters are regarded as random quantities, and a general operational frequency is considered, then mathematical complexities prevent derivation of closed-form results for the pdf of the induced current. However, for lines of arbitrary length, matched at both ends, the following approximate analytical expressions have been derived for the expectation and the standard deviation [58]:

$$\mu_{LF}^{(dBA)} \cong 6 + 20\log_{10} E_0 + 20\log_{10}(2h/Z_C) + 20\log_{10}(L/\lambda), \quad (22)$$

$$\mu_{HF}^{(dBA)} \cong -7.8 + 20\log_{10} E_0 + 20\log_{10}(2h/Z_C), \quad (23)$$

$$\sigma_{LF}^{(dBA)} \cong 3.4 + 20\log_{10} E_0 + 20\log_{10}(2h/Z_C) + 20\log_{10}(L/\lambda), \quad (24)$$

$$\sigma_{HF}^{(dBA)} \cong -10.7 + 20\log_{10} E_0 + 20\log_{10}(2h/Z_C). \quad (25)$$

As shown in Figure 7, the frequency behavior of the estimators in Equations (22)-(25) is approximately piecewise-linear (PWL), and is essentially frequency-independent in the standing-wave region.

In general, if the line terminations are not matched, the statistical behavior of the induced current gets complicated, due to multiple reflections at the line ends. However, in this case it is also possible to derive expressions for the expected value and the standard deviation. In particular, if the line is loaded with equal resistances, *R*, at low frequencies (or, equivalently, for electrically-short transmission lines), the standard deviation of the magnitude of the induced current becomes

$$\sigma_{I_R}^{dB} = 20\log_{10}\left(\frac{2Eh}{Z_C}\right) + 20\log_{10}\left(\frac{L}{\lambda}\right) + 20\log_{10} s(\alpha), \quad (26)$$

where $\alpha = Z_C / R$ and

$$s(\alpha) = \begin{cases} -0.211\alpha^3 + 0.7378\alpha^2 + 0.0052\alpha + 0.9163, & 0.01 \le \alpha < 2 \\ 0.9286\alpha + 0.1629, & 2 \le \alpha < 100 \end{cases}. \quad (27)$$

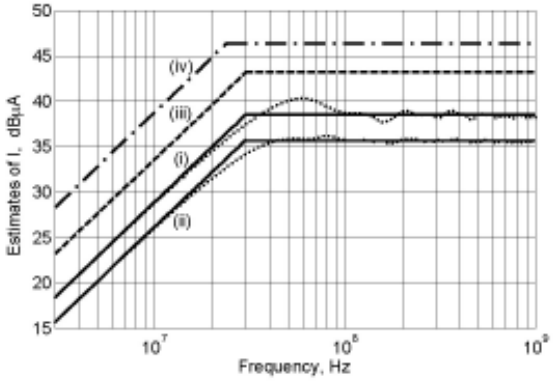

Figure 7. Estimates of the current magnitude in the line loads for a transmission line with length $L = 3$ m, height $h = 3$ cm, and radius $r_w = 0.5$ mm. The plotted curves represent (I) the expected value, (II) the standard deviation, (III) the expected value plus one standard deviation, and (IV) the worst-case envelope. The dotted curves were obtained numerically by repeated runs (10^4 waves with unit amplitude, random direction of incidence and polarization). These curves were included in the plot to assess the accuracy of the piece-wise linear model.

For electrically long lines, Equation (26) is modified to

$$\sigma_{I_R}^{dB} = 20\log_{10}\left(\frac{2Eh}{Z_C}\right) + 20\log_{10} \times \left[\frac{\alpha}{2\sqrt{\left(1+\alpha^2\right)^2 \sin^2\left(2\pi L/\lambda\right) + 4\alpha^2 \cos^2\left(2\pi L/\lambda\right)}}\right] + 20\log_{10} \left[\frac{\sigma_{g3\min}\sigma_{g3\max}}{\sqrt{\sigma_{g3\min}^2(\alpha)\cos^2\left(2\pi L/\lambda\right) + \sigma_{g3\max}^2(\alpha)\sin^2\left(2\pi L/\lambda\right)}}\right] \quad (28)$$

where

$$\sigma_{g3\min}(\alpha) = \begin{cases} -0.6768\alpha^3 + 1.3005\alpha^2 + 0.0048\alpha + 0.5206, & 0.01 \le \alpha < 1 \\ 0.4919\alpha + 0.3699, & 1 \le \alpha < 4 \\ 0.5223\alpha + 0.1716, & 4 \le \alpha < 100 \end{cases} \quad (29)$$

$$\sigma_{g3\max}(\alpha) = \begin{cases} 0.1594\alpha^3 + 0.0567\alpha^2 - 0.0846\alpha + 1.0493, & 0.01 \le \alpha < 4 \\ 0.8788\alpha - 0.0986, & 1 \le \alpha < 4 \\ 0.894\alpha - 0.1125, & 4 \le \alpha < 100 \end{cases} \quad (30)$$

Functions $s(\alpha)$, $\sigma_{g3\min}(\alpha)$, and $\sigma_{g3\max}(\alpha)$, plotted in Figure 8, describe the influence of mismatching on the standard deviation of the induced current. These functions are fitted from coupling data obtained via repeated runs (employing thousands of randomly generated external waves) for different values of α. As illustrated in Figure 9, the frequency profile of the standard deviation, $\sigma_{I_R}^{dB}$, for a mismatched line is asymptotically linear at low frequencies $(L/\lambda \to 0)$, and shows oscillations for $L/\lambda \to 0$.

4.2.4 Statistical Interpolation

The general problem of the probabilistic description of radiated susceptibility of a two-conductor transmission line for arbitrary ranges of variation of the geometrical and electrical parameters of the line, and for a general description of the electromagnetic structure and randomness of the external interfering field, is still an open mathematical problem. However, if the problem is cast in statistical terms, repeated runs and statistical interpolation can be used to derive estimates valid for wide variational ranges of the model parameters (i.e., line length and height, wire separation, and line characteristic impedance). The so called "kriging technique" is a statistical interpolator that may be employed to this end. In [59-60], this technique was used to analyze a transmission line exposed to an external random plane-wave field. For the two-conductor transmission line, this statistical technique provides reliable predictions of the 90th quantile as a measure of the strength of the coupling.

4.2.5 Multiple Interference Sources

If the wiring is exposed to multiple interference sources, the localization and polarization of which are unknown, the model based on a single plane-wave with random parameters is unrepresentative. However, as far as the plane-wave approximation can be applied to each

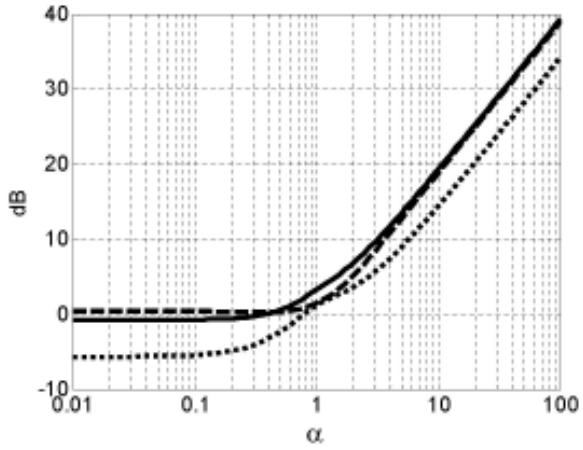

Figure 8. Plots of the functions $s(\alpha)$ (solid line), $\sigma_{g3\max}(\alpha)$ (dashed line), and $\sigma_{g3\min}(\alpha)$ (dotted line) as a function of the mismatch-parameter $\alpha = Z_C/R$.

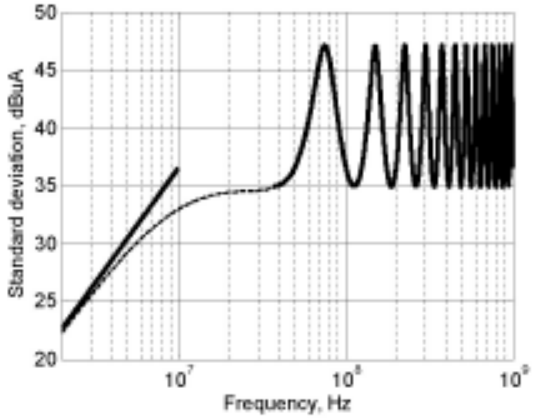

Figure 9. The standard deviation, $\sigma_{I_R}^{dB}$, of the magnitude of the current induced in the loads of a two-conductor transmission line with mismatched loads, excited by a random plane-wave field. For the geometry of the line, see the caption of Figure 7. The line loads were such that $\alpha = Z_C / R = 5$. The dashed curve is a numerical estimate of the standard deviation, obtained by repeated runs (based on 10^4 randomly generated plane waves); the solid curves are the literal expressions of $\sigma_{I_R}^{dB}$ in Equations (26) and (28).

partial source, one may resort to an integral of plane waves over all real angles for the representation of the external interference, i.e.,

$$\mathbf{E}(\mathbf{r}) = \int_{\Omega} \mathbf{F}(\Omega) e^{-j\mathbf{k}\cdot\mathbf{r}} d\Omega \,, \qquad (31)$$

where $\mathbf{F}(\Omega)$ is a complex random variable modeling the angular wave spectrum, and $\mathbf{k}$ is the vector wave number. In [61], this probabilistic model of EMI was applied to investigate the susceptibility of a bifilar transmission line. In the special case of infinite uncorrelated plane waves with random amplitude, polarization, and phase (such as EMI generated in an ideal reverberation chamber), it has been shown that the maximum available power at one end of the line (the other end being connected to a matched load) is

$$P = \frac{E_0^2 b^2}{8 Z_C} \left(1 - \frac{\sin 2\beta L}{2\beta L} \right), \qquad (32)$$

where L is the line length, b is the separation of the wires, β is the propagation constant, Z_C is the line's characteristic impedance, $E_0 = \sqrt{\langle |\mathbf{E}|^2 \rangle}$, and $\langle\ \rangle$ denotes the ensemble average. This result is applicable for general linear objects with linear loads [62].

Statistical modeling has also been exploited to analyze the practical case of complex wiring structures in externally excited metallic enclosures. Descriptions of the statistics of the current response of cables in complicated, highly over-moded cavities are available in [63-66]. These works also provide indications for the numerical simulation of the entire set of statistical phenomena involved in such structures.

5. System-Level EMC Assessment

5.1 Identification of Acceptable Interference Levels

In system-level EMC testing, statistical techniques are primarily used to analyze sets of coupling data in order to identify limits for the tests to be performed [67-68]. Typically, this approach applies whenever the large complexity of the system implies unavailability of data and infeasibility of deterministic analyses. Valid examples of systems belonging to this category are those designed in the military, aerospace, and automotive areas. In practice, extensive experimental campaigns are carried out by operating the system in an electromagnetic environment that resembles, as much as possible, those encountered in real operations. Statistical processing of the measured coupling data is then used to derive frequency-dependent profiles of the maximum acceptable interference levels.

The aforementioned approach may also be adopted for theoretical analyses. As an example, in [69] a bulk current injection immunity test was designed that conforms to specific statistical estimates of radiation-induced interference. There, a statistical characterization of the radiated susceptibility of a wiring harness exposed to external EMI was used to define the proper feeding conditions for the injection probe employed for bulk current injection. This statistically based equivalence scheme allows forcing a correlation between the effects of injected and radiated disturbances.

5.2 Prediction Models

From the viewpoint of EMC prediction at the system level, statistics may also be of considerable value in deriving global EMC properties. These include estimating the distribution of coupling data and physical interpretation of the experimental results. In this framework, a remarkable result was reported in [1], where a statistical prediction model was developed for a large and complex system immersed in external EMI. There, the system was represented in terms of electrically small magnetic and electric dipoles, and coupling with the external field was described via random interactions. In the analysis, the following parameters were treated as random variables: polarization and direction of incidence of the external field (plane wave), size and orientation of the dipoles, mutual coupling strengths among the dipoles, and lumped load impedances. It was shown that interference was dominated at low frequencies by external field coupling with magnetic loops and, in that case, the pdf of the currents induced in the loops

was evaluated analytically. Different distributions of the sizes and orientations of the loops were considered, and it was shown that the resulting current distributions were insensitive to the details of the model, except at the extremely low and high percentiles. In particular, for loops oriented with equal probability in the three-dimensional space, the expected value and standard deviation of the magnitude of the current induced in a loop was [1]

$$\mu_A = \frac{1+\alpha+\alpha^2}{3(1+\alpha)}, \tag{33}$$

$$\sigma_A = \sqrt{\frac{1+\alpha^2}{6} - \left[\frac{1+\alpha+\alpha^2}{3(1+\alpha)}\right]^2}, \tag{34}$$

$$\mu_R = \frac{1+\alpha}{4}, \tag{35}$$

$$\sigma_R = \sqrt{\frac{1+\alpha+\alpha^2}{9} - \left(\frac{1+\alpha}{4}\right)^2}, \tag{36}$$

where the subscripts A and R were used to distinguish the case of loops with equally probable area from the case of loops with equally probable radius, respectively, and $\alpha = r_1/r_2$ was the ratio of the largest to the smallest loop's radius, thus showing the range of spread of the sizes of the loops. In general, the model showed that inclusion of effects of mutual coupling among the loops led to a cumulative current distribution that was roughly log-normal in its central part, and resulted in a standard deviation of some 6 dB.

6. Conclusion

Some applications of probability theory and statistics to EMC prediction and testing have been reviewed. The subjects discussed here do not represent an exhaustive list of the EMC-relevant issues that are worth addressing in a statistical fashion. However, they represent relevant examples of EMC problems in which deterministic schemes were overcome by the potential of probabilistic modeling. Future research in this area is certainly needed, and should be targeted to the ultimate goal of establishing precise and effective information about interference phenomena, as well as providing practical design guidelines.

7. Acknowledgement

This work was supported in part by the Italian Ministry of University (MIUR) under a Program for the Development of Research of National Interest (PRIN grant # 2004093025).

8. References

1. W. R. Graham and Tse Mo, "Probability Distribution of CW Induced Currents on Randomly Oriented Subresonant Loops and Wires," *IEEE Transactions on Antennas and Propagation*, **AP-26**, 1, 1978, pp. 107-117.
2. P. F. Wilson, "Advances in Radiated EMC Measurement Techniques," *Radio Science Bulletin*, **311**, 2004, pp. 65-78.
3. C. R. Paul, *Introduction to Electromagnetic Compatibility*, New York, John Wiley & Sons, Inc., 1992.
4. D. Middleton, "Statistical-Physical Models of Electromagnetic Interference," *IEEE Transactions on Electromagnetic Compatibility*, **EMC-19**, 3, 1977, pp. 106-127.
5. L. R. Espeland and A. D. Spaulding, "Amplitude and Time Statistics for Atmospheric Radio Noise," ESSA Technical Memo. ERL-TM-ITS 250, 1970, US Department of Commerce, Boulder, CO.
6. A. D. Spaulding and L. R. Espeland, "Man-Made Noise Characteristics on and in the Vicinity of Military and Other Government Installations," Office of Telecommunications, Technical Memo. OT-TM-48, 1971, US Department of Commerce, Boulder, CO.
7. D. Middleton, "Man-Made Noise in Urban Environments and Transportation Systems: Models and Measurements," *IEEE Transactions on Communications*, **COM-21**, 11, 1973, pp. 1232, 1241.
8. D. Middleton, "Non-Gaussian Noise Models in Signal Processing for Telecommunications: New Methods and Results for Class A and Class B Noise Models," *IEEE Transactions on Information Theory*, **IT-45**, 4, 1999, pp. 1129-1149.
9. T. K. Blankenship and T. S. Rappaport, "Characteristics of Impulsive Noise in the 450-MHz Band in Hospitals and Clinics," *IEEE Transactions on Antennas and Propagation*, **AP-41**, 1998, pp. 194-203.
10. M. G. Sánchez, L. de Haro, M. C. Ramón, A. Mansilla, C. M. Ortega, and D. Oliver, "Impulsive Noise Measurements and Characterization in a UHF Digital TV Channel," *IEEE Transactions on Electromagnetic Compatibility*, **EMC-41**, 1999, pp. 124-136.
11. W. R. Lauber and J. M. Bertrand, "Statistics of Motor Vehicle Ignition Noise at VHF/UHF," *IEEE Transactions on Electromagnetic Compatibility*, **EMC-41**, 3, 1999, pp. 257-259.
12. M. Uchino, O. Tagiri, and T. Shinozuka, "Real-Time Measurement of Noise Statistics," *IEEE Transactions on Electromagnetic Compatibility*, **EMC-43**, 4, 2001, pp. 629-636.
13. E. L. Bronaugh and D. N. Heirman, "Estimating Measurement Uncertainty a Brief Introduction to the Subject," *IEEE EMC Society Newsletter*, **200**, 2004, pp. 32-44.
14. ANSI/NCSL Z540-2-1997, *American National Standard for Expressing Uncertainty - U.S. Guide to the Expression of Uncertainty in Measurement*, National Conference of Standards Laboratories, (Boulder, CO), 1997.
15. B. N. Taylor and C. E. Kuyatt, "Guidelines for Evaluating and Expressing the Uncertainty of NIST Measurement Results," National Institute of Standards and Technology, Technical Note 1297, (Gaithersburg, MD), 1994.
16. UKAS LAB 34, *The Expression of Uncertainty in EMC Testing*, (Middlesex, UK), 2002.
17. IEC CISPR 16, *Specification for Radio Disturbance and Immunity Measuring Apparatus and Methods-Part 4-2: Un-*

certainties, Statistics and Limit Modeling –Uncertainty in EMC Measurements, International Electrotechnical Commission, (Geneva, Switzerland), 2003.
18. ISO, *Guide to the Expression of Uncertainty in Measurements*, International Organization for Standards, (Geneva, Switzerland), 1993.
19. E. L. Bronaugh and J. D. M. Osburn, "Estimating EMC Measurement Uncertainty Using Logarithmic Terms (dB)," *1999 IEEE International Symposium on Electromagnetic Compatibility*, (Seattle, WA), 1999, pp. 376-378.
20. I. A. Harris and F. L. Warner, "Re-examination of Mismatch Uncertainty when Measuring Microwave Power and Attenuation," *IEE Proceedings*, **128**, 1, 1981, pp. 35-41.
21. D. Carpenter, "A Demystification of the U-Shaped Probability Distribution," *2003 IEEE Symposium on Electromagnetic Compatibility*, (Boston, MA), pp. 521-525.
22. M. Stecher, "Measurement Uncertainty in EMI Emission Measurement," *Proceedings of the 1997 IEEE International Symposium on Electromagnetic Compatibility*, (Austin, TX), pp. 270-273.
23. E. R. Heise and R. E. W. Heise, "A Method to Calculate Uncertainty of Radiated Measurements," *Proceedings of the 1997 IEEE International Symposium on Electromagnetic Compatibility*, (Austin, TX), pp. 359-364.
24. E. R. Heise and R. E. W. Heise, "A Method to Calculate Uncertainty of LISN Conducted Measurements," *Proceedings of the 1998 IEEE International Symposium on Electromagnetic Compatibility*, (Denver, CO), pp. 253-258.
25. E. R. Heise and R. E. W. Heise, "Test Facility Uncertainty Calculation Methodology and Rationale," *Proceedings of the 1999 IEEE International Symposium on Electromagnetic Compatibility*, (Seattle, WA), pp. 365-369.
26. E. R. Heise and R. E. W. Heise, "Uncertainty Rationale for Compliance Margin Factors," *Proceedings of the 2000 IEEE International Symposium on Electromagnetic Compatibility*, (Washington, D.C.), pp. 669-673.
27. E. L. Bronaugh and J. D. M. Osburn, "A Process for the Analysis of the Physics of Measurement and Determination of Measurement Uncertainty in EMC Test Procedures," *Proceedings of the 1996 IEEE International Symposium on Electromagnetic Compatibility*, (Santa Clara, CA), pp. 245-249.
28. M. Fernández, M. Quílez, F. Silva, and G. Montalà, "Bulk Current Injection Test Uncertainty Assessment," *Proceedings of the 1996 IEEE International Symposium on Electromagnetic Compatibility*, (Santa Clara, CA), pp. 69-74.
29. D. N. Heirman, "*CISPR Subcommittee A Uncertainty Activity*," *IEEE Transactions on Electromagnetic Compatibility*, **EMC-44**, 1, 2002, pp. 125-129.
30 J. J. Goedbloed, "Uncertainties in Standardized EMC Compliance Testing," *Proceedings of the 13th International Zurich Symposium on Electromagnetic Compatibility*, (Zurich, Switzerland), 1999, pp. 161-178, (available from the Symposium Secretariat, c/o ETHZ Zentrum, Gloriastrasse 35, CH-8092 Zurich, Switzerland).
31. J. J. Goedbloed and P. A. Beeckman, "Uncertainty Analysis of the CISPR/A Radiated Emission Round-Robin Test Results," *IEEE Transactions on Electromagnetic Compatibility*, **EMC-46**, 2, 2004, pp. 246-262.
32. C. Keller and K. Feser, "Fast Emission Measurement in Time Domain," *Proceedings of the 14th International Zurich Symposium on Electromagnetic Compatibility*, (Zurich, Switzerland), 2001, pp. 373-378, (available from the Symposium Secretariat, c/o ETHZ Zentrum, Gloriastrasse 35, CH-8092 Zurich, Switzerland).
33. F. Krug and P. Russer, "The Time-Domain Electromagnetic Interference Measurement System," *IEEE Transactions on Electromagnetic Compatibility*, **EMC-45**, 2, 2003, pp. 330-338.
34. A. Papoulis and S. U. Pillai, *Probability, Random Variables and Stochastic Processes, Fourth Edition*, New York, McGraw-Hill Inc., 2002.
35. B. Widrow, I. Kollar, and M. Liu, "Statistical Theory of Quantization," *IEEE Transactions on Instrumentation and Measurement*, **IM-45**, 2, 1996, pp. 353-361.
36. D. Bellan, A. Gaggelli, and S. A. Pignari, "Statistical Characterization of Rolling Stock Magnetic Field Emissions," *Proceedings of the 2004 International Symposium on Electromagnetic Compatibility*, (Sendai, Japan), pp. 477-480.
37. "ICNIRP Guidelines for Limiting Exposure to Time-Varying Electric, Magnetic, and Electromagnetic Fields (Up to 300 GHz)," *Health Physics*, **74**, 4, 1998, pp. 494-522.
38. G. T. Capraro and C. R. Paul, "A Probabilistic Approach to Wire Coupling Interference Prediction," *Proceedings of the 4th International Zurich Symposium on Electromagnetic Compatibility*, (Zurich, Switzerland), 1981, pp. 267-272, (available from the Symposium Secretariat, c/o ETHZ Zentrum, Gloriastrasse 35, CH-8092 Zurich, Switzerland).
39. C. R. Paul, "Sensitivity of Crosstalk to Variation in Wire Position in Cable Bundles," *Proceedings of the 7th International Zurich Symposium on Electromagnetic Compatibility*, (Zurich, Switzerland), 1987, pp. 617-622, (available from the Symposium Secretariat, c/o ETHZ Zentrum, Gloriastrasse 35, CH-8092 Zurich, Switzerland).
40. D. Weiner and G. T. Capraro, "A Statistical Approach to EMI Theory and Experiment - Part II," *Proceedings of the 7th International Zurich Symposium on Electromagnetic Compatibility*, (Zurich, Switzerland), 1987, pp. 629-633, (available from the Symposium Secretariat, c/o ETHZ Zentrum, Gloriastrasse 35, CH-8092 Zurich, Switzerland).
41. A. Ciccolella and F. G. Canavero, "Statistical Simulation of Crosstalk in Bundles," *Proceedings of the 11th International Zurich Symposium on Electromagnetic Compatibility*, (Zurich, Switzerland), 1995, pp. 83-88, (available from the Symposium Secretariat, c/o ETHZ Zentrum, Gloriastrasse 35, CH-8092 Zurich, Switzerland).
42. S. A. Pignari, L. Konè, F. G. Canavero, A. Ciccolella, and B. Demoulin, "Statistical Approach to Crosstalk in Random Cable Bundles," (invited paper), *Proceedings of the 16th International URSI Symposium on Electromagnetic Theory*, (Thessaloniki, Greece), 1998, pp. 662-664.
43. S. Salio, F. Canavero, J. Lefèbvre, and W. Tabbara, "Statistical Description of Signal Propagation on Random Bundles of Wires," *Proceedings of the 13th International Zurich Symposium on Electromagnetic Compatibility*, (Zurich, Switzerland), 1999, pp. 499-504, (available from the Symposium Secretariat, c/o ETHZ Zentrum, Gloriastrasse 35, CH-8092 Zurich, Switzerland).
44. S. Shiran, B. Reiser, and H. Cory "A Probabilistic Model for the Evaluation of Coupling Between Transmission Lines", *IEEE Transactions on Electromagnetic Compatibility*, **EMC-35**, 3, 1993, pp. 387-393.
45. D. Bellan, S. A. Pignari, and G. Spadacini, "Characterisation of Crosstalk in Terms of Mean Value and Standard Deviation," *IEE Proceedings-Science, Measurement & Technology*, **150**, 6, 2003, pp. 289-295.
46. A. J. Gibbs and R. Addie, "The Covariance of Near End Crosstalk and Its Application to PCM System Engineering in Multipair Cable," *IEEE Transactions on Communications*, **COM-27**, 2, 1979, pp. 469-477.
47. J. C. Campbell, A. J. Gibbs, and B. M. Smith, "The Cyclostationary Nature of Crosstalk Interference from Digital Signals in Multipair Cable-Part I: Fundamentals," *IEEE Transactions on Communications*, **COM-31**, 5, 1983, pp. 629-637.
48. J. C. Campbell, A. J. Gibbs, and B. M. Smith, "The Cyclostationary Nature of Crosstalk Interference from Digital Signals in Multipair Cable - Part II: Applications and Further Results," *IEEE Transactions on Communications*, **COM-31**, 5, 1983, pp. 638-649.
49. J. W. Lechleider, "Spectrum Management in Telephone Loop Cables, II: Signal Constraints That Depend on Shape," *IEEE Transactions on Communications*, **COM-34**, 8, 1986, pp. 737-743.

50.J. W. Lechleider, "Broad Signal Constraints for Management of the Spectrum in Telephone Loop Cables," *IEEE Transactions on Communications*, **COM-34**, 5, 1986, pp. 641-646.
51.S. Galli, C. Valenti, and K. J. Kerpez, "A Frequency-Domain Approach to Crosstalk Identification in xDSL Systems," *IEEE Journal on Selected Areas in Communications*, **19**, 8, 2001, pp. 1497-1505.
52.S. Galli and K. J. Kerpez, "Methods of Summing Crosstalk from Mixed Sources - Part I: Theoretical Analysis," *IEEE Transactions on Communications*, **COM-50**, 3, 2002, pp. 453-461.
53.K. J. Kerpez and S. Galli, "Methods of Summing Crosstalk From Mixed Sources - Part II: Performance Results," *IEEE Transactions on Communications*, **COM-50**, 4, 2002, pp. 600-607.
54.M. A. Morgan and F. M. Tesche, "Basic Statistical Concepts for Analysis of Random Cable Coupling Problems," *IEEE Transactions on Antennas and Propagation*, **AP-26**, 1, 1978, pp. 185-187.
55.D. Bellan and S. A. Pignari, "A Prediction Model for Crosstalk in Large and Densely-Packed Random Wire-Bundles," *Proceedings of the EMC 2000 International Wroclaw Symposium on Electromagnetic Compatibility*, (Wroclaw, Poland), 2000, pp. 265-269.
56.M. Ianoz, B. I. C. Nicoara, and W. A. Radasky, "Modeling of an EMP Conducted Environment," *IEEE Transactions on Electromagnetic Compatibility*, **EMC-38**, 3, 1996, pp. 400-413.
57.D. Bellan and S. A. Pignari, "A Probabilistic Model for the Response of an Electrically Short Two-Conductor Transmission Line Driven by a Random Plane Wave Field," *IEEE Transactions on Electromagnetic Compatibility*, **EMC-43**, 2, 2001, pp. 130-139.
58.S. A. Pignari and D. Bellan, "A Statistical Piecewise-Linear Model for Transmission Line Susceptibility to External Noise," *Electronics Letters*, **37**, 21, 2001, pp. 1280-1281.
59.V. Rannou, F. Brouaye, M. Hélier, and W. Tabbara, "Coupling of the Field Radiated By a Mobile Phone to a Transmission Line: A Simple Statistical and Probabilistic Approach," *Proceedings of the 14th International Zurich Symposium on Electromagnetic Compatibility*, (Zurich, Switzerland), 2001, pp. 109-112, (available from the Symposium Secretariat, c/o ETHZ Zentrum, Gloriastrasse 35, CH-8092 Zurich, Switzerland).
60.V. Rannou, F. Brouaye, M. Hélier, and W. Tabbara, "Kriging the Quantile: Application to a Simple Transmission Line Model," *Inverse Problems*, **18**, 1, 2002, pp-37-48.
61.Ph. De Doncker and R. Meys, "Electromagnetic Coupling to Transmission Lines Under Complex Illumination," *Electronics Letters*, **40**, 1, 2004, pp. 11, 13.
62.D. A. Hill, "Plane Wave Integral Representation for Fields in Reverberation Chambers," *IEEE Transactions on Electromagnetic Compatibility*, **EMC-40**, 3, 1998, pp. 209-217.
63.R. Holland and R. H. St. John, "Statistical Response of EM-Driven Cables Inside an Overmoded Enclosure," *IEEE Transactions on Electromagnetic Compatibility*, **EMC-40**, 4, 1998, pp. 311-324.
64.R. Holland and R. H. St. John, "Statistical EM Field Models in an Externally Illuminated, Overmoded Cavity," *IEEE Transactions on Electromagnetic Compatibility*, **EMC-43**, 1, 2001, pp. 56-66.
65.R. H. St. John and R. Holland, "Simple Deterministic Solutions for Cables Over a Ground Plane or in an Enclosure," *IEEE Transactions on Electromagnetic Compatibility*, **EMC-44**, 4, 2002, pp. 574-579.
66.R. Holland and R. H. St. John, *Statistical Electromagnetics*, Philadelphia, PA, Taylor & Francis, 1999.
67.D. A. Bull and N. J. Carter, "EMC Testing of Whole Aircraft," *Proceedings of the IEE Colloquium on EMC in Large Systems*, 1994, pp. 4/1-4/5.
68.N. J. Carter, "The Past, Present and Future Challenges of Aircraft EMC," *Proceedings of the EMC'03 IEEE International Symposium on Electromagnetic Compatibility*, (Istanbul, Turkey), 2003, pp. 1-4.
69.G. Spadacini and S. A. Pignari, "A Bulk Current Injection Test Conforming to Statistical Properties of Radiation-Induced Effects," *IEEE Transactions on Electromagnetic Compatibility*, **EMC-46**, 3, 2004, pp. 446-458.

Space Weather Effects on Communications Satellites

H.C. Koons
J.F. Fennell

Abstract

Space near Earth contains a hostile environment for spacecraft. Satellites in space are exposed to such hazards as single-event effects from cosmic rays, internal charging from Van Allen radiation belt electrons, and surface charging from energetic electrons in hot plasma injected into the inner magnetosphere during geomagnetic storms and substorms. These geophysical phenomena are highly variable, and are collectively known as space weather. Problems associated with these hazards include loss of mission, subsystem failure, mission degradation, loss of data, phantom commands, spurious signals, and single-event effects (upsets, latchup, and burnout). Here, we describe the physical phenomena and give numerous examples of their effects on communications satellites.

1. Introduction

When Arthur C. Clark first described the principles for satellite communications from "stations" in geostationary orbit in 1945 [1], there was no such concept as space weather. Today, the space environment (frequently called space weather, in analogy to terrestrial weather) is a major cause of anomalies on communications satellites in geosynchronous orbit [2-8]. Just as terrestrial weather is determined by the seas, mountain ranges, continents, and the polar and equatorial regions, the space weather environment is determined by the plasmas, particles, and magnetic fields in the different regions of space. Each of these can be highly variable, and one must have a basic understanding of these phenomena and of their interaction with satellites in order to understand their differing effects on space systems [2, 9]. Space weather is especially important because human enterprise is increasingly dependent on communication satellites for business data, military operations, news, advertising, entertainment, and business or personal contacts via phone, fax, and video conferences via the Internet.

Satellites in space are exposed to numerous environmental hazards, such as single-event upsets from solar and galactic cosmic rays, internal charging and excessive radiation doses from the Van Allen radiation belt particles, surface charging by hot plasmas energized during geomagnetic storms, collisions with meteoroids and debris, surface damage from atomic ions impinging on the surface, and drag from the neutral atmosphere. The most serious hazards include single-event effects, surface charging, and internal charging. The most serious problem caused by these hazards is the entire loss of a satellite's function, sometimes called loss of mission. Other impacts include subsystem failure, mission degradation, loss of data, phantom commands, spurious signals, safeholds, and latchups, and indirect impacts, such as increased cost of operations, loss of revenue, cost of redesign, etc. [2].

Some space weather effects that are not necessarily considered anomalies include normal solar cell and surface degradation, and expected gravitational, magnetic, thermal, plasma, particulate, and optical effects. Problems in these areas beyond those planned into the satellite's design, however, are considered to be anomalies.

Most of the above will be covered in this paper. The effects on communications satellites will be used as examples of the most important hazards.

2. The Space Environment

We will begin with a relatively simple overview of the space environment, emphasizing the variable weather phenomena that interact with spacecraft. It is a rather daunting list, if you have thought of space as mainly an empty vacuum. We will leave most of the details until we discuss the specific hazards below.

J. F. Fennell is with the Space Science Applications Laboratory, The Aerospace Corporation, 2350 E. El Segundo Blvd., El Segundo, CA, USA 90245; Tel: +1 (310) 336-6519; Fax: +1 (310) 336-1636; E-mail: Joseph.F.Fennell@aero.org.

H. C. Koons passed away after completing this paper.

This is one of the invited Commission H *Reviews of Radio Science*.

2.1 The Sun

The sun is ultimately responsible for many hazards to spacecraft. Particulate radiation in the form of solar cosmic rays (very energetic protons and heavier atomic nuclei of solar origin), eruptive prominences, and coronal mass ejections are sporadic energetic events that can produce hazardous environments and satellite anomalies when the radiation reaches the Earth's vicinity. The sun is also a source for X-rays from some solar flares and for radio noise. These are not significant hazards to spacecraft.

The Earth is in the region of space controlled by the outflow of plasma from the sun. This region is called the heliosphere. The plasma outflow, which consists primarily of thermal protons and electrons, is called the solar wind. It has a highly variable speed and density. It also contains a magnetic field that originates in the upper region of the sun's corona, and is frozen into the solar-wind plasma as it flows outward. The solar-wind plasma is not energetic enough to be a direct hazard. The solar wind is the source of radio emissions that are also not considered to be a hazard.

Solar particle events cause single-event effects and solar-array degradation on spacecraft. Spacecraft surface charging occurs during magnetic storms. Magnetic storms are disturbances in the geomagnetic field driven by the interaction of the solar wind with the Earth's magnetic field. They occur when coronal mass ejections, shockwaves, and high-speed solar streams strike the magnetosphere. Spacecraft internal charging occurs when the radiation-belt fluxes increase following magnetic storms. Atmospheric drag increases when solar X-rays and currents in the ionosphere, driven by geomagnetic storms, heat and raise the height of the neutral atmosphere.

2.2 Galactic Sources

The heliosphere moves through the interstellar medium with the sun. The interstellar medium is the region between the stars. It contains very-low-density plasma, galactic cosmic rays, and electromagnetic radiation from distant stars and galaxies. Galactic cosmic rays are very-high-energy atomic nuclei. The most energetic are believed to be produced in supernova and radio galaxies. The galactic cosmic rays have sufficient energy to penetrate into electronic boxes and to cause upsets to virtually all microprocessors, memory chips, gate arrays, etc. It is amazing to realize that they have traveled for perhaps millions of years before slamming into the electronics on a spacecraft.

2.3 Earth's Magnetosphere

The Earth is protected from the direct impact of the solar wind and from lower-energy solar particles by a teardrop-shaped cavity around the Earth called the magnetosphere. Figure 1 shows an artist's concept of the magnetosphere. It is formed by the interaction of the solar wind with the Earth's magnetic field.

The outer boundary of the magnetosphere is known as the magnetopause. The magnetopause is an electrical current layer that, to a first approximation, entirely confines the Earth's magnetic field. The magnetopause forms where the dynamic pressure of the solar-wind plasma balances the static pressure of the geomagnetic field. Since the solar-wind speed is supersonic, a detached shock appears in front of the magnetosphere. This shock is called the bow shock. The region between the bow shock and the magnetopause is known as the magnetosheath. It is about two Earth radii

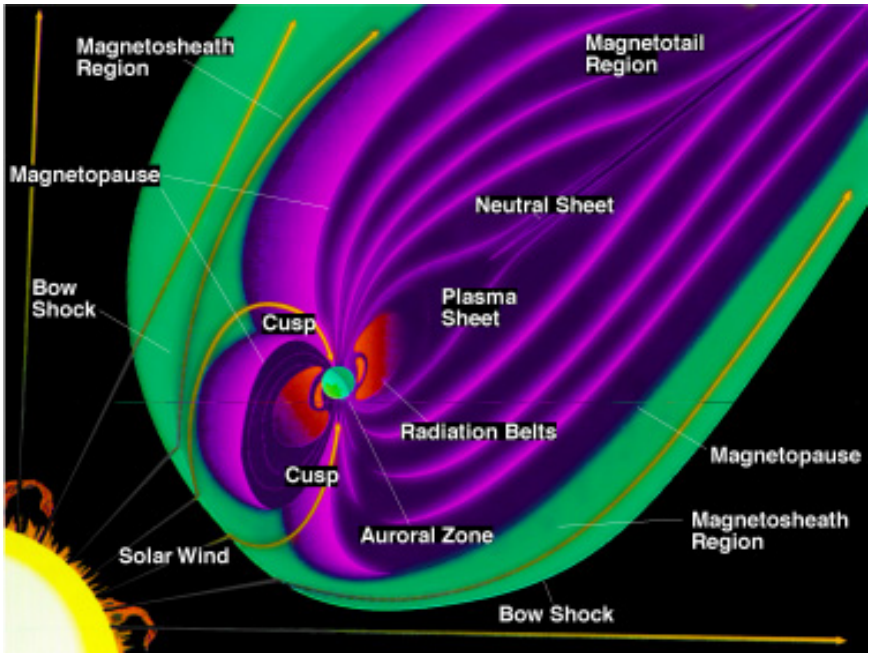

Figure 1. The internal structure of the Earth's magnetosphere (courtesy of Goddard Space Flight Center).

wide along the Earth-sun line, and is a region of considerable plasma turbulence. Along the Earth-sun line, a typical geocentric distance to the magnetopause from the center of the Earth is 10 Earth radii. Occasionally, when the solar-wind velocity is quite high, the distance can be less than 6.6 Earth radii (the distance from the center of the Earth to geosynchronous orbit), and satellites in geosynchronous orbit on the sunward side of the Earth may find themselves in the magnetosheath, outside of the magnetopause. The energy of the particles in the magnetosheath is too low to be a hazard to spacecraft.

Charged particles inside of the magnetosphere are influenced by the Earth's internal magnetic field. This magnetic field is driven by dynamo processes in the Earth's molten core. To a first approximation, the field in the inner magnetosphere is that of a dipole. The magnetosphere contains the Van Allen radiation belts, the plasma sheet, the plasmasphere, the magnetotail, and a number of other uniquely identifiable regions. Several of the regions inside of the magnetosphere provide unique hazards to spacecraft.

Some solar-wind plasma is energized and transported inside of the magnetosphere under the influence of the electric field imposed on the magnetosphere by the interaction of the solar wind with the geomagnetic field. Once inside, it forms different populations with different characteristics. Plasma regions are separated from their neighbors by a boundary on which current flows. Current also flows along and across geomagnetic field lines. These currents give rise to a magnetic field that significantly modifies (distorts) the shape of the dipolar field in the outer magnetosphere. These currents also vary with time, giving rise to significant magnetic-field fluctuations. Stronger disturbances are called magnetic storms.

Since the electrons and protons in the magnetosphere gyrate around and move rapidly along the geomagnetic field lines, the space particle environment is organized by the magnetic field. Magnetic field lines near geosynchronous altitudes map down to the northern and southern polar regions. Electrons from the hot plasma precipitate into the atmosphere in the auroral regions at both ends of the field lines, i.e., the northern and southern auroral zones, generating the optical displays seen there. Processes at low altitudes also accelerate the auroral electrons.

3. Environmental Hazards

3.1 Single-Event Effects

3.1.1 Description

A single energetic ion, such as a cosmic-ray iron nucleus or a trapped energetic proton, can interact with a microelectronic circuit in a manner that causes a change in the operation of the circuit [10, 11]. The energetic ion loses energy as it ionizes atoms in the device along the track it traverses. This creates free charge pairs, which are known as electron-hole pairs, along the ion track. The electric fields in the device sweep up these charges and generate a signal in the device, changing its state. An ion can also undergo a nuclear interaction with the atoms in the device. This generates a shower of energetic nuclei that then suffer ionization losses. Barillot and Calvel [12] have reviewed single-event effect (SEE) occurrences in commercial spacecraft.

The composite cosmic-ray spectrum represents a combination of galactic cosmic rays and solar cosmic rays [13, 14]. The cosmic-ray flux is highly variable at energies below 10 GeV/nucleon. The variability has two sources: (1) the changes of the galactic cosmic-ray access to the near-Earth space during the solar cycle (see Section 4.3), and (2) the enhancement of the cosmic-ray flux caused by energetic solar-particle events. The latter produces the most intense overall flux.

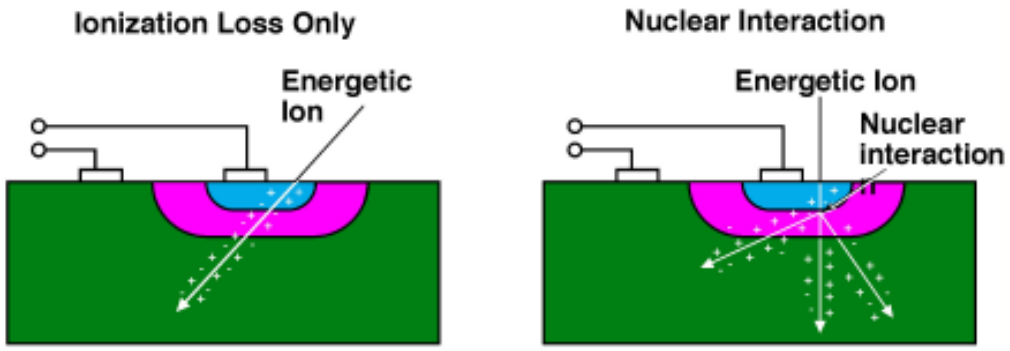

Figure 2. Examples of single-event effects: electrons and holes are swept up by the electric field in the depletion region (the lightest shading, in pink in the color version), resulting in a single-event effect.

3.1.2 Types of Single-Event Effects

All of the different effects caused by the interaction of an energetic ion with a device are collectively known as single-event effects (SEE). Historically, the different types of single-event effects have been identified by the response of the microelectronic device. Examples are shown in Figure 2.

When the free charges created by an ion are collected at the circuit's source and drain points, a current pulse occurs. The pulse can be as large as that produced by a normal input signal. The spurious pulse may change the state of the device. When this happens, the change of state is called a single-event upset (SEU). This can result in the change of a value held in a memory device, such as an instruction in a microprocessor chip, data in a memory chip, an address in an address register, etc. A single-event upset implies that there is no permanent damage done to the circuit. The single-event upset may be self-correcting, depending on the device and how it is operated.

In a single-event latchup (SEL), the free charges created by the ion interact with the parasitic transistors that often exist in microelectronic devices. A latchup can occur when the spurious current spike produced by the free charges activates the parasitic transistors, which combine into the circuit with large positive feedback. The circuit turns fully on, causing a short across the device. The short continues until the device fails (burnout), or until the power is cycled. A single-even latchup can cause permanent damage to a device, including total failure.

The free charge created by the ion in an analog device can cause a voltage spike at the output of the device. Depending on the speed of the amplifier and the following circuitry, the spike can be propagated to other circuits and cause errors. Such errors are called single-event transient effects.

Depending on the structure and function of the microelectronic device, the effect caused by the free charges can show up as normal but unwanted responses from the device. This is especially true for very complex devices such as microprocessors. For example, a single-event upset may cause the execution of an allowed, but inappropriate, instruction by a microprocessor, such as the halt instruction. Devices that have an on-chip diagnostic mode that was only intended for factory use have entered the diagnostic mode as a result of a single-event effect. This means that the device is not performing its intended purpose in the system until the error is corrected. In extreme cases, the device may enter a mode which is destructive, such as can occur with a single-event latchup.

3.1.3 Characterization of Single-Event-Effect Sensitivity

The sensitivity of an electronic device to the free charges that are generated by energetic ions passing through it determines its single-event-effect response. The sensitivity is measured in terms of the effective cross section for upsets per particle per unit area of the device. This cross section depends on the energy loss rate of the ions traversing it. The amount of energy lost by the ion per unit path length in the device is called the linear energy transfer (LET).

The linear energy transfer depends on the type of ion and its energy. Most devices require a minimum linear energy transfer to cause an upset. This minimum is called the threshold linear energy transfer. For most devices, the cross section for an upset increases with increasing linear energy transfer, up to a knee value. Devices with a low linear-energy-transfer threshold (i.e., <10 ions/m^2-sr-sec-MeV/nucleon) can be upset by low-mass high-energy ions, such as protons, helium, oxygen, etc.

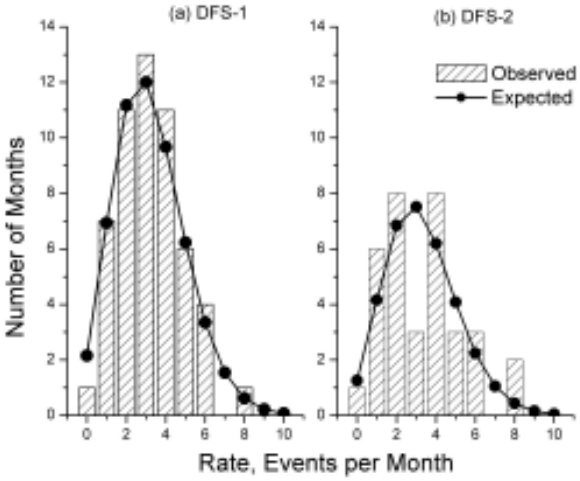

Figure 3. The distribution of single-event upsets on (a) MILSTAR DFS-1 and (b) MILSTAR DFS-2. The expected curve is based on a Poisson distribution (adapted from [15]).

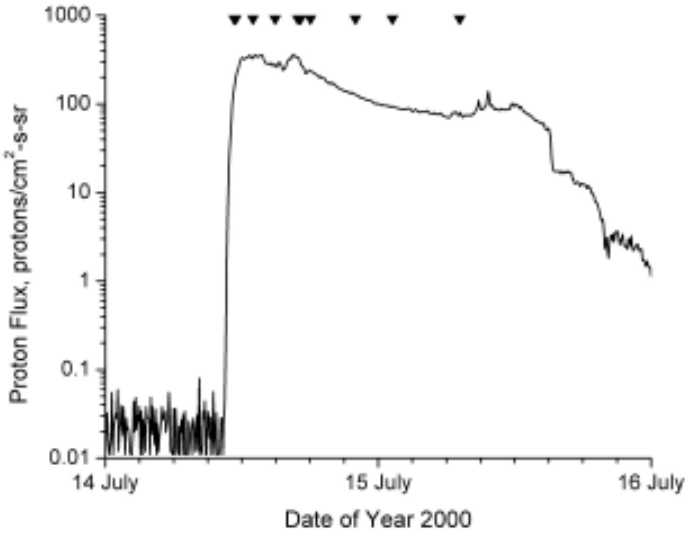

Figure 4. Inverted triangles mark the times of single-event upsets on spacecraft in high-altitude obits during the solar proton event of July, 2000. The time profile of the > 50 MeV protons, measured by the GOES-8 spacecraft during the event, is also shown (proton data courtesy of NOAA).

3.1.4 Anomalies Caused by Single-Event Effects

3.1.4.1 Galactic Cosmic Rays

The MILSTAR DFS-1 and DFS-2 military communication satellites were launched into geosynchronous orbit in February, 1994, and November, 1995, respectively. A database was created to analyze the in-situ occurrence of single-event upsets on the two essentially identical spacecraft. It was found that the upset rate varied from zero to eight upsets per month on each vehicle, with an average of 3.2 upsets on DFS-1 for the first 174 months in orbit, and an average of 3.3 upsets on DFS-2 for the first 112 months in orbit [15].

Single-event upsets caused by galactic cosmic rays should be distributed in time according to a Poisson distribution, because their occurrence can be described as a random variable with a rate that is the number of occurrences per unit time. The Poisson distribution has a single parameter, which, in this case, is interpreted as the average number of occurrences per month. In [15], a chi-squared goodness of fit test was used to see if the distribution of upsets satisfied a Poisson distribution. The hypothesis that the distribution is Poisson is accepted if the value of chi-squared is less than the value at the 0.05 significance level. Figure 3 shows the histograms of the number of months each upset rate occurred as a function of the rate for both spacecraft. Although the average numbers of upsets per month were virtually identical, the significance level from the chi-squared test gave a high value of 0.98 for DFS-1, but a low value of 0.23 for DFS-2. Figure 3 shows that the largest deviations from the expected distribution for DFS-2 occurred at three and eight upsets per month. However, the low value of the significance level for DFS-2 did not imply that the occurrences on DFS-2 did not fit a Poisson distribution. Since the significance level for DFS-2 was still much greater than our acceptance level of 0.05, the hypothesis that the distribution was Poisson can not be rejected. If 100 identical vehicles were launched, statistically, one would expect that about 20 would have worse fits than DFS-2, with a similar number of single-event upset occurrences.

3.1.4.2 Solar Cosmic Rays

Solar particle effects are caused by energetic events, such as solar flares and shocks. They can produce a significant flux of energetic protons and heavier particles. An energetic event can include ions with energies above 100 MeV. Since protons dominate such particle events [14], they are frequently called solar proton events. The larger energetic events cause single-event effects on spacecraft, and they also make a significant contribution to solar-array degradation.

The temporal profile of a solar proton event is determined by the relative positions of the particle emission region and the solar magnetic flux tube that is connected to Earth: the more directly connected, the faster the risetime and the shorter the event. A solar proton event has a proton flux of at least 10 proton flux units (pfu), where 1 pfu = 1 proton/cm^2-s-sr at energies greater than 10 MeV. Energetic solar particles can cause single-event effects on spacecraft, especially during strong ($\geq 10^3$ pfu), severe ($\geq 10^4$ pfu), or extreme ($\geq 10^5$ pfu) solar particle events [16]. The upside-down triangles on Figure 4 show the times of such upsets on spacecraft in geosynchronous and Molniya orbits, during the solar proton event of July, 2000.

3.1.4.3 Inner Radiation Zone and South Atlantic Anomaly

Solar and galactic cosmic rays are the primary source of singe-event effects for electronics that are moderately radiation hardened. Soft parts – that is, parts with low linear-energy-transfer thresholds – can also experience single-event effects from energetic protons. The cosmic-ray flux with linear energy transfer = 10 ions/(m^2-sr-sec-MeV/nucleon) is relatively low. However, the trapped high-energy proton fluxes in the inner radiation belts with this linear energy transfer can be very intense, exceeding 10^8 protons/(m^2-s-sr) for energies > 50 MeV [17]. Programs that plan to fly satellites with low- to middle-altitude orbits or low perigees have to take this into account when developing their systems.

Normally, the inner radiation zone is avoided because the total radiation dose is so large there. However, some low-altitude missions still experience effects from the energetic protons in a region known as the South Atlantic Anomaly. The asymmetries in the geomagnetic field cause the radiation belts to "dip" closer to the Earth in the south Atlantic regions, and satellites that pass through this region can experience single-event effects.

From September, 1988, to May, 1992, UoSAT-2, an amateur-radio communications satellite, flying in a polar orbit at ~ 690 km altitude, experienced almost 9000 single-even upsets (SEUs). The majority of these (75%) occurred in the South Atlantic Anomaly (SAA) region. Figure 5 shows the spatial distribution of upsets on UoSAT-2. The region of the South Atlantic Anomaly is clearly indicated by the high occurrence of upsets over the South American continent and South Atlantic ocean. Events at higher latitudes were attributed to galactic cosmic rays and solar protons [18].

3.2 Surface Charging

3.2.1 Description

Surface charging is the accumulation of electrons from the space environment on the surface of a spacecraft. As electrons accumulate on the surface, they repel lower-energy electrons approaching from the plasma. This ultimately limits the potential to which the surface can charge with respect to the plasma. Since a satellite is essentially always immersed in a space plasma – whether it be in the ionosphere, magnetosphere, or the solar wind – the surface of a spacecraft always charges with respect to the plasma to a potential called the floating potential. This floating potential is a monotonic function of the plasma's temperature. However, charging to large negative values with respect to the plasma is determined by the secondary-emission properties of the surface material, and has been shown to correlate directly with the flux of electrons with energies greater than 30 keV [19]. In the ionosphere, the thermal energy is typically a few eV, while in the plasma sheet, it can be as high as 10 to 20 keV.

If the surface material is an insulator or a conductor isolated from the spacecraft frame, the charges may reside on the surface (or just below the surface) for a long period of time. If the material is a poor conductor or a dielectric, the charges will slowly bleed off to ground (the satellite frame) or to surrounding materials. If the material is a grounded conductor, the surface charges rapidly, and equilibrates with the spacecraft frame.

The floating potential is the potential at which the net current to each surface element on the spacecraft is zero. This is the point at which it is in equilibrium with the

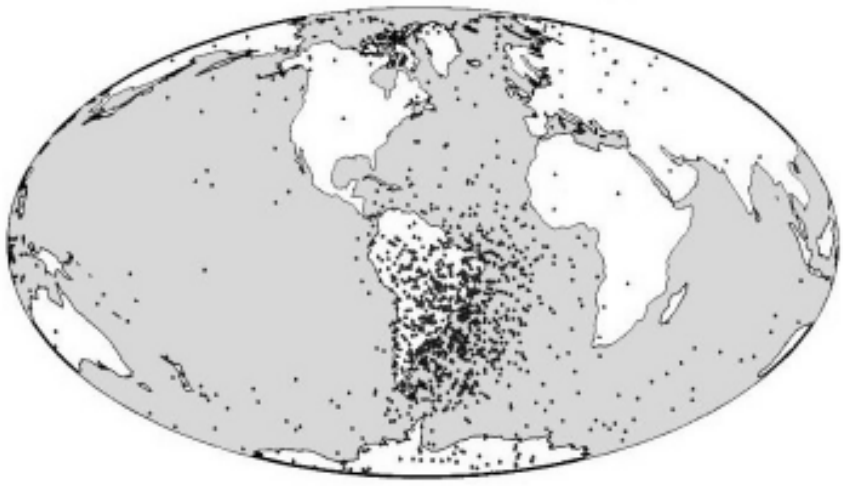

Figure 5. Single-event upsets on the low-altitude UoSAT-2 amateur-radio communications satellite. The majority, from protons in the inner radiation belt, occur in the South Atlantic Anomaly over South America and the South Atlantic Ocean. Upsets scattered over the rest of the globe are from galactic cosmic rays [6] (courtesy of NOAA).

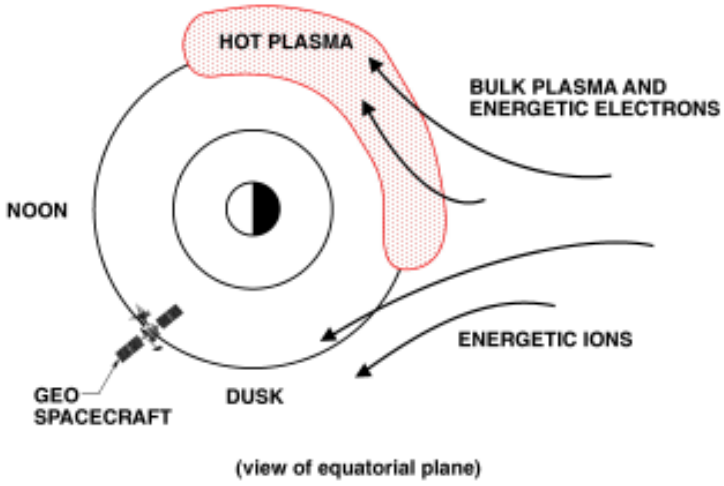

Figure 6. An artist's conception of the region in geosynchronous orbit where hot plasma can cause surface charging (after [25]).

plasma. This can be quite a complex current balance because of the number of different currents involved. For an object as simple as a conducting sphere, the currents include not only the thermal ions and electrons in the plasma, but also secondary electrons that leave the surface when a primary ion or electron strikes it, and photoelectrons that leave the surface when it is struck by photons from the sun. Because the surface is made of materials with differing electrical properties, the current balance and thus the floating potential of each surface element can be different. This generates a differential potential between the spacecraft frame and each material, and between adjacent materials with different electrical properties.

Under most circumstances, the floating potential and the differential potentials are small, and pose no hazard to the vehicle. However, during storms, hot plasmas, with temperatures between 1 and 20 keV, envelop the spacecraft. Dielectric surfaces are then charged to differential potentials as high as 10 kV. This phenomenon is known as surface charging. If the electric field arising from these differential potentials exceeds the breakdown strength for the material, either along the surface or through the material to the spacecraft frame, then an electrostatic discharge (ESD) occurs. The electromagnetic interference and currents resulting from such discharges pose a significant hazard to spacecraft electrical systems. A recent study showed that surface charging is the leading environmental cause of spacecraft mission failures [7].

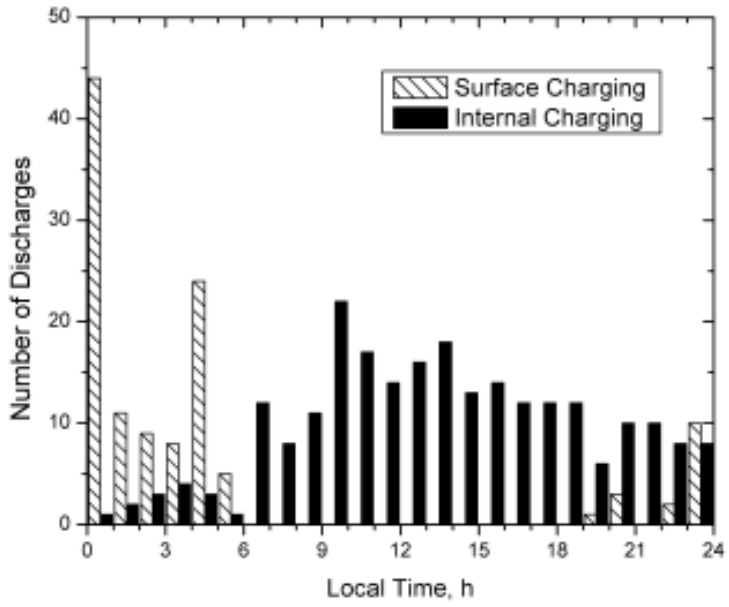

Figure 7. A histogram of the number of occurrences of electrostatic discharges due to surface charging and internal charging on the SCATHA satellite as a function of local time at the spacecraft (adapted from [21]). The data are from a total of 1527 days, between February, 1979, and March, 1988 (reprinted with permission of the American Institute of Aeronautics and Astronautics, Inc.).

3.2.2 Surface Charging in Various Orbits

3.2.2.1 Geosynchronous Orbit

Surface charging in geosynchronous orbit primarily occurs during substorms. During a substorm, the electrons are heated at distances of ~ 20 Earth radii in the magnetotail, and are driven inward toward the Earth. This injection is caused by the rapid acceleration of the electrons by an inductive electric field, generated by the motion of the geomagnetic field as it snaps back to its normal dipolar configuration from a stressed configuration. This primarily occurs on the night side of the Earth. The electrons envelop spacecraft in high-altitude orbits, such as geosynchronous orbit, and those in HEO and MEO orbits on field lines that connect to this region of space. The region where the hot plasma is normally encountered in geosynchronous orbit is shown in Figure 6. Its limits in local time have been measured to be from ~ 19 h LT through midnight to ~ 9 h LT. Surface charging primarily occurs from pre-midnight to local morning, because the energetic electrons drift from their injection point toward dawn.

The first spacecraft mission believed to be lost by a surface-charging anomaly was DSCS-II (9431) on June 2, 1973. It failed when power to its communication subsystem was suddenly interrupted. A review board found that the failure was due to a discharge caused by spacecraft charging as a result of a geomagnetic substorm [20].

Figure 7 shows the local-time distribution of electrostatic discharges due to surface charging on the SCATHA spacecraft [21]. The discharges were attributed to surface charging because, in each case, the Surface Potential Monitor aboard the spacecraft indicated that the dielectric samples on the surface of the vehicle were charged to a relatively high value when these discharges were observed.

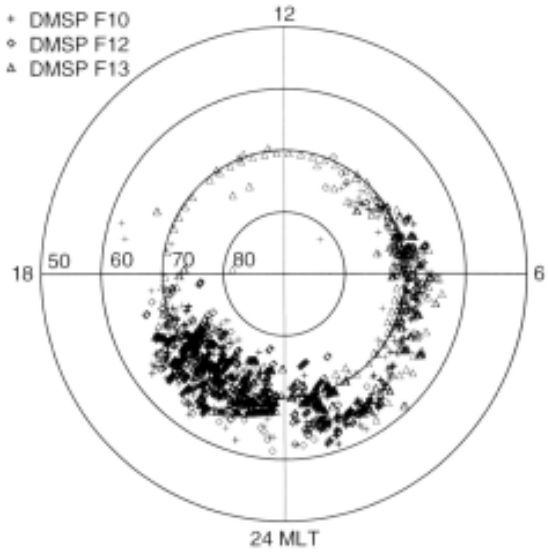

Figure 8. The location in magnetic latitude and magnetic local time of surface-charging events measured on the DMSP satellites at low altitude in the auroral zones [22] (courtesy of the Air Force Research Laboratory).

3.2.2.2 Auroral Zone

Magnetic field lines near geosynchronous altitudes connect to the northern and southern auroral zones at low altitudes. The energetic electrons that precipitate into the atmosphere along these field lines cause optical auroral displays, and also cause satellite surface charging on low-altitude, polar-orbiting spacecraft.

Figure 8 shows the region in LEO (low Earth orbit) where charging was observed on DMSP spacecraft [22]. Each point shows the location where the vehicle frame potential was measured to be more negative than −100 V. Each point occurred in an auroral arc. At low altitudes,

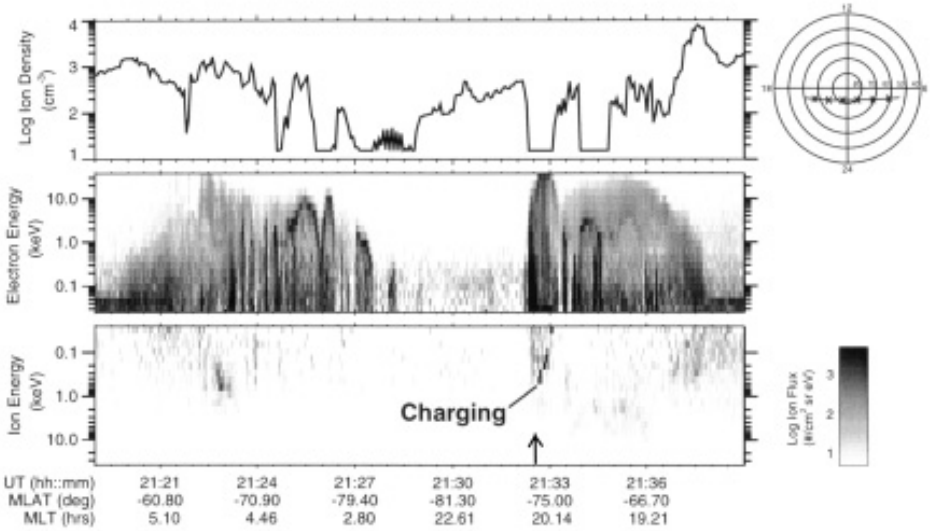

Figure 9. The environmental parameters associated with the surface-charging event and anomaly (at the arrow) on the DMSP F13 spacecraft at 21:32:40 (h:m:s) on May 5, 1995 (after [23], reprinted with permission of the American Institute of Aeronautics and Astronautics, Inc.).

charging only occurred when the vehicle was within an auroral arc. In Figure 9, an intense auroral arc occurred beginning just after 21:32 UT. The electron flux is shown in the middle panel. Within this arc, at the time shown by the arrow, an anomaly attributed to spacecraft surface charging occurred on a DMSP spacecraft [23]. At the time, the environment satisfied the three criteria required for significant charging of the spacecraft frame: (1) the integral number flux must be greater than 10^8 electrons/cm^{-2}-s-sr for electrons with energies greater than 14 keV, (2) the spacecraft must be in darkness, and (3) the background plasma density must be less than 10^{-4} cm^{-3} [24].

3.2.2.3 HEO (Molniya) Orbits

The Molniya orbit is a highly eccentric orbit (HEO), with an inclination of ~ 63° and a period of 12 h. Figure 10 shows the location of frame charging measured by a spacecraft in a Molniya orbit. Spence et al. [25] analyzed a database of approximately 100 anomalies experienced by several satellites in similar orbits. They mapped the anomalies from the location of the spacecraft at the time of the anomaly to the magnetic equator along magnetic field lines, and showed that most of the anomalies mapped to the dawn sector, between 0000 MLT and 1000 MLT. This is just the region where surface charging was seen to occur in Figure 10. Based on this mapping, they attributed these anomalies to surface charging. On a later vehicle, the same type of anomalies were shown to correlate with frame charging.

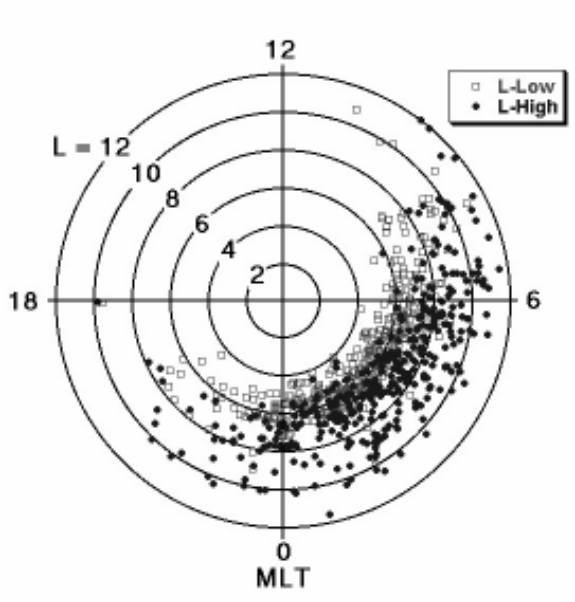

Figure 10. The location in Magnetic Local Time and L-shell where the spacecraft frame potential was less than -30 V in a Molniya orbit. The squares indicate the low L-shell limit of the charging (no data were taken below L ~ 4) and the circles show the high L-shell limit for each orbit. The points were not connected to simplify the drawing.

3.2.3 Surface Charging Mitigation and Risk

The space environment may dictate parts and materials selection in some applications and orbits. Failure to consider the environment leads to technical risks in parts and materials selection, EMC design, software and firmware design, and weight budget. Redesign, rework, and retest required by late recognition of environmental impacts may cause cost overruns and schedule delays. An example is the MARECS B spacecraft, a maritime European communications satellite. It was removed from the Ariane launch vehicle and returned to the factory for retest and rework because of a large number of environmental anomalies on MARECS A [26, 27]. Anomalies caused by the space environment increase the need for monitoring a spacecraft's state of health, increase the manpower required to operate the spacecraft, and result in inefficient workarounds when the are frequent. The most serious risk is that of subsystem or mission failure.

3.3 Internal Charging

3.3.1 Description

Internal charging is caused by energetic electrons that have penetrated into or through satellite surface material. These electrons deposit their charge on and inside cables, circuit boards, and other dielectrics, or on ungrounded conductors. Over time, the charge can build up electric fields in and between materials to breakdown levels, leading to electrostatic discharges into sensitive circuits. Internal charging is sometimes called bulk charging or deep dielectric charging. The penetrating electrons normally must have relatively high energies, i.e., > 300 keV. In geosynchronous orbit, the peak fluxes of the penetrating electrons occur two to five days after a magnetic storm, or after the onset of a high-speed solar-wind stream. Discharges have occurred on spacecraft for enhanced electron fluence levels in the range from ~ 3 ´ 10^9 to 10^{12} electrons/cm^2 in a few hours to days.

Internal charging occurs where the energetic electron fluxes are high. This occurs along field lines with L values in the range of $3 < L < 7$. The fluxes are highest where the L value is lowest in this range. The L value is the distance in Earth radii from the center of the Earth to the point at which a magnetic field line crosses the magnetic equator, measured in the magnetic equatorial plane. Energetic electrons drift around the Earth on paths of constant L value.

Internal charging causes logic errors, phantom commands, erroneous data, electronic noise, and, in some cases, loss of device, subsystem, or system functionality. Most of the time, the results of internal charging are nonfatal. However, in rare cases it can cause serious harm to a spacecraft.

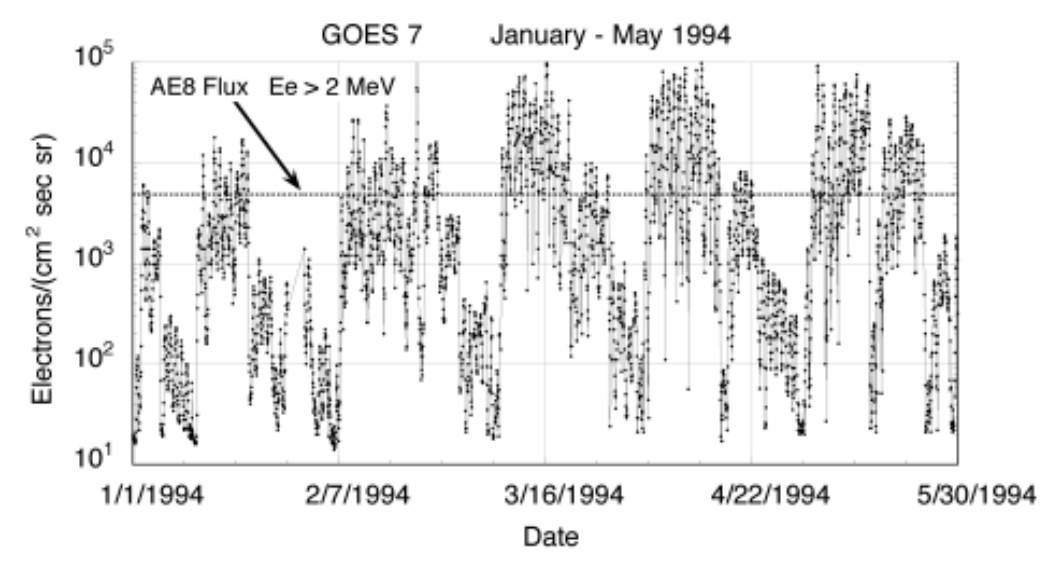

Figure 11. The daily averaged energetic electron fluxes for electrons with energies > 2 MeV from January to May, 1994 (data courtesy of NOAA). The average fluxes from the AE8 electron model are shown for comparison [28].

In geosynchronous orbit, the local time distribution of electrostatic discharge due to internal charging shows a peak in the relative occurrence coincident with a peak in the electron flux near noon [21]. The geomagnetic field is distorted at this altitude by the plasma currents that flow on the magnetospheric boundary, and a geosynchronous satellite is closest to that boundary at local noon. The causes the high-energy electron flux to be greater at noon, whereas the L value, on average, is lowest than at midnight and points in between. This flux asymmetry gives rise to the enhanced occurrence of internal electrostatic discharge around noon.

The electron fluxes in the outer radiation belt are highly variable, as shown by the example in Figure 11. The data covered a five-month period in 1994, when the solar wind consisted of a succession of high-speed and low-speed streams in a quasi-periodic manner. The electron fluxes at geosynchronous orbit generally peaked in conjunction with the high-speed solar wind streams, and dropped during the low-speed intervals. The maximum > 2 MeV electron fluxes exceeded the average flux values from the AE8 radiation-belt model [28] by more than an order of magnitude.

3.3.2 Communication Satellite Examples

A. L. Vampola [29] was the first to describe specific anomalies caused by internal charging. He identified anomalies on NTS-2 (a demonstration satellite for the Global Positioning System), Voyager 1, Meteosat-1, and DSP. The anomaly on DSP was the failure of a shutter designed to protect a sun sensor from direct exposure to the sun. The probable cause of the DSP anomaly was spurious pulses in an exposed cable, which were due to discharges in the dielectric in the cable. Based on the local time distribution of the anomalies attributed to electrostatic discharge on a number of spacecraft, Vampola estimated that half were due to surface charging and half to internal charging.

On January 20, 1994, the Anik E-2 communications satellite, owned by Telsat Canada, spun out of control because of a failure in one of its momentum wheel controllers in its guidance system. The anomaly was attributed to burnout from an electrostatic discharge to a pin on a multi-vibrator chip from an ungrounded spot shield. The primary controller and its backup both failed during this event. Service was restored using ground-based control in August, 1994 [30]. Anik E-1 suffered a similar failure in its primary controller during the same event. Full service was restored to Anik E-1 in about eight hours by successfully switching to a backup circuit.

3.4 Total Radiation Dose

3.4.1 Description

There are two basic sources of the total radiation dose for satellites flying in near-Earth space. The primary source is the radiation trapped in the Van Allen radiation belts. The secondary source is energetic protons from solar particle events. Both of these sources are highly variable. The radiation belts are populated by multiple sources. The high-energy protons in the inner radiation belt are derived from cosmic-ray albedo neutrons, created when cosmic rays strike the atmosphere, and from transient injections of solar and outer-belt protons during large storms. In addition, some energetic, anomalous, cosmic-ray ions are captured by charge exchange as they are passing near the Earth. The ionic component of the outer radiation belt has two sources: transport inward from the solar wind, and up-flow from the

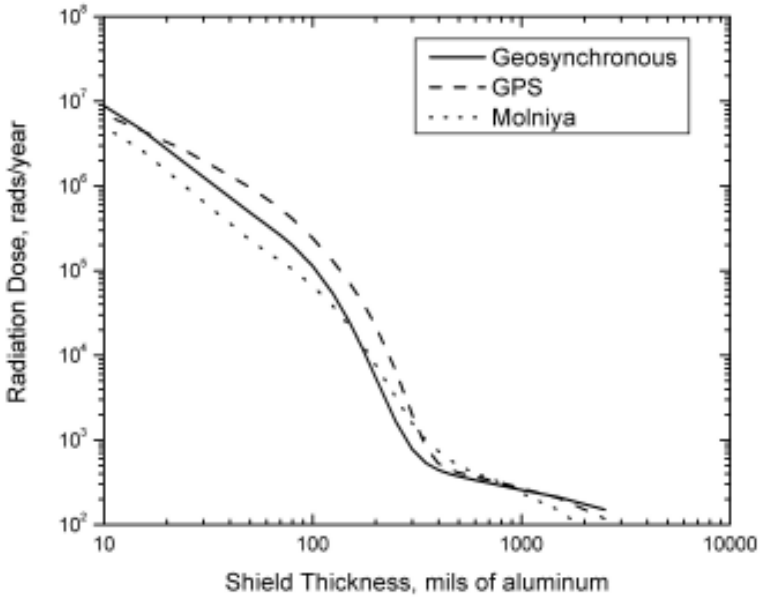

Figure 12. The yearly total radiation dose (one-half the dose at the center of an aluminum sphere) as a function of the shielding thickness for three typical orbits.

Earth's ionosphere. Most electrons in the radiation belts are of solar-wind origin, and come from the plasma-sheet plasma that is transported toward the Earth from the magnetotail by convection and fluctuating electric and magnetic fields. The complete story as to how this happens is still unfolding.

3.4.2 Radiation Protection and Radiation-Belt Models

Protection from ionizing radiation is provided by the use of electronic components (radiation-hardened parts) that are specifically designed to tolerate the environment, and by shielding. Radiation hardening requires manufacturing processes that are different from those used in commercial foundries [31]. For example, nonstandard starting materials, incorporating epitaxial layers or insulating substrates, may enhance radiation immunity. Proprietary procedures, involving novel implants or modifications of layer thickness, are also used. A new technique, known as radiation hardness by design, RHBD, uses circuit-design strategies to mitigate damage from total radiation dose and upsets and data loss from single-event effects. Radiation hardness by design includes such strategies as using multiple circuits with voting logic and redundant transistors. Parts from foundries dedicated to the production of radiation-hardened parts can cost as much as 100 times more than the equivalent commercial parts, because of their complexity and the small space-electronics market.

Models that specify the average particle environment are used to estimate the long-term average dose from the trapped radiation [28, 32]. These models are used to calculate the orbit-averaged particle spectra and total fluence for both protons and electrons. Solar proton fluences are treated statistically, using historical data to provide the probability of particle fluxes as a function of energy and mission duration [33].

The models can also be used to predict the long-term dose for spacecraft orbits where few measurements have been made. Typically, the trapped, radiation-belt models are used to generate the average electron and proton spectra for a one-year exposure. This is then multiplied by the number of years planned for the mission to give the expected radiation-belt contribution to the total radiation dose. The solar proton dose is calculated separately, and added to the radiation-belt contribution to give the total radiation dose. Particle-transport codes are used to propagate the particles through the spacecraft's shielding. They also keep track of the X-rays and gamma rays (bremsstrahlung) produced by the particles as they pass through material. The codes then add up the energy that is transmitted through the shielding into the underlying materials or devices. This energy is usually expressed as the absorbed dose for silicon (the most common material in microcircuits). The result provides an estimate of the shielding provided by a design for protecting electronics and other items (solar arrays, optics, humans, etc.) from the radiation that will be accumulated in that orbit during a mission.

The satellite designer will normally select parts that have been tested for total radiation dose and for single-event effects. He or she will know the intrinsic hardness of the parts in kilorads. He or she will then use curves, such as those shown in Figure 12, to select the additional shielding required for the orbit and the planned duration of the mission. Figure 12 shows the results of a total radiation dose calculation for satellites in geosynchronous, Molniya, and GPS orbits. The values are given in rads/year, and are assumed to be about the same at any time during a solar cycle. Missions are presently being planned to survive for 15 or more years.

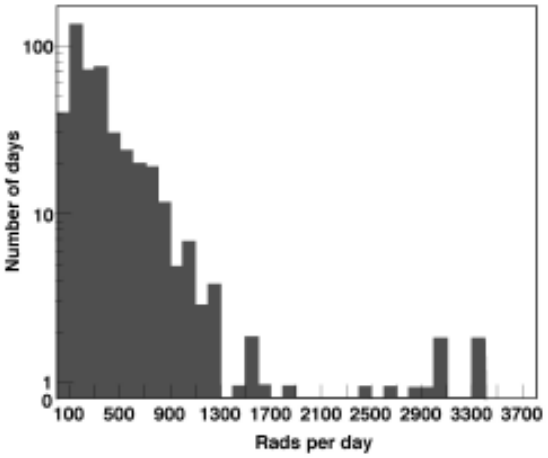

Figure 13. A histogram of the daily electron dose rate experienced in a GPS orbit over a 13-month period.

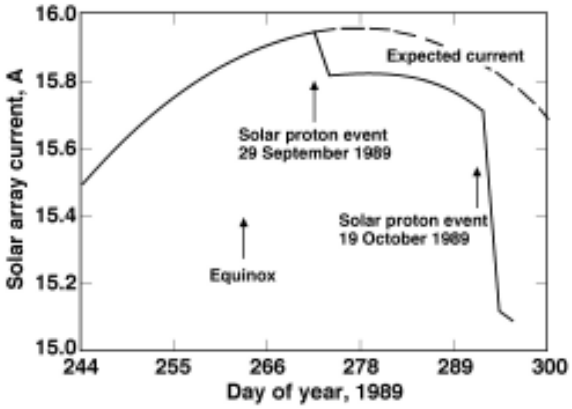

Figure 14. The solar-array current observed on GOES-7 during the fall of 1989 (after [35], reprinted with permission of the American Institute of Aeronautics and Astronautics, Inc.).

3.4.3 Electron Radiation Dosage in GPS Orbit

Some GPS satellites have carried dosimetry to verify the model predictions for total radiation dose for the GPS orbit. Figure 13 shows the dose in rads/day behind a 75-mil aluminum shield during about a thirteen-month period While the long-term average dose was close to the expected value, the day-to-day and week-to-week variations were large. Sometimes, the peaks and valleys in the dose rate were more than an order of magnitude greater or less than the average. Most of the dose-rate variations experienced by this GPS satellite were caused by variations in the trapped energetic electron fluxes. The high values of the dose rate dominated the long-term average. That is, the majority of total dose could be accumulated in a relatively short time, especially if a succession of storms occurred. The peak dose rates might also be hazardous for devices with marginal radiation or dose-rate tolerance.

3.5 Solar-Cell Degradation

Energetic protons from solar particle events damage solar arrays and reduce their ability to generate current [34]. This can significantly reduce the lifetime of a communications satellite. Solar arrays are covered with thin glass covers to shield the solar cells from all protons with energies < 10 MeV, because at geosynchronous orbit there are very few trapped protons with energies > 10 MeV. However, solar proton events can generate high fluences of > 10 MeV protons in a few days. The fluence of > 50 MeV protons can be substantial. As an example, the GOES 7 solar array current was reduced by nearly 10% as a result of two large solar proton events in 1989, as shown in Figure 14 [35].

3.6 Atmospheric Effects

During storms, the upper atmosphere heats and expands in response to increases in auroral currents, solar X-rays, solar ultraviolet radiation, and the precipitation of radiation-belt and plasma-sheet particles into the atmosphere. During a large storm, the density of the neutral atmosphere at Shuttle and space-station altitudes may reach 100 times its quiet-time value. These episodic increases in the atmospheric density are superimposed upon longer-term trends in the overall heating and expansion of the atmosphere in response to the 11-year solar cycle.

Low-altitude satellite orbits are always decaying, due to atmospheric drag. The increased atmospheric densities from the increase of the solar ultraviolet emissions during the peaks of the solar cycle and during large geomagnetic disturbances can cause significant ephemeris errors, and can hasten the decay of satellites. Figure 15 shows the satellite-tracking problems caused by such ephemeris errors due to increased drag during the large magnetic storm of March, 1989 [36]. The temporal profile of the storm is given by the Daily Magnetic Index, Ap. This showed a peak in magnetic activity on March 13. The histogram showed that the tracking problems began as the storm was subsiding, and lasted for about a week before all of the spacecraft (including large debris) was located and identified. Although this does not affect geosynchronous spacecraft, it does cause tracking errors that can lead to failures to acquire telemetry or transponder signals for low-altitude spacecraft, such as those used by radio amateurs.

4. Solar-Cycle Effects

Sunspots have been monitored for over 250 years. The official international Sunspot Number is issued by the Solar Index Data Center [37]. The times of the solar

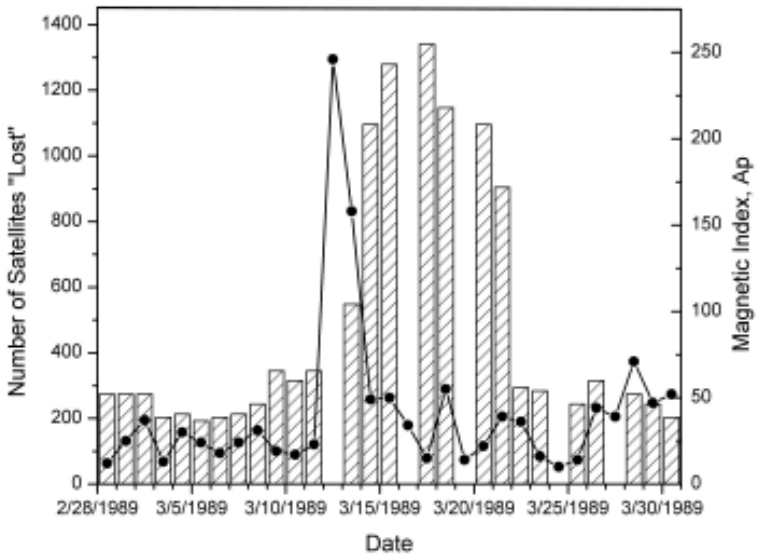

Figure 15. Satellite tracking problems after the March 13-14, 1989 magnetic storm. The histogram shows the number of satellites the tracks of which were lost as a result of the atmospheric disturbances caused by this severe storm [36]. The storm intensity was measured by the daily magnetic index, Ap.

maximum and solar minimum are based on the thirteen-month, running, smoothed, sunspot numbers. The number of sunspots varies with a cycle that has a period of about eleven years. This is known as the solar cycle. The current cycle is Solar Cycle 23. It began at solar minimum in 1996 and peaked in April of 2000. The next minimum is currently predicted to occur in December 2006. The maximum, smoothed, sunspot number varies by a factor of about five from the lowest to the highest, for the 23 cycles to date.

A number of solar and geomagnetic activity parameters are shown in Figure 16. The upper-left panel shows that the number of optical solar flares correlates closely with the sunspot number. But the hazards do not correlate so well with the sunspot number. For example, moderate to severe geomagnetic storms, shown in the lower-left panel, show only a weak relationship to the solar cycle. Nymmik [38] has shown that the number of solar particle events per year is very nearly a linear function of the average sunspot number. However, the distribution for the number of events per year as a function of the > 30 MeV proton fluence is independent of the sunspot number. Thus, the number of events maximizes at solar maximum, but a severe event can occur at any time during the solar cycle. Wren et al. [5, 39] have shown that the number of anomalies attributed to internal charging on a geosynchronous communications satellite is at a minimum during solar maximum, and maximizes during the declining phase of the solar cycle. They showed that this generally agrees with the variation in the two-day fluence of > 2 MeV electrons, as measured by the GOES spacecraft in geosynchronous orbit.

Spacecraft design must be based on worst-case estimates for each of the hazards, since each can have extreme levels at any time during a solar cycle. For high reliability, a short spacecraft mission around solar minimum must have the same protection as a long mission spanning more than one solar cycle, for all hazards except total radiation dose. Even for that, it must be protected against a major solar proton event.

5. Extreme Events and Anomalies

Examination of more than a solar cycle of the GOES daily-average electron flux data indicates that the extended period of energetic-electron flux enhancements in early 1994 was exceptional during solar cycle 22. However, the 1994 fluxes were not the highest. The highest daily-average electron fluxes observed by GOES occurred in response to a large solar event and magnetic storm that happened in late March, 1991. The distribution of daily average flux levels showed that they exceeded 10^4 electrons/(cm^2-s) about 6% of the time.

The statistics of extreme values can be used to study the extreme values that can be expected for the integral flux of energetic electrons in geosynchronous orbit. Using a data set that extended from January 1, 1986, through August 31, 1999, Koons [40] used extreme-value analysis to show that the extreme values fitted a generalized Pareto distribution [41], with an upper end point at an average daily flux of 2.34×10^5 electrons/(cm^2-s). The largest sample in the 13.67-year data set was 7.94×10^4 electrons/(cm^2-s) on March 28, 1991. A large storm in July, 2004, produced a higher daily-average flux of 9.63×10^4 electrons/(cm^2-s) on July 29. The analysis by Koons gave an expected value of 9.57×10^4 electrons/(cm^2-s) for a 50-year storm and 1.08×10^5 electrons/(cm^2-s) for a 100-year storm. Because the electron data were taken by sensors on different spacecraft in 1991 and 2004, caution must be exercised in comparing the data.

Severe space-weather events are expected to cause an increase in anomalies on spacecraft in most orbits. Information from NASA Earth and space-science missions from the severe storm period from October 19 to November 4, 2003, indicated that 59% of the spacecraft and about 18% of the instrument groups experienced some effect from the solar activity. Spacecraft-by-spacecraft details were given in [42].

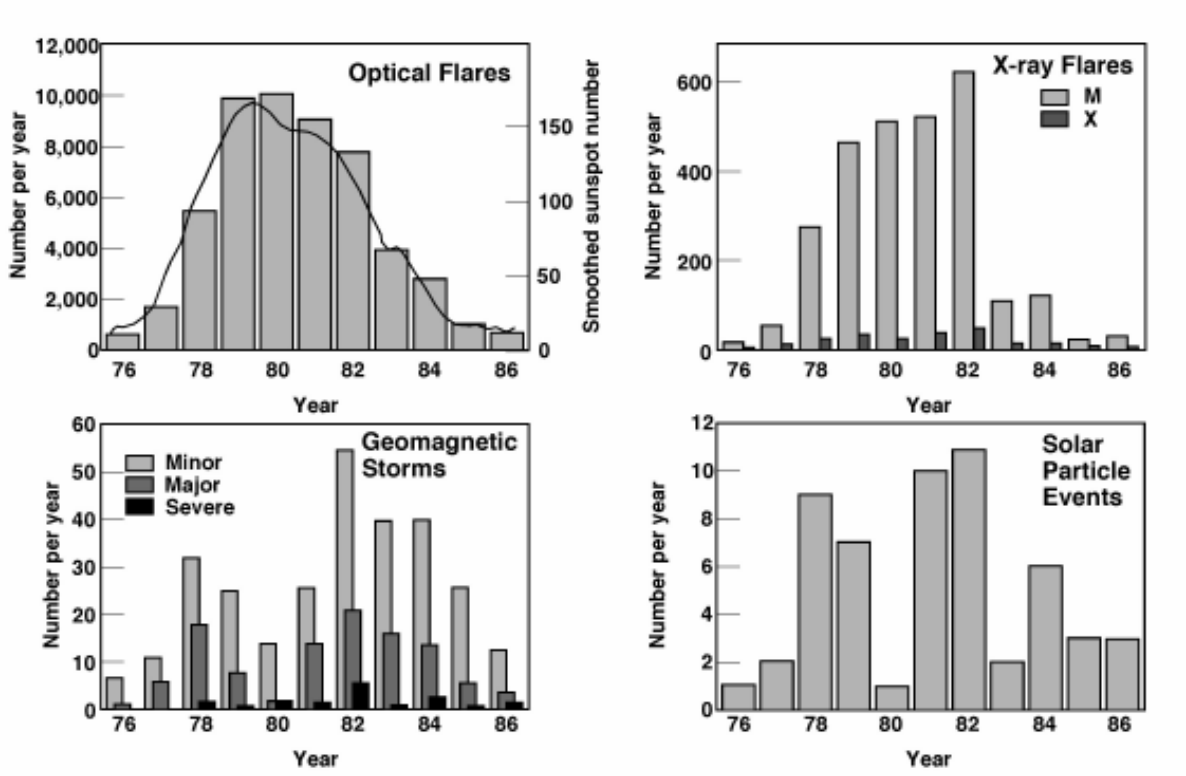

Figure 16. The solar and geomagnetic activity parameters for Solar Cycle 21. The solar cycle is shown by the curve for the smoothed sunspot number in the upper-left panel (courtesy of NOAA).

6. Conclusions

Space weather continues to be a serious hazard to modern communications spacecraft. The most serious effect is loss of mission. However, millions of dollars are spent addressing the design problems associated with the interaction of the space environment with spacecraft. Specification models are available for most of the phenomena. However, only about 40 years of data have been collected – none continuously. What has been collected and is available is insufficient to accurately specify, even in a statistical sense, the environment to be expected during a specific mission. We frankly don't know the size of the worst environment that the sun can throw at us. It is essential that high-quality data be continuously collected on each of the phenomena, and that we continue to make the effort to better understand the interaction of each with spacecraft materials and components, if we wish to design spacecraft that are safe from the environment.

7. Acknowledgements

The authors wish to thank James L. Roeder and Paul O'Brien for helpful discussions. This work was supported in part by The Aerospace Corporation IR&D Program, and in part by NASA Grant NAG5-10938.

8. References

1. A. C. Clarke, "Extra-Terrestrial Relays," *Wireless World,* October 1945, pp. 305-308.
2. B. F. James, O. W. Norton, and M. B. Alexander, "The Natural Space Environment: Effects on Spacecraft," *NASA Reference Publication 1350,* November 1994 (available from National Aeronautics and Space Administration, Marshall Space Flight Center, MSFC, Alabama 35812 USA).
3. R. D. Leach and M. B. Alexander, "Failures and Anomalies Attributed to Spacecraft Charging," *NASA Reference Publication 1375,* August 1995 (available from National Aeronautics and Space Administration, Marshall Space Flight Center, MSFC, Alabama 35812 USA).
4. K. L. Bedingfield, R. D. Leach, and M. B. Alexander, "Spacecraft System Failures and Anomalies Attributed to the Natural Space Environment," *NASA Reference Publication 1390*, August 1996 (available from National Aeronautics and Space Administration, Marshall Space Flight Center, MSFC, Alabama 35812 USA).
5. G. L. Wrenn, "Conclusive Evidence for Internal Dielectric Charging Anomalies on Geosynchronous Communications Spacecraft," *Journal of Spacecraft and Rockets,* **32,** 3, 1995, pp. 514-520.
6. J. H. Allen and D. C. Wilkinson, "Solar-Terrestrial Activity Affecting Systems in Space and on Earth," in J. Hruska, M. A. Shea, D. F. Smart, and G. Heckman (eds.), *Solar-Terrestrial Predictions – IV, Proceedings of a Workshop at Ottawa, Canada, May 18-22, 1992*, Vol. 1, September 1993, pp. 75-107 (available from National Oceanic and Atmospheric Administration, Environmental Research Laboratories, Boulder, CO, USA).
7. H. C. Koons, J. E. Mazur, R. S. Selesnick, J. B. Blake, J. F. Fennell, J. L. Roeder, and P. C. Anderson, "The Impact of the

Space Environment on Space System," *Aerospace Report No. TR-99(1670)-1*, The Aerospace Corporation, El Segundo, CA, 1999.
8. H. C. Koons, J. E. Mazur, R. S. Selesnick, J. B. Blake, J. F. Fennell, J. L. Roeder, and P. C. Anderson, "The Impact of the Space Environment on Space System," in Proceedings of the 6th Spacecraft Charging Technology Conference, November 2-6, 1998, *AFRL-VS-TR-20001578*, Air Force Research Laboratory, Hanscom, MA, September 2000, pp. 55-59, pp. 7-11.
9. J. F. Fennell, J. L. Roeder, and H. C. Koons, "Substorms and Magnetic Storms from the Satellite Charging Perspective," in Ling-Hsiao Lyu (ed.), *Space Weather Study Using Multipoint Techniques, Proceedings of the COSPAR Colloquium*, Taipei, Taiwan, September 27-29, 2000, Amsterdam, Pergamon, 2002, pp. 163-173.
10. J. H. Adams, Jr., R. Silberberg, and C. H. Tsao, "Cosmic Ray Effects on Microelectronics," *IEEE Transactions on Nuclear Science*, **NS-29**, 1, 1982, 169-172.
11. E. Normand, "Single-Event Effects in Avionics," *IEEE Transactions on Nuclear Science*, **43**, 2, 1996, pp. 461-474.
12. C. Barillot and P. Calvel, "Review of Commercial Spacecraft Anomalies and Single-Event-Effect Occurrences," *IEEE Transactions on Nuclear Science*, **43**, 2, 1996, pp. 453-460.
13. D. F. Smart and M. A. Shea, "Chapter 6: Galactic Cosmic Radiation and Solar Energetic Particles," in A. S. Jursa (ed.), *Handbook of Geophysics and the Space Environment*, pp. 6-1-6-29, Air Force Geophysics Laboratory, Air Force Systems Command, United States Air Force, 1985, (available from the National Technical Information Service, Springfield, VA 22161 USA).
14. J. H. Adams, Jr., R. Silberberg, and C. H. Tsao, "Cosmic Ray Effects on Microelectronics, Part I: The Near-Earth Particle Environment," *NRL Memorandum Rpt. 4506*, August 1981.
15. H. C. Koons and M. W. Chen, "An Update on the Statistical Analysis of MILSTAR Processor Upsets," in *1999 Government Microcircuit Applications Conf., Digest of Papers*, **24**, March 1999, pp. 816-819.
16. *S. E. C. User Notes*, Issue 28, NOAA, Space Environment Center, Boulder, CO, January 2000.
17. W. N. Spjeldvik and P. L. Rothwell, "Chapter 5: The Radiation Belts," in A. S. Jursa (ed.), *Handbook of Geophysics and the Space Environment*, p. 5-28, Air Force Geophysics Laboratory, Air Force Systems Command, United States Air Force, 1985, (available from the National Technical Information Service, Springfield, VA 22161 USA).
18. J. H. Allen, "Satellite Anomalies, Recent Events, and Possible Causes," *Space Weather Study Using Multipoint Techniques, Proceedings of the COSPAR Colloquium*, Taipei, Taiwan, September 27-29, 2000, (available from the SCOSTEP website homepage at http://www.ngdc.noaa.gov/stp/SCOSTEP/scostep.html), slide 50.
19. I. Katz, M. Mandell, G. Jongeward, and M. S. Gussenhoven, "The Importance of Accurate Secondary Electron Yields in Modeling Spacecraft Charging," *Journal of Geophysical Research*, **91**, 12, 1986, pp. 13739-13744.
20. R. D. Leach and M. B. Alexander, "Failures and Anomalies Attributed to Spacecraft Charging," *NASA Reference Publication 1375*, August 1995, p. 16, (available from National Aeronautics and Space Administration, Marshall Space Flight Center, MSFC, Alabama 35812 USA).
21. H. C. Koons and D. J. Gorney, "The Relationship Between Electrostatic Discharges on Spacecraft P78-2 and the Electron Environment," *Journal of Spacecraft and Rockets*, **28**, 6, 1991, pp. 683-688.
22. P. C. Anderson, "Surface Charging in the Auroral Zone on the DMSP Spacecraft in LEO," in Proceedings of the 6th Spacecraft Charging Technology Conference, November 2-6, 1998, *AFRL-VS-TR-20001578*, Air Force Research Laboratory, Hanscom, Mass., September 2000, pp. 55-59.
23. P. C. Anderson and H. C. Koons, "Spacecraft Charging Anomaly on a Low-Altitude Satellite in an Aurora," *Journal of Spacecraft and Rockets*, **33**, 5, 1996, pp. 734-738.
24. M. S. Gussenhoven, D. A. Hardy, F. rich, W. J. Burke, and H. -C. Yeh, "High Level Charging in the Low-Altitude Polar Auroral Environment," *Journal of Geophysical Research*, **90**, A11, 1985, pp. 11000-11023.
25. H. E. Spence, J. B. Blake, and J. F. Fennell, "Surface Charging Analysis of High-Inclination, High-Altitude Spacecraft: Identification and Physics of the Plasma Source Region," *IEEE Transactions on Nuclear Science*, **40**, 6, 1993, pp. 1521-1524.
26. J. J. Capart and J. J. Dumesnil, "The Electrostatic-Discharge Phenomena on Marecs-A," *ESA Bulletin*, No. 34, May 1983, pp. 22-27.
27. M. Frezet, E. J. Daly, J. P. Granger, and J. Hamelin, "Assessment of Electrostatic Charging of Satellites in Geostationary Environment," *ESA Journal*, **13**, 2, 1989, pp. 89-116.
28. J. I. Vette, "*The AE-8 Trapped Electron Model Environment*," NSSDC/WDC-A-R&S 91-24, Goddard Space Flight Center, MD, 1991.
29. A. L. Vampola, "Thick Dielectric Charging on High-Altitude Spacecraft," *Journal of Electrostatics*, **20**, 1987, pp. 21-30.
30. H. C. Koons, J. E. Mazur, R. S. Selesnick, J. B. Blake, J. F. Fennell, J. L. Roeder, and P. C. Anderson, "The Impact of the Space Environment on Space System," *Aerospace Report No. TR-99(1670)-1, Appendix A*, The Aerospace Corporation, El Segundo, CA, 1999, pp. 7-9.
31. D. C. Mayer and R. C. Lacoe, "Designing Integrated Circuits to Withstand Space Radiation," *Crosslink*, The Aerospace Corporation, **4**, 2, 2003, pp. 30-35.
32. D. M. Sawyer and J. I. Vette, "AP-8 Trapped Proton Environment," *NSSDC/WDC-A-R&S 76-06*, Goddard Space Flight Center, MD, 1976.
33. J. Feynman, G. Spitale, J. Wang, and S. Gabriel, "Interplanetary Proton Fluence Model: JPL 1991*," Journal of Geophysical Research*, **98**, 8, 1993, pp. 13281-13294.
34. L. J. Lanzerotti, D. W. Mauer, H. H. Sauer, and R. D. Zwickl, "Large Solar Proton Events and Geosynchronous Communication Spacecraft Solar Arrays," *Journal of Spacecraft and Rockets*, **28**, 5, 1991, pp. 614-616.
35. D. C. Marvin and D. J. Gorney, "Solar Proton Events of 1989: Effects on Spacecraft Solar Arrays," *Journal of Spacecraft and Rockets*, **28**, 6, 1991, pp. 713-719.
36. D. J. Gorney, H. C. Koons, and R. L. Walterscheid, "Some Prospects for Artificial Intelligence Techniques in Solar-Terrestrial Prediction," *Solar-Terrestrial Predictions – IV, Proceedings of a Workshop at Ottawa, Canada, May 18-22, 1992*, Vol. 2, September 1993, pp. 550-564 (available from National Oceanic and Atmospheric Administration, Environmental Research Laboratories, Boulder, CO, U.S.A.).
37. Solar Index Data Center, Royal Observatory of Belgium, Av. *Circulaire*, **3**, B-1180 Brussels, Belgium.
38. R. A. Nymmik, "Relationships among Solar Activity, SEP Occurrence Frequency, and Solar Energetic Particle Event Distribution Functions," *Proc. 26th International Cosmic Ray Conference*, **6**, 1999, pp. 280-283.
39. G. L. Wrenn, D. J. Rodgers, and K. A. Ryden, "A Solar Cycle of Spacecraft Anomalies Due to Internal Charging," *Annales Geophysicae*, **20**, 2002, pp. 953-956.
40. H. C. Koons, "Statistical Analysis of Extreme Values in Space Science," *Journal of Geophysical Research*, **106**, A6, 2001, pp. 10915-10921.
41. R. -D. Reiss and M. Thomas, *Statistical Analysis of Extreme Values*, Boston, MA, Birkhäuser Verlag, 1997.
42. L. P. Barbieri and R. E. Mahmot, "October-November 2003's Space Weather and Operations Lessons Learned," *Space Weather*, **2**, 2004, pp. 15-29, doi:10.1029/2004SW000064.

Radio-Frequency Radiation Safety and Health

James C. Lin

Mental Process of Children and Mobile-Phone Electromagnetic Fields

Shortly before merging with and becoming a part of the Health Protection Agency's Center for Radiation, Chemical and Environmental Hazards, the National Radiological Protection Board (NRPB) in the UK issued a report with an advisory to parents: not to let children under the age of eight use mobile phones. The report was a follow-up to a similar study issued five years ago. Little had changed during that time in terms of being able to assure the safety of mobile-phone use on the public's health, the NRPB report suggested.

On the other hand, several companies have made major strides in marketing cellular mobile telephones to children during the past year. Perhaps, it is the attraction of a potentially lucrative market: the most significantly under-penetrated groups with identifiable interest in cellular mobile telephony, in the US. However, the marketing of mobile phones to youngsters has been controversial [1]. Nevertheless, more than 20 million 5- to 19-year-olds already had mobile phones by the end of 2004, according to technology research firm IDC.

Are mobile phones harmful, so that a cautious approach of risk management, especially in relation to children, should be taken? Are the brains of children more susceptible to the radio-frequency (RF) fields emitted by mobile phones than those of adults?

Some fear any disturbance to brain activity in children could lead to impaired learning ability or behavioral problems. Moreover, any lasting biochemical effects could have important consequences, especially in the young, who still have years of development ahead of them. However, there is a paucity of scientific data. Because of ethics issues concerning research studies involving children, very few studies have targeted teens or pre-teens. Thus, the questions cannot be easily answered, based on existing scientific knowledge.

In a supplement issue published in October, 2005, the *Bioelectromagnetics* journal carried two studies of young users of standard 902 MHz Global System for Mobile Communication (GSM) cellular mobile telephones: one paper reported a slight trend toward the speeding up of simple reaction time [2], whereas the other study did not detect any change in cognitive functions [3]. The phones were provided by the same manufacturer in both studies.

Some people experience difficulties with attention, remembering names, or with finding the right words, at times. These are normal, everyday lapses in cognitive functions, and are seldom mistaken as something that is more serious. However, for subjects who perform poorly on tests of several different types of cognitive function, these can be indicative of symptoms or problems that are of a more serious nature. Some investigators have reported that exposure to mobile-phone microwave fields can affect such cognitive functions as attentional function, short-term memory tasks, information manipulation, or response reaction times, in adults.

In the recent UK investigation [2], the effect on cognitive function was studied in 18 children who were 10 to 12 years of age: all were born between January, 1991, and June, 1992, on the Isle of Man. The group consisted of nine boys and nine girls, living within a 10-mile radius of the research center, and whose parents had given consent. The research protocol was reviewed and approved by the local ethics committee for human research. The response rate to the invitation to participate in the study was 100%, and all children satisfactorily completed the testing program. Exposures were from a standard Nokia 3110 mobile-phone handset, mounted on a plastic headset in normal use position. The output powers were 0 W (power off), 0.25 W peak (0.025 W mean), or 2 W peak (0.25 W mean). The SAR in the brain was approximately 0.28 W/kg, near the top (0.44 W/kg) of the range for GSM phones operating at a 0.25 W mean output power.

James Lin is with the University of Illinois-Chicago, 851 South Morgan Street (M/C 154), Chicago, Illinois 60607-7053, USA; E-mail: lin@uic.edu.

This is one of the invited *Reviews of Radio Science* from Commission K.

The study was conducted as a single group, in which each child was given a single training session, and then three test sessions in a randomized, three-way crossover design, which compared the three conditions. The only response needed was through a module with "Yes" and "No" buttons. Each test was conducted at approximately the same time of day for each child on sequential days, 24 h or 48 h after the training session. The same person tested all the children – working to a strict script and timetable – in order to minimize variation in tester influence. Each session took about 30-35 min to complete.

The cognitive drug research (CDR) cognitive assessment system was used, in a form slightly modified to suit children. The system had been extensively validated for adults to demonstrate impairment or enhancement of cognitive efficiency due to therapeutic agents. It provides a parallel series of tests, with three measures of performance: (a) reaction time in ms, (b) accuracy for percent correct, and (c) a sensitivity index, which is a measure of the effect of distracting or novel information. The sensitivity index combines the accuracy score of an original response with that of the distracted response. For example, a digit vigilance task: requiring a "Yes" response when numbers matched, a "beep" sometimes intervened and required a "No" response. The CDR cognitive assessment tests took about 30-35 min to complete.

This study found some trends toward faster reaction times, higher accuracy, and higher sensitivity in the presence of microwave radiation from a GSM mobile phone compared to the sham-exposure (power-off) condition. However, none of these effects reached statistical significance. Specifically, the study showed that the simple reaction-time measurement during sham exposure was considerably slower (p-vale = 0.02) than during exposure to 0.025 W and 0.25 W. However, the effects did not reach statistical significance after a statistical correction for multiple comparisons. Given the trend toward the longest reaction time under the sham condition, the effect of mobile-phone microwave exposure on all measures of reaction time was examined in a two-way analysis of variance. Still, none of the ten measures of reaction time approached statistical significance.

The study from Finland also investigated the potential effects of standard 902 MHz GSM mobile phones on young children's cognitive function. It recruited twice as many subjects but used a different study design, which involved a two-way counterbalance methodology. A total of 16 boys and 16 girls participated, with informed consent from one parent and the subjects themselves. The subjects were healthy native speakers of Swedish who ranged from 10 to14 years of age (mean 12.1 years, SD 1.1), and happened to be right-handed. The experiment was conducted according to the ethical guidelines and procedures stated in the principles of professional ethics for psychologists in the Nordic countries. The subjects performed a battery of eight cognitive tests twice in a counterbalance order: while exposed to a mobile phone with power on, and during exposure to an inactive phone. The tests were selected from those used by the research team earlier with adults, which consisted of four reaction-time tasks and four short-term memory tests. In all the tasks, the subjects were instructed to react to the stimuli presented on a computer screen by pressing a specific button of the computer keyboard as quickly and accurately as possible. Each task was preceded by a practice task, and each stimulus was presented until the subject responded or 2 s had elapsed.

Each subject performed the tasks twice, in separate sessions, with the mobile phone on, and with the mobile phone off for sham exposure. These sessions were separated by 24 hours. The study employed a double-blind design, in which both the subject and the experimenter were unaware of the exposure condition. Moreover, the order of exposure was counterbalanced over subjects and sex. The phone, in a leather and vinyl case, was held in the normal-use position on the left side of the head, fitted with an adjustable rubber cap. The average 10-g and 1-g SARs were 0.99 and 1.44 W/kg, respectively, on the cheek approximately 2 cm anterior and 1 cm inferior to the auditory canal, with a maximum value of 2.07 W/kg for the typical 0.25 W emitted power from GSM mobile phones. The duration of the RF or sham exposure for each session was approximately 50 min. The loudspeaker for the phone was removed to eliminate any auditory cues to the exposure condition. The temperature between the mobile phone and the skin was measured with a thermocouple sensor for four subjects. An average difference of 0.1°C was measured in the temperature rise between the phone and skin for a 50-min RF or sham exposure. Since the thermocouple was in the RF field from the mobile phone, its use could have interfered with the thermocouple's normal operation. Indeed, an initial temperature rise was observed. This was followed by a gradual change, which showed little variation with the RF-exposure condition. It is conceivable that the initial rise in skin temperature could have served as a thermal cue to the RF-exposure condition. It is interesting to note that the subject's ability to detect the power-on status of mobile phones was not statistically more accurate in the estimates of the phone's power-off status. Also, there were no statistically significant differences between genders, nor with the order of RF exposure.

Also, the statistical analyses showed no significant differences between the mobile-phone power on-off conditions in reaction times or response accuracy over all tests or in any one of the tasks. Moreover, there were no systematic directional differences in reaction time and accuracy across exposure conditions: In some tasks, subjects performed faster and more accurately during the mobile-phone on condition, while in others, the opposite was observed. Thus, it was concluded that RF electromagnetic energy from a standard GSM mobile phone has no effect on 10-14 year olds' cognitive function, as measured by response time and accuracy.

Comparing the results of this study to those of the UK investigation, it should be noted that SARs from the two studies cannot be directly compared. Measurements in the UK study were for maximum SAR in brain tissues, not the maximum values for tissues on the cheek that were given for the Finish study. But the maximum output power was used for the standard factory models of GSM mobile phones. In both studies, the acoustic transducers in the phones were removed to eliminate any auditory cues to the exposure condition. Also, the procedure removed a potentially confounding low-level buzzing sound under high-power operations.

While one of the two cognitive-function studies of young users of standard 902 MHz GSM mobile phones found some trends toward faster reaction times, higher accuracy, and higher sensitivity in the presence of microwave radiation from mobile-phone exposure than under sham exposure conditions, none of these effects reached statistical significance. Moreover, the other study did not detect any change in cognitive functions.

It should be noted that both studies were limited to the acute effects of mobile phones on a battery of cognitive functions of children. Ethical considerations of research involving youngsters have kept the numbers of subjects small in both studies, which must be regarded as initiatory and preliminary. Nevertheless, these limitations make it difficult to draw any firm conclusions concerning the sensitivity of young children to microwave radiation from mobile phones.

Undoubtedly, discussions on the ethical aspects of using children as research subjects will continue. Likewise, the trend of mobile-phone use remains: more and more children are using mobile phones as part of their daily routines. Thus, the research needed – to establish whether biological effects or cognitive changes occur in children from mobile-phone microwave exposure, and at what level they could occur – has to rely primarily on laboratory investigations using young animals, conducted with properly designed protocols and expertly carried out in a number of independent laboratories. Otherwise, NRPB's advice to parents not to let children under the age of eight use mobile phones may continue to fall on receptive ears and to remain a source of controversy.

References

1. J. C. Lin, "Radio-Frequency Radiation Safety and Health: Children and the Risk of Mobile Telecommunication ," *URSI Radio Science Bulletin*, 305, 2003, pp. 46-49.
2. A. W. Preece , S. Goodfellow, M. G. Wright, S. R. Butler, E. J. Dunn, Y. Johnson, T. C. Manktelow, and K. Wesnes, "Effect of 902 MHz Mobile Phone Transmission on Cognitive Function in Children," *Bioelectromagnetics*, Supplement, **7**, 2005, pp. S138-S143.
3. C. Haarala, M. Bergman, M. Laine , A. Revonsuo, M. Koivisto, and H. Hämäläinen, "Electromagnetic Field Emitted by 902 MHz Mobile Phones Shows No Effects on Children's Cognitive Function," *Bioelectromagnetics*, Supplement, **7**, 2005, pp. S144-S150.

News from ITU-R

The Current Status of Studies within ITU-R Study Group 7 (Science Services)

Studying the past, the present and the future: These words, to a certain extent, reflect the ITU-R Radiocommunication Study Group 7 (SG 7) terms of reference and its main activities.

ITU-R Study Group 7 is named "Science services," where "services" refer to those of standard frequency and time signals, space research, space operation, remote sensing using Earth exploration satellite, meteorological satellite (MetSat), meteorological aids (MetAids), and radio astronomy (RAS).

Although the services are qualified by the word "science," we use information provided by them every day when we read the weather forecast (to check whether we need an umbrella or not), use the telephone, operate a computer, watch television, switch on a radio-controlled alarm, take a plane, etc. In particular, the services involve:

- Studies of the Universe and its origins and searching for extraterrestrial intelligence;
- Dissemination, reception, and exchange of standard frequency and time signals, which are used by industry (telecommunications, computers, etc.) and by everyone in everyday life;
- Studies of radio communication systems and applications for use with manned and unmanned spacecraft (including those embedded in the space suits of astronauts); communication links between satellites and planetary bodies, and the transmission/reception of tele-command, tracking, and telemetry data;
- Studies of the Earth's environment (soil moisture, salinity, water vapor, ocean ice, oil spills, chemicals, forest fire, etc.) and climate (rain, snow, ice, winds, ocean topography, etc.), and carrying out scientific and meteorological measurements (temperature, atmospheric pressure, ocean surface temperature, wind speed, cloud coverage, weather forecasting, hurricane tracking), etc.

ITU-R Study Group 7 consists of four Working Parties (WP):

- WP 7A: Time signals and frequency standard emissions
- WP 7B: Space radio communication applications[1]
- WP 7C: Remote sensing systems[2]
- WP 7D: Radio astronomy

SG 7 addresses different aspects of spectrum management relevant the above-mentioned services, such as spectrum requirements and operational aspects and the protection of systems from unwanted emissions, taking into account the technical characteristics.

The Study Group has a direct bearing on prediction, detection, and radio communications relating to disasters and emergencies. The meteorological aids, meteorological-satellite, and Earth-exploration-satellite services play a major role in the prediction and detection of disasters, and in retrieving and relaying data from monitoring equipment (e.g., on buoys) to land-based siren systems. More advanced systems involve remote sensing of the ocean temperature, the variations of which can be linked with seismic activity.

The systems linked with Study Group 7 are used in activities such as:

- weather forecasting and climate change prediction
- detection and tracking of earthquakes, tsunamis, hurricanes, forest fires, oil leaks;
- providing alerting/warning information;
- damage assessment;
- providing information for planning relief operations.

In support of further development of the services relevant to the prediction and detection of disasters, as well as supporting the regulatory decisions made at World Radiocommunication Conferences (WRC), Study Group 7 has developed many texts, e.g., Recommendations and Reports, which address the technical characteristics of the services concerned, as well as related spectrum issues.

Further information concerning SG 7 activities may be obtained from the SG 7 Web page, at

http://www.itu.int/ITU-R/study-groups/index.asp?link=rsg7&lang=en.

Recognizing the importance of the above-mentioned studies, and in order to provide a new generation of systems belonging to "Science services" with the required spectrum and protection, the World Radiocommunication Conference 2003 (WRC-03) proposed including in the agenda of the next conference, WRC-07, several agenda items relevant to these services. They are:

- Agenda item 1.2: *concerning* allocations and related regulatory issues for EESS (passive), SRS (passive), and MetSat in the frequency bands 18.1-18.4 GHz, 10.6-10.68 GHz, and 36-37 GHz *(of which one of the major issues is the allocation of an additional 100 MHz for EESS and SRS in 18.0-18.4 GHz band);*

- Agenda item 1.3: *concerning* extended allocation to EESS (active) and SRS (active) in the 9500-9800 MHz band *(additional allocation of 200 MHz)*;

- Agenda item 1.20: *concerning* protection of EESS (passive) (in the bands 1400-1427 MHz, 23.6-24, 31.3-31.5, 50.2-50.4 GHz) from unwanted emissions of active services;

- Agenda item 1.21: *concerning* compatibility between radio astronomy and active space services in order to review and update threshold levels used for consultation.

In carrying out the relevant studies in accordance with the requests from the Radiocommunication Assembly and WRC-03, Working Parties of ITU-R Study Group 7 have held five series of meetings since 2003 (except WP 7A, which had 3 meetings) that resulted in drafts of:

- 7 new and 10 revised ITU-R Recommendations;
- 4 new and 1 revised ITU-R Questions;
- 4 new ITU-R Reports.

All these texts were considered at a meeting of Study Group 7, held in conjunction with those of the WPs, during the period 7 to 15 November, 2005, in Geneva. Further details of the outcome of these meetings are given below.

1. Working Party 7A: Time Signals and Frequency Standard Emissions

WP 7A covers standard frequency and time signal services, both terrestrial and satellite. Its scope includes the dissemination, reception and exchange of standard frequency and time signals and coordination of these services, including the application of satellite techniques on a worldwide basis.

WP 7A developed drafts of two new ITU-R Questions, which were adopted by SG 7:

- Interference between standard frequency and time signal services operating between 20 and 90 kHz

- Interference to standard-frequency and time signal services in the low-frequency band caused by noise from electrical sources

One of the most important and the most controversial areas of study that WP 7A has undertaken since 2000 relates to a possible revision of Recommendation ITU-R TF.460-6. This recommendation defines and describes the use of Coordinated Universal Time (UTC) for radio communication and telecommunication purposes. The implication of changes to the UTC time scale, or identification of an alternative time scale, could have a significant impact on radio communication, telecommunication, and computer systems.

At the WP 7A meeting in October 2004, a contribution on the future of UTC proposed:

a) to discontinue the insertion of leap seconds on the UTC time scale starting from December 2007;

b) to allow the maximum difference between UT1 (based on the Earth's rotation) and UTC to increase from the current value of ±0.9 second to ±1 hour, the consequence of which being that no correction would occur for several centuries given the present behavior of the Earth.

As a reaction to the proposal, further contributions were discussed at the meeting of WP 7A held in November, 2005. However, since no clear consensus emerged, it has been decided that more time is required for studying the matter.

WP 7A developed the Handbook "Selection and Use of Precise Frequency and Time Systems," available at

http://www.itu.int/publications/publications.aspx?lang=en&parent=R-HDB-31

which describes basic concepts, frequency and time sources, measurement techniques, characteristics of various frequency standards, operational experience, problems, and future prospects. Currently, experts in WP 7A are preparing a new edition of this handbook.

2. Working Party 7B: Space Radiocommunication Applications

WP 7B is responsible for space operation, space research, Earth exploration-satellite, telemetry, and MetSat telemetry. It studies communication systems for use with manned and unmanned spacecraft; communication links between planetary bodies; the use of data relay satellites; and the transmission and reception of tele-command, tracking, and telemetry data. Within this scope, WP 7B helps enable the implementation of both scientific studies and technology programs by means of efficient use of the radio-frequency spectrum.

Based on the results of the latest studies, WP 7B prepared drafts of three new and four revised ITU-R Recommendations, which were subsequently considered by SG 7:

- New Recommendation ITU-R SA.[THz]: Technical and operational characteristics of interplanetary and deep-space systems operating in the space-to-Earth direction around 283 THz.

- New Recommendation ITU-R SA.[MET 18 GHz]: System characteristics and sharing criteria for meteorological satellite systems operating around 18 GHz *(discussion to be continued)*;

- New Recommendation ITU-R SA.[Int.Budget]: Maximum allowable degradation to radio communication links of the space research and space operation services arising from interference from emissions and radiations from other sources;

- Revision of Recommendation ITU-R SA.609-1: Protection criteria for telecommunication links for manned and unmanned near-Earth research satellites;

- Revision of Recommendation ITU-R SA.1157: Protection criteria for deep-space research;

- Revision of Recommendation ITU-R SA.1014: Telecommunication requirements for manned and unmanned deep-space research;

- Revision of Recommendation ITU-R SA.1159-2; Performance criteria for data dissemination, data collection and direct data readout systems in the Earth exploration-satellite service and meteorological-satellite service.

Working Party 7B also compiled several new ITU-R Reports concerning technical and operational aspects of space radio communication applications. These reports were adopted by SG 7:

- Report SA.[SRS 14GHZ]: Use of the 13.75 to 14.0 GHz band by the space research service and the fixed-satellite service;

- Report ITU-R SA.[S-VLBI]: Protection of the space VLBI telemetry link;

- Report ITU-R SA.[VIS STAT]: Means of calculating low-orbit satellite visibility statistics.

WP 7B is also developing a draft of Report ITU-R SA.[MARS NETWORK]: A telecommunication relay network for Mars exploration.

Further information on space research systems is documented in the Space Research Communications Handbook, available at

http://www.itu.int/publications/publications.aspx?lang=en&parent=R-HDB-43

which presents the basic technical and spectrum requirements for the many different space research programs, missions, and activities. It discusses space research functions and technical implementations, factors that govern frequency selection for space research missions, and space research protection and sharing considerations.

3. Working Party 7C: Remote Sensing Systems

WP 7C covers remote-sensing applications in the Earth-exploration-satellite service (EESS), both active and passive, systems of the MetSat and MetAids services, as well as space research sensors, including planetary sensors.

The sharp demand for greater precision in weather forecasting and prediction of climate change, coupled with significant technological progress in Earth exploration and meteorological studies, has resulted in a considerable increase in the amount of data used by EESS and MetSat systems. That is why WP 7C is considering the possibility of implementing future meteorological systems in optical frequency bands and, as a result, has developed a draft new Recommendation ITU-R RS~~SA~~.[OPTICAL METAIDS]: Technical and operational characteristics of ground-based meteorological aids systems operating in the frequency range 272-750 THz. WP 7C has also completed studies and submitted to SG 7 the following drafts of new and revised ITU-R Recommendations:

- Draft revised Recommendation ITU-R RS~~SA~~[3].577-5: Preferred frequencies and required bandwidths for spaceborne active sensors operating in the Earth exploration-satellite (active) and space research (active) services;

- Draft revision of Recommendation ITU-R RS~~SA~~[3].1165-1: Technical characteristics and performance criteria for systems in the meteorological aids service in the 403 MHz and 1680 MHz bands;

- Draft revision to Recommendation ITU-R RS~~SA~~[3].1166-2: Performance and interference criteria for spaceborne active sensors;

- Draft new Recommendation ITU-R RS~~SA~~[3].[USE 1.7 GHz]: Use of the band 1668.4-1710 MHz by the meteorological aids service and meteorological-satellite service (space-to-Earth)

- Draft new Recommendation ITU-R RS~~SA~~[3].[MITIGATE]: Mitigation technique to facilitate the use of the 1215-1300 MHz band by the Earth exploration-satellite service (active) and the space research service (active).

WP 7C has also proposed one new and one revised ITU-R Questions:

- New Question ITU-R [MITIGATION]: Characterization of technical parameters and interference effects and possible interference mitigation techniques for passive sensors operating in the Earth exploration-satellite service (passive);

- Revision of Question ITU-R 235/7: Technical and operational characteristics of applications of science services operating above 275 GHz.

Draft new Report ITU-R RS~~SA~~.[ACTIVE 13.5 GHz] Active sensing near 13.5 GHz was considered and approved by SG 7.

WP 7C, in cooperation with the World Meteorological Organization (WMO), is compiling a new version of the Handbook "Use of Radio Spectrum for Meteorology," which describes modern meteorological systems, tools, and methods, available at

http://www.itu.int/publications/productslist.aspx?lang=e&CategoryID=R-HDB&product=R-HDB-45

Another Handbook is in preparation on the Earth exploration satellite service, which will complement the handbook on the use of radio spectrum for meteorology.

4. Working Party 7D: Radio Astronomy

WP 7D covers radio aspects of the radio astronomy service. Its scope includes radio astronomy and radar astronomy sensors, both Earth-based and space-based, including space very-long-baseline interferometery (space-VLBI).

Several drafts of new and revised RA-Series of ITU-R Recommendations were submitted to SG 7 and sent to ITU-R Member States for adoption/approval. They are:

- New Recommendation ITU-R RA.[EESS-RAS]: Mutual planning between the EESS (active) and the RAS in the 94 GHz and 130 GHz bands;

- Revised Recommendation ITU-R RA.611: Protection of the radio astronomy service from spurious emissions;

- Revised Recommendation ITU-R RA.517-3: Protection of the radio astronomy services from transmitters operating in adjacent bands.

WP 7D proposed a new ITU-R Question concerning radio quiet zones. The second edition of the Radio Astronomy Handbook, available at

http://www.itu.int/pub/R-HDB-22/en

developed by WP 7D provides many details on the use of the radio spectrum for radio astronomy.

ITU-R Radiocommunication Study Group 7 is also developing text for the CPM (Conference Preparatory Meeting) Report to be considered by CPM-07 in the first quarter 2007.

Alexandre V. Vassilliev
Kevin A. Hughes
ITU Radiocommunication Bureau
E-mail: kevin.hughes@itu.int

[1] Previously "Space radio systems," WP 7B was renamed at the November, 2005, SG 7 meeting.

[2] Previously "Earth exploration-satellite service (EESS) and meteorological elements," WP 7C was renamed at the November, 2005, SG 7 meeting.

[3] Study Group 7 decided to introduce new RS-Series of ITU-R Recommendations and Reports for remote sensing. This recommendation, as well as other ITU-R Recommendations and Reports concerning remote sensing systems, will use the acronym RS (e.g., Recommendation ITU-R RS.577).

IUCAF Annual Report for 2005

1. Introduction

The Scientific Committee on Frequency Allocations for Radio Astronomy and Space Science, IUCAF, was formed in 1960 by URSI, IAU, and COSPAR. Its brief is to study and coordinate the requirements of radio frequency allocations for passive (i.e., non-emitting) radio sciences, such as radio astronomy, space research and remote sensing, in order to make these requirements known to the national and international bodies that allocate frequencies. IUCAF operates as a standing inter-disciplinary committee under the auspices of ICSU, the International Council for Science.

2. Membership

At the end of 2005 the composition of membership for IUCAF was:

URSI	S. Reising (Com F)	USA
	U. Shankar (Com J)	India
	W. Swartz (Com G)	USA
	A. Tzioumis (Com J)	Australia
	W. van Driel (Com J,Chair)	France
IAU	H. Chung	Korea
	R.J. Cohen	UK
	D.T. Emerson	USA
	M. Ohishi	Japan
	K.F. Tapping	Canada
COSPAR	J. Romney	USA
at large:	W.A. Baan	Netherlands
	K. Ruf	Germany

IUCAF also has a group of Correspondents, in order to improve its global geographic representation and for issues on spectrum regulation concerning astronomical observations in the optical and infrared domains.

3. International Meetings

During the period of January to December 2005, its Members and Correspondents represented IUCAF in the following international meetings:

February:	ITU-R Task Group 1/9 (Compatibility between passive and active services) in Geneva, Switzerland
March:	ITU-R Working Party 7D (radio astronomy) in San Diego, USA
May:	ITU-R Task Group 1/8 (Compatibility between ultra-wideband devices (UWB) and radiocommunication services) in San Diego, USA
June:	Second Summer School in Spectrum Management for Radio Astronomy in Castel San Pietro, Italy
September:	ITU-R Task Group 1/9 (Compatibility between passive and active services) in Geneva, Switzerland
October:	ITU-R Task Group 1/8 (Compatibility between ultra-wideband devices (UWB) and radiocommunication services) in Geneva, Switzerland
	Space Frequency Coordination Group meeting SFCG-25 in Beijing, China
	URSI General Assembly in New Delhi, India
November:	ITU-R Working Party 7D (radio astronomy) in Geneva, Switzerland

Additionally, many IUCAF members and Correspondents participated in numerous national or regional meetings (including CORF, CRAF, RAFCAP, the FCC etc.), dealing with spectrum management issues.

3.1 IUCAF Business Meetings

During the year 2005 IUCAF had a face-to-face committee meeting before each of the ITU meetings of Working Parties and Task Groups of relevance to IUCAF, with the purpose of discussing issues on the agenda of the meetings in preparation for the public sessions. During these ITU sessions, typically lasting a week to 10 days, a number of ad-hoc meetings of IUCAF are held to discuss further its strategy. Other IUCAF business, such as action plans for future workshops and summer schools or initiatives and future contributions to international spectrum management meetings, are also discussed.

Although such face-to-face meetings have been convenient and effective, throughout the year much IUCAF business is undertaken via e-mail communications between the members and correspondents.

4. Contact with the Sponsoring Unions and ICSU

IUCAF keeps regular contact with the supporting Unions and with ICSU. The Unions play a strong supporting role for IUCAF and the membership is greatly encouraged by their support.

IUCAF members actively participated in national URSI meetings, in IAU Colloquia and Symposia and in the 2005 URSI General Assembly.

IUCAF members are actively involved in the work of the URSI Scientific Commission on Telecommunication (SCT), whose brief is to form a liaison in matters of spectrum management between URSI and the International Telecommunication Union (ITU).

IUCAF members have played an active role in the redaction of the URSI White Paper on Solar Power Satellites (SPS). IUCAF's objective was to ensure that a White Paper published by URSI presents a balanced discussion of the SPS technology, including an honest comparison with other competing technologies and an evaluation of the risks involved, in particular to radio science. Unwanted radio emissions from SPS systems must be suppressed sufficiently to avoid interference with other radio services and applications, in accordance with the provisions of the Radio Regulations of the ITU.

In 2005, IUCAF has been working actively towards strengthening its links with other passive radio science communities and defining a concerted strategy in common spectrum management issues.

5. Protecting the Passive Radio Science Services

At the International Telecommunication Union, the work in the various Working Parties and Task Groups of interest to IUCAF was focused largely on the preparations for WRC-07, the ITU World Radiocommunication Conference to be held in 2007.

Of particular concern to IUCAF in ITU-R Working Parties 7C and 7D, specializing in Earth exploration by satellites and in radio astronomy, respectively, is the protection of the 1400-1427 MHz passive band, which is used to measure soil moisture and ocean salinity and which contains the heavily observed interstellar 21-cm neutral hydrogen line, from unwanted emissions from fixed-satellite service (FSS) feeder links in the nearby bands 1 390-1 392 MHz and 1 430-1 432 MHz. Studies have suggested suppressing these frequency allocations to the FSS, and a decision on this issue will be made at WRC-07.

ITU-R Task Group 1/8, which finished its work in 2005, dealt with the introduction of unregistered low power ultra-wide bandwidth (UWB) devices (including vehicular anti-collision radars) transmitting across large parts of the radio spectrum, into bands that are already allocated to a variety of other services and in some of which "all emissions are prohibited" according to the ITU Radio Regulations. Studies have shown that unless appropriately controlled, the operation of such devices is likely to be harmful to the passive radio services.

ITU-R Task Group 1/9 deals with the protection of passive services, specifically the radio astronomy service and the Earth exploration-satellite (passive) service, from unwanted emissions of active services in adjacent and nearby bands. Its goal is to review and update, if appropriate, the tables of threshold levels used for consultation between the passive radio and active services that appear in Recommendation ITU-R SM.1633. Of particular concern to IUCAF is the protection of the 1610.6-1613.8 MHz and 22.21-22.5 GHz radio astronomy bands, which contain spectral lines of important interstellar molecules.

Within the Space Frequency Coordination Group, IUCAF has worked towards a Resolution on the sharing of the band 94-94.1 GHz between the radio astronomy service and Space agencies operating powerful satellite-borne cloud profile radars, which can potentially damage, and even destroy, receivers in radio telescopes observing in the direction of such radars. In particular, IUCAF is serving as the international coordination point between radio observatories and the operators of the Cloudsat radar.

6. IUCAF-Sponsored Meetings

The Second Summer School in Spectrum Management for Radio Astronomy was held in Castel San Pietro, Italy, from 6 to 10th June, 2005. Its main sponsors were IUCAF and RadioNet, the European Commission-funded Integrated Infrastructure Initiative (I3) for advanced radio astronomy in Europe.

The purpose of SS2005 was to offer a comprehensive view of both regulatory and technical issues related to the radio astronomers' use of the spectrum, as well as a view of how these issues are dealt with by other passive radio services, such as the Earth exploration satellite service. It was aimed specifically at young scientists and engineers involved in radio astronomy.

The number of participants (21), the quality and scope of the presentations all showed the importance that the astronomical community attributes to spectrum management as a tool necessary for maintaining the quality of radio astronomical data by limiting the levels of radio interference.

7. Publications and Reports

IUCAF has a permanent web address, http://www.iucaf.org , where the latest updates on the organization's activities are made available. All contributions to IUCAF-sponsored meetings are made available on this website.

8. Conclusion

IUCAF interests and activities range from preserving what has been achieved through regulatory measures or mitigation techniques, to looking very far into the future of high frequency use and giant radio telescope use. Current priorities, which will certainly keep us busy through the next years, include band-by-band studies for cases where allocations are made to satellite down-links close in frequency to the radio astronomy bands, to satellite up-links and terrestrial radio services in the vicinity of bands allocated to the Earth Exploration Satellite Service(passive), the coordination of the operation in shared bands of radio observatories and powerful transmissions from downward-looking satellite radars, the possible detrimental effects of ultra-wide band transmissions on all passive services, and studies on the operational conditions that will allow the successful operation of future giant radio telescopes.

IUCAF is thankful for the moral and financial support that has been given for these continuing efforts by ICSU, URSI, the IAU, and COSPAR during the recent years. IUCAF also recognizes the support given by radio astronomy observatories, universities and national funding agencies to individual members in order to participate in the work of IUCAF.

Wim van Driel, IUCAF Chair
Meudon, France
March 6, 2006
IUCAF website: http://www.iucaf.org
IUCAF contact: iucafchair@iucaf.org

Conferences

CONFERENCE REPORTS

Multiconference on Advanced Optoelectronics and Lasers - CAOL'2005

Yalta, Crimea, Ukraine 12 - 17 September 2005

The 2nd IEEE/LEOS International Multiconference on Advanced Optoelectronics and Lasers, CAOL'2005 was held from 12th to 17th of September, in resort "Russia". The Crimean city Yalta is famous in the world for its unique, salubrious climate and even greater for a historic Conference in Yalta which summed up the World War II as well as laid the foundation of post-war period. It had been held in Livadia Palace in February, 1945. Just taking into consideration the Yalta's fame, this city was chosen for holding regular Conference on Advanced Optoelectronics and Lasers.

These Conference was organized by the Kharkov National University of Radio Electronics in collaboration with V. N. Karazin National University, Ukraine, University of Guanajuato, Mexico as well as with other scientific centres. 2005 Multiconference included 3 conferences: 2nd Conference "Advanced Optoelectronics and Lasers" (CAOL'2005); 7th Conference "Laser and Fiber Optical Networks Modeling" (LFNM'2005) (held from 1999); 2nd Conference "Precision Oscillations in Electronics and Optics", POEO 2005. Both these accompanying events organically supplement and extend the circle of the participants from the point of view of the application of theoretical methods and computer modeling of optoelectronic and laser systems as well as neighboring areas which are currently developed in optoelectronics. It should be noted that POEO conference is a unique one in its way, since it joins specialists on precision signal processing and optics, where these problems become more important.

In Yalta, it was presented scientific organizations from 37 countries. The quantity of presented from 5 continents papers made up 216 including: West and Central Europe – 28, America – 5, Asia – 12, Australia – 1, Africa – 2. As usual, around two thirds of participants were from CIS – 168, among them Belorussia – 18, Russia – 63, Ukraine – 87.

Fig 1 Joint conference photo

The topics of the Multiconference embraced mathematical, physical and technical problems of modern laser physics, photonics, optics and signal processing. The most fully it was presented directions concerning semiconductor nanoengineering and photonic crystals, nonlinear optics as well as optical measurements, wave distribution in optical systems and precision oscillations.

Conference proceedings with the volume of 1000 pages has been published before the conference beginning and include 2 volumes of CAOL Proceedings (672 pages) and 1 volume of LFNM Proceedings with a volume of 328 pages. At that, more than 350 papers have been submitted from which 279 papers have been accepted.

During a week, participants had an opportunity to exchange ideas, communicate not only at the time of plenary, section or poster sessions but also in informal atmosphere, in the beach and, of course, at conference banquet. Contacts of well-known scientists with PhD students and students who constituted one third out of general number of participants were especially wholesome.

It can be concluded that the Multiconference met with success. It showed a great potential in continuing investigations in the photonics area that opens possibilities to develop new generation of optoelectronic devices for various applications. In particular, this potential contains in works related to photonic crystals and devices based on them, creation of new nanolasers and other active elements based on quantum-confined structures, creation of ultrabroadband systems and data transmission devices, including those for application in optical computers.

Lastly, the conference CAOL would not be possible without collaboration and supporting of our sponsors. The financial support obtained from URSI, USAF and technical help received from IEEE/LEOS, EOS, local chapters of IEEE and SPIE has allowed solving many organization difficulties in the beginning of conference preparation, as well as providing travel grants to invite speakers and young scientists from Ukraine, Belarus, Russia.

All information about last and future conferences of these series you can find on the web site http://lfnm.kture.kharkov.ua/ and http://caol.kture.kharkov.ua/

Igor A. Sukhoivanov
i.sukhoivanov@ieee.org

CONFERENCE ANNOUNCEMENT

International Symposium on Recent Observations and Simulations of the Sun-Earth System (ISROSES)

Varna, Bulgaria, 17 - 22 September 2006

We cordially invite you to participate in the International Symposium on Recent Observations and Simulations of the Sun-Earth System (ISROSES). This symposium will be held in the five-star "Grand Hotel Varna" located in the famous Bulgarian seaside resort "St Konstantin and Elena" near the beautiful city of Varna, Bulgaria, during 17-22 September, 2006.

The main objective of this symposium is to bring together scientists from solar, heliospheric, magnetospheric, and earth sciences communities worldwide to present and discuss recent advances in modeling and observations of the Sun-Earth System (SES). The meeting will enable better communication amongst these communities of scientists, and will stimulate fruitful discussions to improve present understanding of solar dynamics and the response of geospace. Papers on wave-particle interactions and the role of waves in understanding the solar-magnetosphere-ionosphere-atmosphere system are encouraged. A special issue of the Journal of Atmospheric and Solar-Terrestrial Physics (JASTP) is planned to publish papers presented at this meeting.

Scientific Organizing Committee

1. Tom Bogdan, NCAR, Boulder, Colorado, USA
2. Joe Borovsky, LANL, Los Alamos, New Mexico, USA
3. Charles Farrugia, University of New Hampshire, Durham, New Hampshire, USA
4. Klaus Galsgaard, Niels Bohr Institute, Copenhagen, Denmark
5. Joe Giacalone, University of Arizona, Tucson, Arizona, USA
6. Tamas Gombosi, University of Michigan, Ann Arbor, Michigan, USA
7. Marcel Goossens, Katholieke Universiteit Leuven, Leuven, Belgium
8. Nat Gopalswamy, NASA/GSFC, Greenbelt, Maryland, USA
9. Richard Horne, British Antarctic Survey, Cambridge, UK
10. Vladimir Kuznetsov, IZMIRAN, Russian Academy of Sciences, Russian Federation

11. Dora Pancheva, University of Bath, Bath, UK
12. Judit Pap, NASA/GSFC, Greenbelt, Maryland, USA
13. Nathan Schwadron, Boston University, Boston, Massachusetts, USA
14. David Sibeck, NASA/GSFC, Greenbelt, Maryland, USA

The Conference Conveners are Vania Jordanova (Los Alamos National Laboratory, Los Alamos, NM, USA; vania@lanl.gov) and Ilia Roussev (University of Hawaii at Manoa, Honolulu, HI, USA; iroussev@ifa.hawaii.edu)

Important Dates

1 April 2006: Deadline for abstract submissions.
1 April 2006: Deadline for travel support applications.
1 May 2006: Deadline for early bird registration.

Further information about this meeting may be found at: http://www.isroses.org/

Eleventh International Workshop on Technical and Scientific Aspects of MST Radar (MST 11)

Gadanki/Tirupati, India, 11 - 15 December 2006

The international workshop on MST radar, held about every 2-3 years, is a major event that gathers together experts from all over the world, engaged in research and development of radar techniques to study the mesosphere, stratosphere, troposphere (MST) and the ionosphere. It also offers excellent opportunities to young scientists, research students and new entrants to the field for close interaction with the experts on the technical and scientific aspects of MST radar techniques.

The eleventh MST radar workshop – MST 11 - will focus on the following topics, which are somewhat extended as compared to the previous workshops:

- Radar scattering processes in the atmosphere and ionosphere
- Wind and temperature deduction in the lower and middle atmosphere
- Gravity waves, momentum flux, and turbulence
- Meteorological phenomena in tropical, middle and polar latitudes
- Wind profiler applications
- Stratosphere-troposphere exchange
- Scientific, technical and signal processing achievements, new developments and highlights from the MST radar facilities and wind profilers from around the world.
- MF and meteor radar science, and technology
- Coherent ionospheric scatter radars (PMSE, Sporadic E layers, ESF, EEJ)
- Contributions of MST/ST radars and radio occultation technique for studies of lower, middle and upper atmosphere
- Radar networks
- Multi-instrument studies with strong MST radar involvement
- Input of MST radars to CAWSES and IPY

As during the MST10 workshop, a brain-storming session on novel perspectives and unsolved issues will be held at MST 11, with the aim to highlight open questions and potential solutions, to generate proposals for innovative approaches, define new programs and offer recommendations.

We also expect some input from the Permanent Working Groups of the MST radar community on:
(1) System Calibration and Definitions
(2) Data Analysis, Validation and Parameter Deduction Methods
(3) Accuracies and Requirements for Meteorological Applications
(4) International Collaborations

The MST 11 workshop will be held in Gadanki/ Tirupati, India. Tirupati is close to the Indian MST radar facility at Gadanki, which has been recently renamed as National Atmospheric Research Laboratory (NARL). NARL is known for its operation of the high sensitivity MST radar and co-located instrumentation. Tirupati is a lively Indian city with high-standard hotels and modern facilities, and can be reached from Chennai International Airport (formerly Madras) in three hours by car.

The International Steering Committee, which is presently preparing MST 11, consists of J.L. Chau (Peru), K.S. Gage (USA), W.K. Hocking (Canada), E. Kudeki (USA), D. Narayana Rao (India), I. Reid (Australia), J. Röttger (Germany) and T. Tsuda (Japan),

The National and Local Organizing Committees are being established with our Indian colleagues by Prof. D. Narayana Rao.

The Scientific and Technical Program Committee is being created to plan the sessions before the release of the Second Circular.

The Eleventh International Workshop on Technical and Scientific Aspects of MST Radar – MST 11 - will be co-sponsored by the Scientific Committee on Solar Terrestrial Physics (SCOSTEP), the International Union of Radio Science (URSI Commissons F and G) and other bodies t.b.d., as being done in the past.

Those who are interested in attending the MST11 and would like to receive the Second Circular of MST11, may please send an e-mail to: profdnrao@narl.gov.in by March 31, 2006

Please include the following in your mail: 1. Name and affiliation, 2. Complete postal address, 3. Telephone and fax numbers including the international code, 4. E-mail address, 5. An indication whether you are planning to present paper(s), 6. Potential topic of your paper(s).

The **Second Circular of MST11**, which will be distributed in April 2006, will contain details about abstract submission and the deadlines, the venue, logistics etc. for the meeting.

URSI CONFERENCE CALENDAR

May 2006

ISSTT 2006 - International Symposium on Space Technologies
Paris, France, 10-12 May 2006
Contact : Chantal Levivier, ISSTT 2006, Observatoire de Paris, 61, avenue de 'lObservatoire, F-75 014 Paris, France, E-mail : isstt2006@mesiog.obspm.fr, Web : http://wwwusr.obspm.fr/gemo/ISSTT06/Accueil/PageAccueil.html

EUSAR 2006 - 6th European Conference on Synthetic Aperture Radar
Dresden, Germany, 16-18 May 2006
Contact: VDE CONFERENCE SERVICES, Stresemannallee 15, D-60596 Frankfurt am Main, Germany, Tel. : +49 69-63 08-275 / 229, Fax: +49 69-96 31 52 13, E-mail : vde-conferences@vde.com , Web : http://www.eusar.de

June 2006

11th Workshop on the Physics of Dusty Plasmas
Williamsburg, Virginia, USA, 28 June - 1 July 2006
cf. announcement in the Radio Science Bulletin of December 2005, p. 52
Contact : Dr. W.E. Amatucci, Space Experiments Section, Plasma Physics Division, Code 6755, Naval Research Laboratory, Washington, DC 20375, USA, Tel. : +1 202 404 1022, Fax : +1 202 767 3553, E-mail : bill.amatucci@nrl.navy.mil , Web : http://www.conted.vt.edu/dustyplasma

July 2006

Workshop on Waves and Turbulence Phenomena in Space Plasmas
Kiten, Bulgaria, 1-9 July 2006
Contact : Prof. Ivan Zhelyazkov, Sofia University, Faculty of Physics, 5 James Bourchier Blvd, BG-1164 Sofia, Bulgaria, Fax +359 2-9625 276, E-mail : izh@phys.uni-sofia.bg

36th COSPAR Scientific Assembly
Beijing, China, 16-23 July 2006
cf. announcement in the Radio Science Bulletin of June 2005 p. 85
Contact : COSPAR Secretariat, 51, bd. de Montmorency, F-75016 Paris, France, Tel : +33-1-45250679, Fax : +33-1-40509827, E-mail : cospar@cosparhq.org, Web : http://meetings.copernicus.org/cospar2006/

IRST2006 - Ionospheric Radio Systems and Techniques Conference
London, United Kingdom, 18-21 July 2006
cf. announcement in the Radio Science Bulletin of June 2005 p. 85
Contact : IRST 2006 ORGANISER, The IEE, Event Services, Michael Faraday House, Six Hills Way, Stevenage, Hertfordshire SG1 2AY, United Kingdom, Tel : +44 1438 765647, Fax : +44 1483 765659, E-mail: eventsa2@iee.org.uk, Web : http://conferences.iee.org/IRST2006/

September 2006

ISROSES - International Symposium on Recent Obsrvations and Simulations of the Sun-Earth System
Varna, Bulgaria, 17-22 September 2006
cf. announcement in the Radio Science Bulletin of March 2006 p. 53
Contact : E-mail : isroses2006@abv.bg, Web : http://www.isroses.org/

Vertical Coupling in the Atmospheric/Ionospheric System
Varna, Bulgaria, 18-22 September 2006
Contact : Dr. Dora Pancheva, Centre for Space, Atmospheric & Oceanic Science, Dept. of Electronic and Electrical Engineering, University of Bath, Bath BA2 7AY, United Kingdom, Fax : +44 1225-386305, E-mail : eesdvp@bath.ac.uk, Web : http://www.iaga.geophys.bas.bg/

International Conference on Ultrawideband
Waltham, MA, USA, 24-27 September 2006
Contact : Dr. A. F. Molisch, Mitsubishi Electric Research Labs, 201 Broadway, Cambridge, MA 02139, USA, Fax : +1 617 621 7550, E-mail : Andreas.Molisch@ieee.org , http://www.icuwb2006.org/

October 2006

IRI Workshop 2006 - New Measurements for Improved IRI TEC Representation
Buenos Aires, Argentina, 16-20 October 2006
Contact : Marta Mosert, Av. Espana 1512 (sur), Capital, CP 5400, Ciudad de San Juan, Argentina, Fax +54 2644213653, mmosert@casleo.gov.ar , Web : http://www.casleo.gov.ar/WSIRI2006 (not yet operable)

November 2006

EuCAP 2006 - European Conference on Antennas and Propagation
Nice, France, 6-10 November 2006
Contact : EuCAP 2006 Secretariat, ESA Conference Bureau, Postbus 299, NL-2200 AG Noordwijk, The Netherlands, Tel. : +31 71 565 5005, Fax : +31 71 565 5658, E-mail : eucap2006@esa.int, Web : www.eucap2006.org and http://www.congrex.nl/06a08/

December 2006

Eleventh International Workshop on Technical and Scientific Aspects of MST Radar (MST11)
Gadanki/Tirupati, India, 11-15 December 2006
cf. announcement in the Radio Science Bulletin of March 2006, p. 54
Contact: Dr. J. Roettger, Max-Planck-Institut fur Aeronomie, Max-Planck-Str. 2, D-37191 Katlenburg-Lindau, Germany, Tel. +49 5556-979 163, Fax +49 5556-979 240, E-mail roettger@linmpi.mpg.de

APMC 2006 - 2006 Asia-Pacific Microwave Conference
Yokohama, Japan, 12-15 December 2006
cf. announcement in the Radio Science Bulletin of September 2005 p. 44
Contact : Dr. Takashi Ohira, 2-2-2 Hikaridai, Keihanna Science City, Kyoto 619-0288, Japan, Fax : +81 774-95 1508, E-mail : ohira@atr.jp , Web : http://www.apmc2006.org

April 2007

URBAN 2007 - Urban Remote Sensing Joint Event 2007
Paris, France, 11-13 April 2007
Contact : Paolo Gamba, Dipartimento di Elettronica, Università di Pavia, Via Ferrata 1, 27100 Pavia, Italy, Fax +390 382-422583, e-mail : paolo.gamba@unipv.it , Web : http://tlc.unipv.it/urban-remote-sensing-2007/index.html

August 2007

ISAP 2007 - International Symposium on Antennas and Propagation
Niigata, Japan, 20-24 August 2007
Contact : Yoshihiko Konishi (Publicity Chair), Mitsubishi Electric Corporation, 5-1-1 Ofuna, Kamakura, 247-8501 Japan, E-mail : isap-2007@mail.ieice.org, Web : http://www.isap07.org

AP-RASC 2007 - Asia-Pacific Radio Science Conference
Perth, Western Australia, August or September 2007 (exact date not fixed yet)
Contact : Dr. Phil Wilkinson, Deputy Director IPS Radio and Space Services, Department of Industry, Tourism and Resources, P O Box 1386, Haymarket, NSW 1240, AUSTRALIA, Tel : +61 2 9213 8003, Fax : +61 2 9213 8060, E-mail: phil@ips.gov.au, Web : http://www.ap-rasc07.org/

August 2008

URSI GA08 - XXIXth URSI General Assembly
Chicago, IL, USA, 9-16 August 2008
Contact : URSI Secretariat, c/o INTEC, Ghent University, Sint-Pietersnieuwstraat 41, B-9000 Ghent, Belgium, Tel. : +32 9 264 3320, Fax : +32 9 264 4288, E-mail : info@ursi.org

An up-to-date version of this Conference Calendar, with links to various conference web sites can be found at www.ursi.org/ Calendar of supported meetings

If you wish to announce your meeting in this meeting in this calendar, you will gind more information at www.ursi.org URSI cannot held responsible for any errors contained in this list of meetings

News from the URSI Community

NEWS FROM A MEMBER COMMITTEE

TURKEY
URSI-TURKEY'2006 Scientific Congress & National Committee Meeting

06 – 08 September 2006, Hacettepe University, Ankara, TÜRKÝYE

The International Union of Radio Science (URSI), an organization under the International Council for Science, includes the scientists in the fields of electromagnetic fields, electronics, signal processing, communications and medical electronics.

A Member Committee of URSI (represented by TUBÝTAK in Turkey) is established in a territory by its Academy of Sciences or Research Council, or by a similar institution or association of institutions.

The General Meeting and Scientific Congress of URSI-Turkey Member Committee will be held in September 6-8, 2006, at the Beytepe Campus of Hacettepe University, Ankara. The presentation of the ongoing research at the Turkish Universities and Research Institutions in such a comprehensive platform will reveal the research potential of our country and will help inform scientists working on the same topics, and stimulate the co-operations.

Topics

- Electromagnetic Metrology
- Fields and Waves
- Signals and Systems
- Electronics and Photonics
- EM Noise and Interference
- Wave Propagation and Remote Sensing
- Ionospheric Radio Propagation
- Waves and Plasmas
- Radio Astronomy
- EM in Biology and Medicine
- Microwave Integrated Circuits and RF MEMS

Deadlines

Deadline for abstract submission	1 June 2006
Notification of evaluation results	22 June 2006
Deadline for submission of full papers	17 July 2006

Abstracts

Attendees will send the abstracts that explain technical content in Turkish to ursi@ee.hacettepe.edu.tr via e-mail. Abstracts should be in form of Word or pdf files. In addition, abstracts should include title of abstract, subject of abstract, author names, addresses, phones, fax numbers, e-mail addresses.

Student Paper Contest

In URSI-Turkey' 2006 Congress, a paper contest will be arranged for M.Sc. and Ph.D. students. For these papers, the first author should be the student. This case should be made clear while submission via e-mail.

Contact

URSI-2006 Ulusal Kongresi
Prof. Dr. Erdem YAZGAN
Hacettepe Üniversitesi
Elektrik ve Elektronik Müh. Bölümü
Beytepe TR-06800 Ankara, TÜRKÝYE
Tel: (312) 297 70 50 70 or (312) 297 70 00,
Fax: (312) 299 21 25
e-mail: ursi@ee.hacettepe.edu.tr
web: www.ee.hacettepe.edu.tr/~ursi
http://ursi.ee.hacettepe.edu.tr

Wireless Networks

The journal of mobile communication, computation and information

Editor-in-Chief:
Imrich Chlamtac
Distinguished Chair in Telecommunications
Professor of Electrical Engineering
The University of Texas at Dallas
P.O. Box 830688, MS EC33
Richardson, TX 75083-0688
email: chlamtac@acm.org

Wireless Networks is a joint publication of the ACM and Baltzer Science Publishers. Officially sponsored by URSI

Aims & Scope:
The wireless communication revolution is bringing fundamental changes to data networking, telecommunication, and is making integrated networks a reality. By freeing the user from the cord, personal communications networks, wireless LAN's, mobile radio networks and cellular systems, harbor the promise of fully distributed mobile computing and communications, any time, anywhere. Numerous wireless services are also maturing and are poised to change the way and scope of communication. WINET focuses on the networking and user aspects of this field. It provides a single common and global forum for archival value contributions documenting these fast growing areas of interest. The journal publishes refereed articles dealing with research, experience and management issues of wireless networks. Its aim is to allow the reader to benefit from experience, problems and solutions described. Regularly addressed issues include: Network architectures for Personal Communications Systems, wireless LAN's, radio , tactical and other wireless networks, design and analysis of protocols, network management and network performance, network services and service integration, nomadic computing, internetworking with cable and other wireless networks, standardization and regulatory issues, specific system descriptions, applications and user interface, and enabling technologies for wireless networks.

For a complete overview on what has been and will be published in Telecommunication Systems please consult our homepage:

BALTZER SCIENCE PUBLISHERSHOMEPAGE
http://www.baltzer.nl/winet

Special Discount for URSI Radioscientists

Euro 62 / US$ 65
(including mailing and handling)

Wireless Networks ISSN 1022-0038
Contact: Mrs. Inge Heleu
Fax +32 9 264 42 88 E-mail ursi@intec.rug.ac.be
Non members/Institutions: contact Baltzer Science Publishers

BALTZER SCIENCE PUBLISHERS
P.O.Box 221, 1400 AE Bussum, The Netherlands
Tel: +31 35 6954250 Fax: +31 35 6954 258 E-mail: publish@baltzer.nl

The Journal of Atmospheric and Solar-Terrestrial Physics

SPECIAL OFFER TO URSI RADIOSCIENTISTS

AIMS AND SCOPE

The *Journal of Atmospheric and Terrestrial Physics* (JASTP) first appeared in print in 1951, at the very start of what is termed the "Space Age". The first papers grappled with such novel subjects as the Earth's ionosphere and photographic studies of the aurora. Since that early, seminal work, the Journal has continuously evolved and expanded its scope in concert with - and in support of - the exciting evolution of a dynamic, rapidly growing field of scientific endeavour: the Earth and Space Sciences. At its Golden Anniversary, the now re-named *Journal of Atmospheric and Solar-Terrestrial Physics* (JASTP) continues its development as the premier international journal dedicated to the physics of the Earth's atmospheric and space environment, especially the highly varied and highly variable physical phenomena that occur in this natural laboratory and the processes that couple them. The *Journal of Atmospheric and Solar-Terrestrial Physics* is an international journal concerned with the inter-disciplinary science of the Sun-Earth connection, defined very broadly. The journal referees and publishes original research papers, using rigorous standards of review, and focusing on the following: The results of experiments and their interpretations, and results of theoretical or modelling studies; Papers dealing with remote sensing carried out from the ground or space and with in situ studies made from rockets or from satellites orbiting the Earth; and, Plans for future research, often carried out within programs of international scope. The Journal also encourages papers involving: large scale collaborations, especially those with an international perspective; rapid communications; papers dealing with novel techniques or methodologies; commissioned review papers on topical subjects; and, special issues arising from chosen scientific symposia or workshops. The journal covers the physical processes operating in the troposphere, stratosphere, mesosphere, thermosphere, ionosphere, magnetosphere, the Sun, interplanetary medium, and heliosphere. Phenomena occurring in other "spheres", solar influences on climate, and supporting laboratory measurements are also considered. The journal deals especially with the coupling between the different regions. Solar flares, coronal mass ejections, and other energetic events on the Sun create interesting and important perturbations in the near-Earth space environment. The physics of this subject, now termed "space weather", is central to the Journal of Atmospheric and Solar-Terrestrial Physics and the journal welcomes papers that lead in the direction of a predictive understanding of the coupled system. Regarding the upper atmosphere, the subjects of aeronomy, geomagnetism and geoelectricity, auroral phenomena, radio wave propagation, and plasma instabilities, are examples within the broad field of solar-terrestrial physics which emphasise the energy exchange between the solar wind, the magnetospheric and ionosphericplasmas, and the neutral gas. In the lower atmosphere, topics covered range from mesoscale to global scale dynamics, to atmospheric electricity, lightning and its effects, and to anthropogenic changes. Helpful, novel schematic diagrams are encouraged. Short animations and ancillary data sets can also be accommodated. Prospective authors should review the *Instructions to Authors* at the back of each issue.

Complimentary Information about this journal:
http://www.elsevier.com/locate/JASTP?
http://earth.elsevier.com/geophysics

Audience:
Atmospheric physicists, geophysicists and astrophysicists.

Abstracted/indexed in:
CAM SCI Abstr
Curr Cont SCISEARCH Data
Curr Cont Sci Cit Ind
Curr Cont/Phys Chem & Sci
INSPEC Data
Meteoro & Geoastrophys Abstr
Res Alert

Editor-in-Chief:
T.L. Killeen, National Centre for Atmospheric Research, Boulder, Colorado, 80307 USA

Editorial Office:
P.O. Box 1930, 1000 BX Amsterdam, The Netherlands

Special Rate for URSI Radioscientists 2003:
Euro 149.00 (US$ 149.00)
Subscription Information
2002: Volume 65 (18 issues)
Subscription price: Euro 2659 (US$ 2975)
ISSN: 1364-6826

CONTENTS DIRECT:
The table of contents for this journal is now available pre-publication, via e-mail, as part of the free ContentsDirect service from Elsevier Science. Please send an e-mail message to cdhelp@elsevier.co.uk for further information about this service.

For ordering information please contact Elsevier Regional Sales Offices:

Asia & Australasia/ e-mail: asiainfo@elsevier.com
Europe, Middle East & Africa: e-mail: nlinfo-f@elsevier.com
Japan: Email: info@elsevier.co.jp
Latin America : e-mail: rsola.info@elsevier.com.br
United States & Canada : e-mail: usinfo-f@elsevier.com

Information for authors

Content

The *Radio Science Bulletin* is published four times per year by the Radio Science Press on behalf of URSI, the International Union of Radio Science. The content of the *Bulletin* falls into three categories: peer-reviewed scientific papers, correspondence items (short technical notes, letters to the editor, reports on meetings, and reviews), and general and administrative information issued by the URSI Secretariat. Scientific papers may be invited (such as papers in the *Reviews of Radio Science* series, from the Commissions of URSI) or contributed. Papers may include original contributions, but should preferably also be of a sufficiently tutorial or review nature to be of interest to a wide range of radio scientists. The *Radio Science Bulletin* is indexed and abstracted by INSPEC.

Scientific papers are subjected to peer review. The content should be original and should not duplicate information or material that has been previously published (if use is made of previously published material, this must be identified to the Editor at the time of submission). Submission of a manuscript constitutes an implicit statement by the author(s) that it has not been submitted, accepted for publication, published, or copyrighted elsewhere, unless stated differently by the author(s) at time of submission. Accepted material will not be returned unless requested by the author(s) at time of submission.

Submissions

Material submitted for publication in the scientific section of the *Bulletin* should be addressed to the Editor, whereas administrative material is handled directly with the Secretariat. Submission in electronic format according to the instructions below is preferred. There are typically no page charges for contributions following the guidelines. No free reprints are provided.

Style and Format

There are no set limits on the length of papers, but they typically range from three to 15 published pages including figures. The official languages of URSI are French and English: contributions in either language are acceptable. No specific style for the manuscript is required as the final layout of the material is done by the URSI Secretariat. Manuscripts should generally be prepared in one column for printing on one side of the paper, with as little use of automatic formatting features of word processors as possible. A complete style guide for the *Reviews of Radio Science* can be downloaded from http://www.ips.gov.au/IPSHosted/NCRS/reviews/. The style instructions in this can be followed for all other *Bulletin* contributions, as well. The name, affiliation, address, telephone and fax numbers, and e-mail address for all authors must be included with all submissions.

All papers accepted for publication are subject to editing to provide uniformity of style and clarity of language. The publication schedule does not usually permit providing galleys to the author.

Figure captions should be on a separate page in proper style; see the above guide or any issue for examples. All lettering on figures must be of sufficient size to be at least 9 pt in size after reduction to column width. Each illustration should be identified on the back or at the bottom of the sheet with the figure number and name of author(s). If possible, the figures should also be provided in electronic format. TIF is preferred, although other formats are possible as well: please contact the Editor. Electronic versions of figures *must* be of sufficient resolution to permit good quality in print. As a rough guideline, when sized to column width, line art should have a minimum resolution of 300 dpi; color photographs should have a minimum resolution of 150 dpi with a color depth of 24 bits. 72 dpi images intended for the Web are generally *not* acceptable. Contact the Editor for further information.

Electronic Submission

A version of Microsoft *Word* is the preferred format for submissions. Submissions in versions of T_EX can be accepted in some circumstances: please contact the Editor before submitting. *A paper copy of all electronic submissions must be mailed to the Editor, including originals of all figures.* Please do *not* include figures in the same file as the text of a contribution. Electronic files can be send to the Editor in three ways: (1) By sending a floppy diskette or CD-R; (2) By attachment to an e-mail message to the Editor (the maximum size for attachments *after* MIME encoding is about 7 MB); (3) By e-mailing the Editor instructions for downloading the material from an ftp site.

Review Process

The review process usually requires about three months. Authors may be asked to modify the manuscript if it is not accepted in its original form. The elapsed time between receipt of a manuscript and publication is usually less than twelve months.

Copyright

Submission of a contribution to the *Radio Science Bulletin* will be interpreted as assignment and release of copyright and any and all other rights to the Radio Science Press, acting as agent and trustee for URSI. Submission for publication implicitly indicates the author(s) agreement with such assignment, and certification that publication will not violate any other copyrights or other rights associated with the submitted material.

APPLICATION FOR AN URSI RADIOSCIENTIST

I have not attended the last URSI General Assembly, and I wish to remain/become an URSI Radioscientist in the 2006-2008 triennium. Subscription to *The Radio Science Bulletin* is included in the fee.
(please type or print in BLOCK LETTERS)

Name: Prof./Dr./Mr./Mrs./Ms. _____
Family Name *First Name* *Middle Initials*

Present job title: _____

Years of professional experience: _____

Professional affiliation: _____

I request that all information, including the bulletin, be sent to my ☐ home ☐ business address, i.e.:

Company name: _____

Department: _____

Street address: _____

City and postal / zip code: _____

Province / State: _____ Country: _____

Phone: _____ ext: _____ Fax: _____

E-mail: _____

Areas of interest (please tick)

☐ A Electromagnetic Metrology
☐ B Fields and Waves
☐ C Signals and Systems
☐ D Electronics and Photonics
☐ E Electromagnetic Noise & Interference
☐ F Wave Propagation & Remote Sensing
☐ G Ionospheric Radio and Propagation
☐ H Waves in Plasmas
☐ J Radio Astronomy
☐ K Electromagnetics in Biology & Medicine

The fee is 50 Euro.
(The URSI Board of Officers will consider waiving of the fee if the case is made to them in writing)

Method of payment: VISA / MASTERCARD (we do not accept cheques)

Credit Card No ☐☐☐☐ ☐☐☐☐ ☐☐☐☐ ☐☐☐☐ Exp. date: _____

Date: _____ Signed _____

Please return this signed form to:

The URSI Secretariat
c /o Ghent University / INTEC
Sint-Pietersnieuwstraat 41
B-9000 GENT, BELGIUM
fax (32) 9-264.42.88